LUT UNIVERSITY
LUT School of Energy Systems
LUT Mechanical engineering

Ilkka Suoranta

IMPLEMENTATION OF A LASER SENSOR SYSTEM IN A MULTI-ROBOT WELDING CELL

14.6.2021

Examiners: Prof. Timo Björk
M. Sc. (Tech.) Hannu Lund

TIIVISTELMÄ

LUT-Yliopisto
LUT School of Energy Systems
LUT Kone

Ilkka Suoranta

Laseranturijärjestelmän käyttöönotto monirobottihitsausasemassa

Diplomityö

2021

94 sivua, 57 kuvaa, 8 taulukkoa ja 5 liitettä

Tarkastajat: Prof. Timo Björk
DI Hannu Lund

Hakusanat: robottihitsaus, laseranturi, railonhaku, railonseuranta, jigitön hitsaus

Tämä diplomityö on tehty LUT-yliopiston hitsaustekniikan laboratoriolle osana EFREA-projektia (Energy-efficient systems based on renewable energy for Arctic conditions). Yksi projektin tavoitteista on kehittää ratkaisuja, joilla hitsauksen laatu ja tuottavuus kevyiden rakenteiden valmistuksessa voidaan varmistaa. Optiset anturit, joilla on keskeinen rooli mukautuvien ja älykkäiden robottihitsausjärjestelmien kehittämisessä, on esimerkki tällaisesta ratkaisusta.

Työssä perehdytään optisten antureiden mahdollisuuksiin ja rajoitteisiin robottihitsauksessa. Tyypilliset sekä kehittyvät optiset anturimenetelmät ja niiden sovelluskohteet esitellään kirjallisuuskatsauksessa. Katsauksen perusteella optisten antureiden avulla voidaan parantaa robottiaseman joustavuutta, sekä varmistaa hitsauksen laatu myös muuttuvissa olosuhteissa.

Työn keskeinen tarkoitus on optisen laseranturijärjestelmän käyttöönotto hitsauslaboratorion monirobottiasemassa. Tavoitteena on kehittää menetelmät, joilla laseranturia voidaan hyödyntää monirobottiaseman eri käyttötarkoituksiin, sekä selvittää näiden menetelmien tarkkuus ja käytettävyys.

Käytännön osuudessa esitellään laseranturimenetelmät railonhakuun, railonseurantaan sekä kappaleiden paikoitukseen jigittömässä hitsauksessa. Railonhaku- ja seurantamenetelmien toimivuus varmistettiin käytännön kokeilla. Työkappaleiden paikoitusmenetelmää ei testattu käytännössä, mutta siihen liittyvät robottiohjelmat luotiin ja menetelmän toimintaa simuloitiin. Kokeet osoittivat, että railonhaku laseranturilla on huomattavasti tarkempaa verrattuna tavanomaiseen langalla hakuun. Railonseurantatestit todistivat, että menetelmä itsessään toimii ja sen tarkkuus on riittävä hyvän laadun varmistamiseksi. Valokaaren aiheuttamat häiriöt kuitenkin johtivat merkittäviin seurantavirheisiin hitsauksen aikana, joten jatkokehitystä tarvitaan luotettavan railonseurannan toteuttamiseksi. Keskeisenä tuloksena työssä annetaan kehitysehdotuksia laseranturimenetelmien käytettävyyden ja luotettavuuden parantamiseksi.

ABSTRACT

LUT University
LUT School of Energy Systems
LUT Mechanical Engineering

Ilkka Suoranta

Implementation of a laser sensor system in a multi-robot welding cell

Master's thesis

2021

94 pages, 57 figures, 8 tables and 5 appendices

Examiner: Prof. Timo Björk
M. Sc. (Tech.) Hannu Lund

Keywords: robotic welding, laser sensor, seam finding, seam tracking, jigless welding

This master's thesis is done for the LUT University's laboratory of welding technology as a part of project EFREA (Energy-efficient systems based on renewable energy for Arctic conditions). One of the goals of the project is to develop solutions that ensure the quality and productivity in welding manufacturing of lightweight structures. An example of such solution is optical sensing, which is a key technology in the development of adaptable and intelligent robotic welding systems.

This thesis gives an overview on the possibilities and restrictions of utilizing optical sensors in robotic welding. The typical and emerging optical sensing methods and their applications are presented in a literature review. Based on the review, optical sensors can increase the flexibility of a robot system, and ensure high weld quality under varying circumstances.

Main purpose of this thesis is to implement a laser sensor system in the multi-robot welding cell of the welding laboratory. The aim is to develop methods for utilizing the laser sensor for different tasks of the welding cell, and to investigate the accuracy and usability of the developed methods.

The experimental section presents methods for utilizing the laser sensor for seam finding, seam tracking and workpiece positioning in jigless welding. Functionality of the seam finding and seam tracking methods was verified with practical experiments. The workpiece positioning method was not tested in practice, but the required robot programs were created, and its functions were simulated. The experiments showed that seam finding with the laser sensor provides superior accuracy in comparison to the conventional touch sensing method. Accuracy of the seam tracking method was proven to be sufficient for ensuring high weld quality. However, disturbances caused by arc light led to significant tracking errors during welding, so further development is needed in order to realize reliable seam tracking. As a key result, development proposals for improving the usability and reliability of the proposed laser sensor methods are given.

ACKNOWLEDGMENTS

I would like to thank D.Sc. Tuomas Skriko and M.Sc. Hannu Lund for your valuable guidance and comments during this study, as well as for giving me the opportunity to do my master's thesis on this very interesting topic. I would also like to thank M.Sc. Sakari Penttilä and laboratory engineer Esa Hiltunen for assisting and advising me not only during this thesis, but also during my previous work for the welding laboratory.

Furthermore, I would like to thank my parents for all the support and encouragement throughout my life and studies. Lastly, I would like to express my deepest gratitude to my wife Melisa, daughter Else and son Vilho for giving me the strength to finish my studies and this "robottikirja" in time.

Ilkka Suoranta
Lappeenranta 14.6.2021

TABLE OF CONTENTS

LIST OF ABBREVIATIONS

6-DOF	Six Degrees of Freedom
AI	Artificial Intelligence
ANN	Artificial Neural Network
CCD	Charge-Coupled Device
CMOS	Complementary Metal Oxide Semiconductor
DLP	Digital Light Processing
GMAW	Gas Metal Arc Welding
I/O	Input / Output
IoT	Internet of Things
IPC	Information Processing Center
IWS	Intelligent Welding System
MAWC	Measurement-Aided Welding Cell
REFP	Reference Point
SAR	Spatial Augmented Reality
TCP	Tool Center Point
TOF	Time of Flight
WPS	Welding Procedure Specification

1 INTRODUCTION

This master's thesis is done for LUT University's welding laboratory as a part of ENI CBC project EFREA (Energy-efficient systems based on renewable energy for Arctic conditions). The project aims, among other things, to develop solutions which ensure the quality and productivity in welding manufacturing of lightweight structures for extreme temperatures. With regard to this topic, in this thesis the possibilities and restrictions of utilizing optical sensing in a multi-robot welding cell are examined and tested in practice.

This thesis is also a further study for Lund (2019) master's thesis "Development of a multi-robot welding cell for jigless welding", in which the concept of jigless welding was examined and developed. In jigless welding, welding assemblies are carried out without workpiece fixturing by using an additional robot to handle the workpieces. The concept was tested in LUT welding laboratory's multi-robot welding cell, which consists of a welding robot, a material handling robot and a workpiece positioner. In his thesis, Lund (2019, pp. 76–80) recognized the need for machine vision in the system, as it could be used for robot path correction and for ensuring the accuracy of workpiece positioning. Laser triangulation was proposed to be the most suitable machine vision method for this purpose, and in this study, a laser triangulation- based sensor system is integrated to the cell.

1.1 Background

The welding industry has been shifting from using manual labor to automated systems for decades due to harshness of welding work, lack of skilled welders and increased demands on productivity and quality. Robotic welding is already widely adopted in high volume production, where the variety of welding tasks is low, and robots can be operated in teach-and-playback mode with limited adaptability. However, in order to efficiently utilize welding robots in lower production volumes and in more challenging applications, the robot system must have the ability to adapt to the varying circumstances and tasks. This drives the industry to develop solutions which minimize the time and resources required for programming, set-ups and weld preparations, and which ensure the weld quality during the process. Recent developments in enabling technologies such as optical sensors, artificial intelligence (AI), modelling and simulation, digitalization and internet of things (IoT) has

brought new possibilities to move towards these goals, and to realize increasingly more adaptable and flexible robotic welding systems. (Rout et al. 2019, pp. 12–13; Wang et al. 2020, pp. 373–374)

The need for sensors in robotic welding is apparent, because there is always differences between the preprogrammed robot path and the actual joint location and geometry due to factors such as inaccurate prefabrication, workpiece positioning and heat distortions. Advantages of using optical sensing have been widely acknowledged, as the method can be used for measuring various geometries and features from the welding assembly, and the measurement data can be utilized in e.g. adaptive process control, quality assurance, robot guidance, seam finding and seam tracking. So far, optical sensors have not reached widespread adoption in industry due to the complexity and practical issues they add to the system, and more conventional sensing methods are usually used for the essential tasks. Nevertheless, optical sensors play a key role in the development of advanced robotic welding systems, as they provide crucial measurement data that cannot be obtained with other sensors. (Rout et al. 2019, pp. 12–16; Kah et al. 2015, pp. 1–5)

1.2 The research problem and objectives

Many studies in the field of robotic welding focus on developing solutions related to optical sensors, such as machine vision algorithms for seam recognition or methods for intelligent welding process control, but the results often remain on theoretical level. On the contrary, robot suppliers provide optical sensor systems as a turnkey solution alongside robot stations. However, when a modern optical sensor is integrated to an older generation robot station, practical restrictions and compatibility issues often occur, but studies of such technical integration are rare. The research problem in this study is that the laser sensor system that is being implemented does not have built-in features for robotic welding tasks, and it is not fully compatible with the robot controller. Therefore, it is challenging to utilize the laser sensor to its full potential in the multi-robot welding cell.

The aim of this study is to realize the possibilities of a laser vision sensor in the LUT welding laboratory's multi-robot welding cell. This includes development of the methods and program routines for seam tracking, seam finding and handling robot guidance by utilizing the laser sensor. The following research questions are set to guide the focus of this study:

- What are the possibilities and restrictions of using optical sensors in robotic welding?
- For what tasks and how the laser sensor can be utilized in the multi-robot welding cell?
- Is the accuracy of the laser sensor methods sufficient to ensure high weld quality?

The first research question is answered by conducting a literature review on the topic. To find answers to the latter research questions, features of the laser sensor and the robot system are investigated, the laser sensor methods are implemented, and practical experiments are carried out.

1.3 Research methods

The literature review of this thesis introduces the principles and future outlook of robotic welding, and presents the typical and emerging optical sensing methods and their applications in robotic welding cells. Finally, the possibilities and restrictions of optical sensor utilization are discussed based on the literature findings. The review is done on the basis of peer-reviewed studies, technical documentations and commercial sources. Studies were searched with keywords such as “robotic welding”, “seam tracking”, “seam finding”, “vision-aided robotic welding”, “machine vision”, “laser triangulation”, “laser vision sensor”, “flexible welding cell”, “jigless welding”, “multi-robot welding cell”, “vision-guided robotics”, “machine vision” and “intelligent welding”. The references were selected based on their relevancy to the topic, with emphasis on the latest publications, preferably published after year 2015. Other sources, such as system suppliers are used to provide examples of optical sensor utilization in industrial applications.

The experimental section deals with the laser sensor implementation in the multi-robot welding cell, which consists of a welding robot, a handling robot with magnetic gripper and a servo-controlled workpiece positioner. Technical documentations such as user manuals are utilized in investigating the system configuration, and in implementation of the laser sensor methods for seam finding, seam tracking and handling robot guidance. Also the robot manufacturer's technical support is consulted. The accuracy and functionality of seam finding and seam tracking with the laser sensor is verified with practical experiments. Visual quality of the resulting welds is inspected with a weld quality assurance software based on laser scanning, and the weld quality level is determined in accordance with standard ISO

5817. The possibility of using the laser sensor for handling robot guidance in jigless welding is not tested in practice, but the method is developed with the help of a simulation software.

1.4 Scope and limitations

The focus of the study is on laser sensor systems, robotic gas metal arc welding (GMAW) and optical sensing solutions which can be utilized in the jigless multi-robot welding cell. The principles and future outlook of robotic welding, and other optical sensing methods than laser triangulation- based sensors are only briefly introduced in the literature review.

In the experimental section, the developed methods and achieved results apply directly only to the LUT welding laboratory's multi-robot welding cell and the specific laser sensor system. Moreover, the sensor functions were tested with T-joints of structural steel plates with surface in delivery condition, so the results may not be valid for other joint types or highly reflective materials, such as aluminum or machined surfaces. Functionality of the laser sensor methods is evaluated mainly based on accuracy, and the effect of seam tracking to the weld quality is inspected only visually. Practical restrictions of the developed methods are discussed in more detail in chapter 6.

1.5 Contribution

The literature review provides an overview on how optical sensors can be utilized in modern robotic welding cells, and what are the emerging technologies of the field. To summarize the literature findings, a table of the reviewed studies and industrial use cases is compiled. It can be used as a reference for comparing the accuracy and applicability of different optical sensing methods in robotic welding.

Experimental section of this thesis sets a basis for further development of the LUT welding laboratory's multi-robot welding cell in terms of optical sensor utilization. Practical methods for using the laser sensor for seam finding and seam tracking are developed and tested. In addition, a new method for using a search function for handling robot guidance in jigless welding is proposed. These methods can be applied in robotic welding cells by Yaskawa and with different type of laser triangulation sensors. As a key result, accuracy of the developed laser sensor methods is determined and proposals for further development are given.

2 PRINCIPLES AND FUTURE OUTLOOK OF ROBOTIC GAS METAL ARC WELDING

Arc welding is one of the most typical applications for industrial robots. Over the past decades, welding robots have become increasingly more common as the systems have become more capable and affordable for small and medium sized enterprises. The motivation for robotizing welding in general is to increase productivity and to decrease production costs. Also better, and especially more consistent weld quality can be achieved when compared to manual welding, as the human factor is removed from the process, and robots are able to work tirelessly with high precision. (Pires et al. 2005, pp. 17–23) The following subchapters introduces the principles and emerging technologies in the field of robotic welding.

2.1 Robotic welding system

Configuration of a typical arc welding robot system is presented in figure 1. It is based on an industrial robot with six-degrees-of-freedom (6-DOF), which refers to the ability to move and rotate the robot tool along three perpendicular coordinate axes. The system is operated through a robot controller, which controls the motions of the robot and external axes, and communicates with other devices such as welding power source and sensors. (Lin & Luo 2015, pp. 2404–2439)

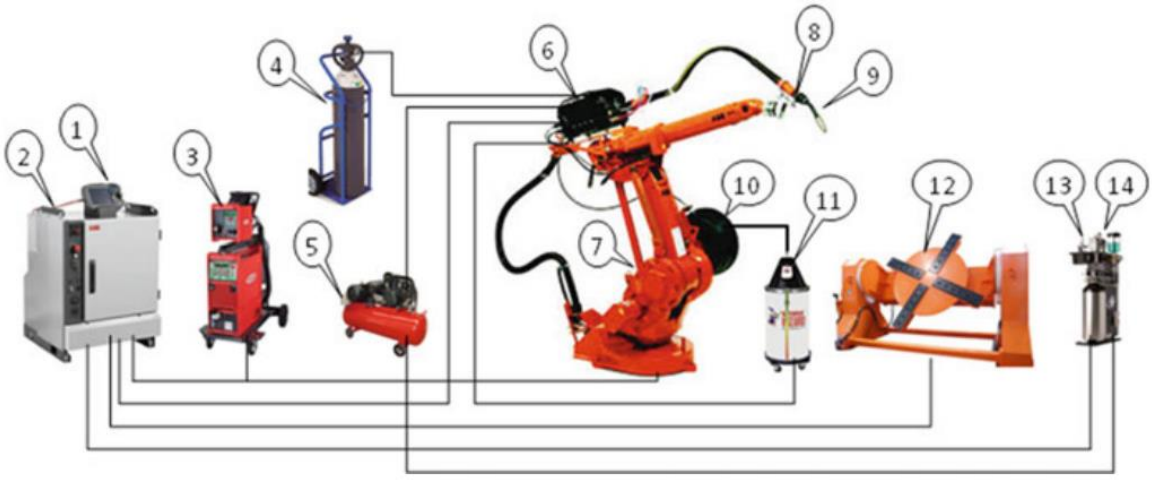

Figure 1. Components of a typical welding robot system: 1. teach pendant 2. robot controller 3. welding power source 4. shielding gas cylinder 5. air compressor 6. wire feeder 7. robot 8. collision detector 9. torch 10. wire spool 11. wire drum 12. workpiece positioner 13. & 14. station for torch cleaning and robot tool calibration. (Lin & Luo 2015, p. 2429)

At its simplest, a robotic welding cell can consist of a stationary robot and a welding fixture. This solution can be suitable for small workpieces, but usually more reachability is needed in order to approach the joints in the desired welding position and tool angle. More reachability can be realized by mounting the robot on a transporter, and by using a workpiece positioner with degrees of freedom. According to Lin & Luo (2015, pp. 2419–2420) mounting the robot on a transporter generally makes the system more flexible, and as a result the arc time and productivity increases. Depending on the required working area, different robot transporter options are linear track, gantry and column. In figure 2 can be seen an example of a welding robot attached to a three-axis gantry, making it possible to weld at two separate workstations. (Lin & Luo 2015, pp. 2418–2422)

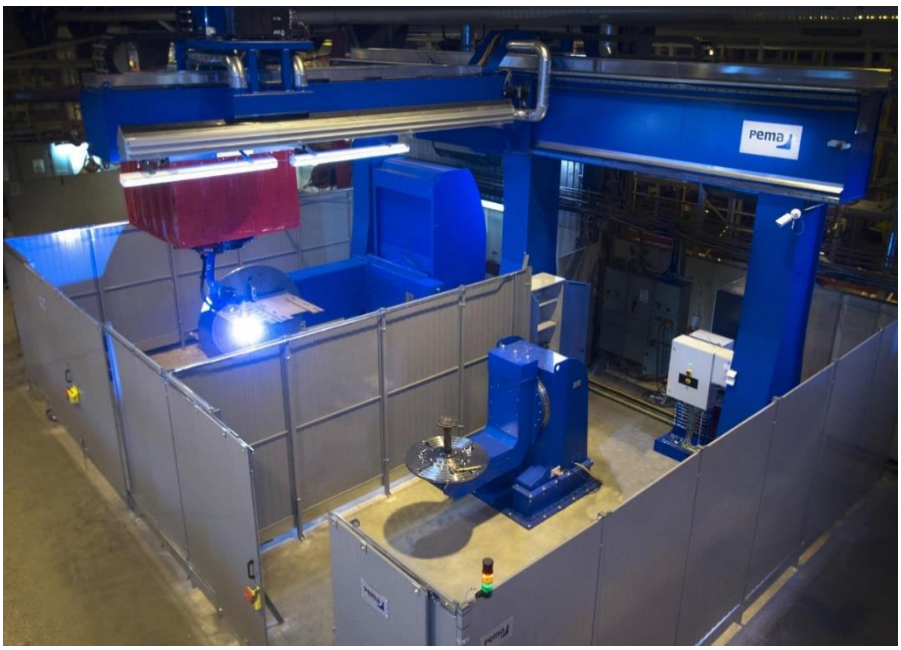

Figure 2. Welding robot station consisting of a three-axis gantry and two workpiece positioners. (Bell 2020)

A robotic workpiece positioner is an external axis which can be controlled in a coordinated manner with the welding robot. The main function of a workpiece positioner is to offer the workpiece at optimal orientation for the robot, in terms of desired welding position and accessibility of the joint. Numerous workpiece positioner solutions have been developed for handling products of different shape and size, and some example models are presented in figure 3. (Lin & Luo 2015, pp. 2419–2424)

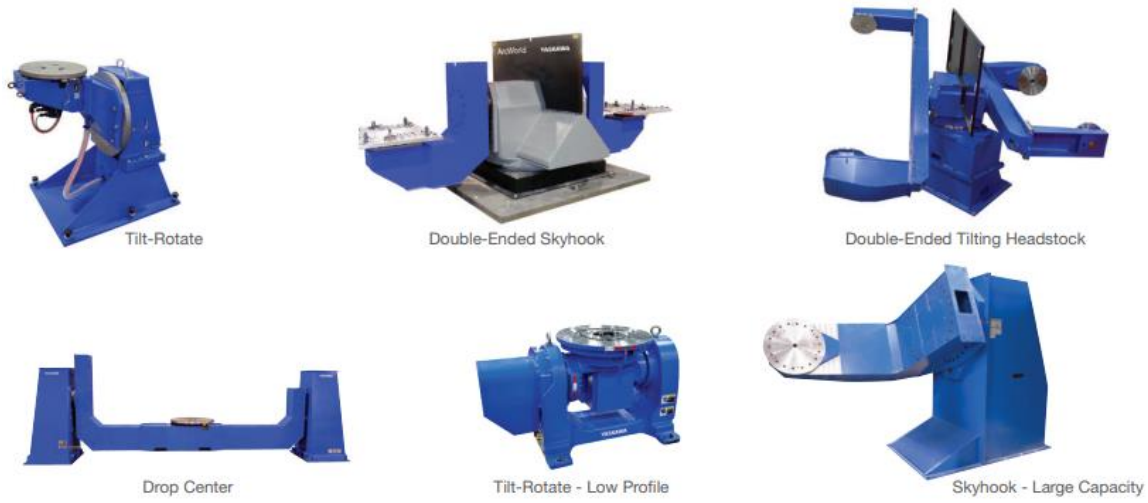

Figure 3. Workpiece positioner solutions (Yaskawa 2020, p. 21)

Robotic welding cells are usually tailored for the user's needs to serve specific tasks, and the optimal use of transporters, workpiece positioners and other devices such as sensors must be carefully considered in the system design (Lin & Luo 2015, p. 2424). However, robot manufacturers have brought compact and modular off-the-shelf type welding cells to the markets. Such systems include all the necessary solutions considering safety, workpiece positioning and compatibility, so they can be implemented in production fast and effortlessly. In figure 4 can be seen an example of a modular welding cell, which is consists of three welding robots, two- sided workpiece positioner and safety devices. (Yaskawa 2020, pp. 6–10)

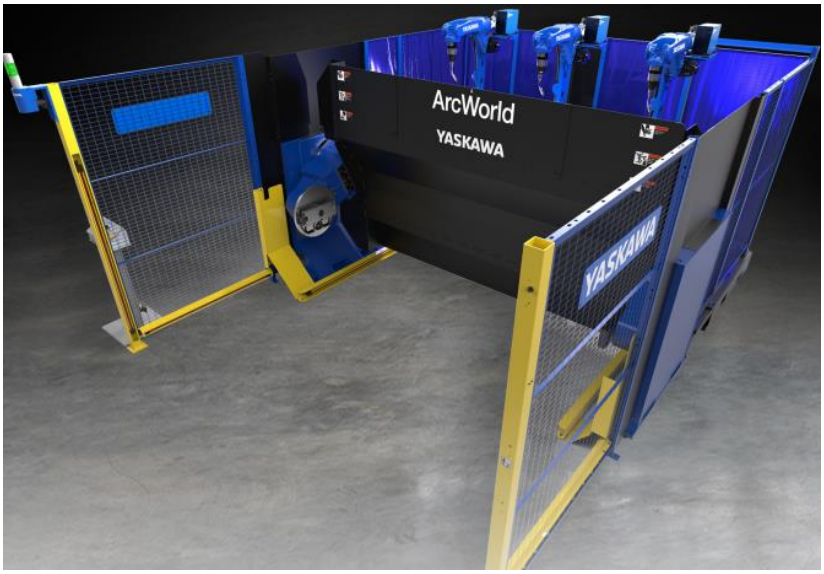

Figure 4. A compact and modular multi-robot welding cell. (Yaskawa 2020, p. 10)

2.2 Multi-robot welding cells and jigless welding

In a multi-robot welding cell, two or more 6-DOF industrial robots operate in a coordinated and synchronous manner. The cell may consist solely of welding robots as shown in figure 4, but also material handling robots can be utilized. A handling robot can pick the workpieces and place them into workpiece positioner, or alternatively it can hold the entire workpiece during welding, and thus provide optimal accessibility and welding positions for the welding robot. If the handling robot holds the workpiece during welding, the workpiece must be either already tack welded, or the robot holds the entire welding fixture. (Lin & Luo 2015, pp. 2424–2426; Tuominen 2016, pp. 374–379)

Multi-robot solutions are being developed to meet the growing demand for more flexible automated welding systems, and one example of such solution is jigless welding. Generally, a welded product requires a tailored jig, as it is necessary to hold the workpieces in place during welding and to prevent heat distortions. However, the costs related to their design, manufacturing and installation is limiting the suitability of robotic welding for low volume – high variation production. Therefore, efforts have been made to realize fully jigless robotic welding cells, where a handling robot brings components to the welding assembly one by one and holds them in position during tack welding (Lund 2019). According to Bejlegaard et al. (2018, p. 306), compared to traditional methods jigless welding could provide improved flexibility without sacrificing productivity, as well as reduced manufacturing costs and changeover times between different product types. Figure 5 shows an example layout of a multi-robot welding cell for jigless welding. (Bejlegaard et al. 2018, pp. 305–311)

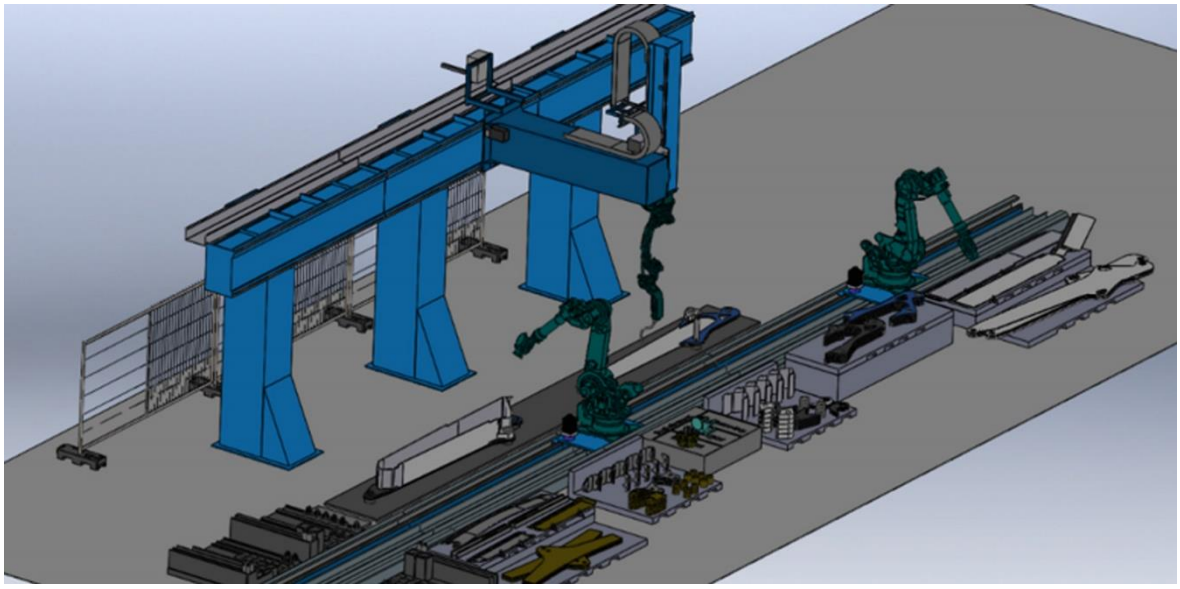

Figure 5. A model of jigless welding cell, consisting of a gantry- mounted welding robot and two track- mounted handling robots. (Bejlegaard et al. 2018, p. 309)

According to Bejlegaard et al. (2018, p. 309) and Lund et al. (2020, pp. 302–303), the main challenges in jigless welding are ensuring the accuracy of workpiece positioning and compensating the distortions caused by heat input. These challenges could be overcome by developing methods for predicting the heat distortions and for estimating the optimal welding sequence, and by utilizing optical sensor measurements and feedback control for workpiece handling (Lund 2019, pp. 80–84). Studies by Tuominen (2016, pp. 376–377) and Lund et al. (2020, pp. 303–308) propose that the heat distortions in jigless welding could be compensated by positioning the components so, that the desired product dimensions are achieved after welding and cooling. Other considerable issues regarding jigless welding cells are tight tolerance requirements, versatility of the handling robot gripper, increased programming workload and high initial investment (Bejlegaard et al. 2018, pp. 308–309).

2.3 Intelligent welding

Development of intelligent welding systems (IWS) is a central research topic in the welding automation field. Intelligent welding can be defined as solutions, which utilize advanced technologies such as AI and machine vision to replace the need of human operations in the welding process. A fully intelligent welding system would be able to sense, learn, predict, make decisions and adapt like manual welder during welding tasks. According to Wang et al. (2020, p. 379), IWS applications are being developed for various purposes before, during

and after welding, such as robot program generation, simulations, task sequencing, path optimization, process monitoring, process control and quality inspections. (Wang et al. 2020, pp. 373–379)

One characteristic IWS application is adaptive process control, where an AI- based system controls the welding parameters and optimizes the process in real-time based on sensor data and pre-trained knowledge bank. The input data for the control system can be obtained with different types of sensors, which measure e.g. the process parameters, temperatures or certain geometries from the groove, weld pool or weld bead. Intelligent welding process control systems have been developed based on several different AI- approaches, such as neural networks, fuzzy logic and machine learning (Wang et al. 2020, p. 385). Penttilä et al. (2019) proposed an artificial neural network (ANN) based parameter control method for ensuring the quality and penetration in multi-pass welding. In the study, a laser sensor was used to provide geometrical data of the root gap width, root face height and tack weld location. Based on the data, the control system optimized the welding process by adjusting wire feed rate and arc voltage during welding in order to achieve the desired outcome. (Penttilä et al. 2019, pp. 3369–3385)

2.4 Digitized welding production

Digitalisation of welding production is part of a larger trend to digitize manufacturing industries in general, which is commonly referred as Industry 4.0. Industry 4.0 combines concepts such as industrial IoT, cyber-physical systems, big data and cloud computing to interconnect the systems, machines and information throughout the product's value chain. In terms of welding production, the vision is that the design, manufacturing and quality control data could be stored and processed in a cloud-based digital environment, including e.g. CAD- drawings, simulation models, welding procedure specifications (WPS), process parameters and scanning results of welded structures. Among other things, this would enable to link the achieved weld quality to the used manufacturing procedures and parameters, and this information could be then utilized in further product design, production planning, process optimization and quality predictions. An example of the information flow in digitized welding production is presented in figure 6. (Reisgen et al. 2019, pp. 1121–1131; Wang et al. 2020, p. 381)

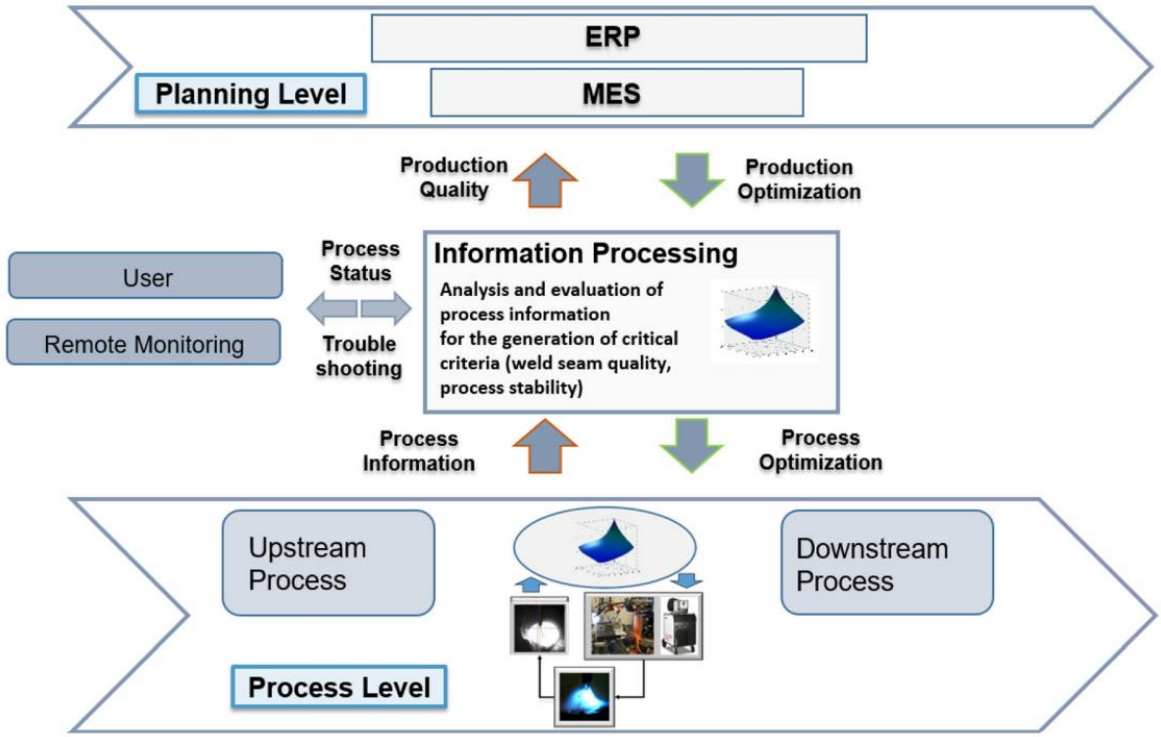

Figure 6. Information flow in digitized welding production. (Reisgen et al. 2019, p. 1130)

In digitized welding production the product information, such as plate thickness, joint type, material, process parameters, geometry of the final product and weld quality can be collected to databases, which can be utilized in different knowledge- based methods (Wang et al. 2020, pp. 381–382). Lund et al. (2020) proposed a knowledge-based method for estimating welding distortions in a simulation software for jigless welding applications. In the method, the position of a multi-robot welding cell's handling robot was adjusted to compensate the expected distortions based on a knowledge database. The database consists of welding distortion data for different plate thicknesses and weld types, measured with a laser scanner. (Lund et al. 2020, pp. 302–308)

2.5 Simulation and offline- programming

So far, the conventional method to program a welding robot has been online- programming in teach-and-playback mode, where the desired path is taught to the robot by using a manual teach pendant. However, offline- programming with simulation software is becoming increasingly more popular, in which the program is created basis on 3D models of the robot station and workpiece. The main advantage of offline- programming is that the production is uninterrupted during programming work, resulting in increased productivity. (Kah et al.

2015, pp. 3–4) Simulation software and models of robotic welding cells have also other roles in digitized welding production than program generation, such as functioning as a digital twin (DT), which can be used for e.g. monitoring and operating the physical system, and for testing new methods and procedures in virtual reality (Ratava et al. 2019, pp. 497–504).

According to Larkin et al. (2017, p. 48), costs related to programming is a limiting factor in the viability of robotic welding for small production volumes. The basic online- and offline programming methods share some drawbacks, as they are time consuming, and the outcome is highly dependent on operator skill. Also, programs created with a simulation software must be often manually calibrated when they are exported to the robot station. Therefore, development has been made to enable more automated and flexible program generation for welding robots. Larkin at al. (2017, pp. 48–58) created an automated offline- programming method, that was able to define the weld paths and plan the robot trajectory based on 3D CAD model of the workpiece. When the program is exported to the robot station, the final calibration could be done within the robot program by utilizing an optical sensor.

Nowadays, some partly automated offline- programming solutions are already commercially available, and efforts are being made to utilize more advanced technologies in robot programming. According to Wang et al. (2020, p. 383), “In the future, more integrated intelligent programming methods are expected as more accurate sensor/vision technologies, 3D CAD/PLM software, and intelligent algorithms are developed, blurring the boundary between online and offline programming.”

3 UTILIZATION OF OPTICAL SENSORS IN ROBOTIC WELDING CELLS

In general, optical sensors in robotic gas metal arc welding are used to extract geometrical data from different details of the welding assembly, such as workpiece location and orientation, or dimensions of the weld groove, weld pool and weld bead. This data can then be utilized in different feedback control, process optimization, quality inspection and robot guidance applications. (Rout et al. 2019, pp. 12–37) This chapter discusses the optical sensor utilization for seam finding, seam tracking and jigless welding applications. The focus is on laser triangulation sensors, which are commonly referred with term “laser sensor”, but some applications for alternative optical sensing methods are also presented.

3.1 Optical sensing methods for robot guidance

Optical sensing methods can be classified into subgroups of active vision and passive vision. In active vision, a known pattern of light is projected to the object and captured in image, and the 3D measurement data can be obtained with different methods based on e.g. light travel time, deformation of the light pattern or trigonometric calculations. In passive vision only a camera is needed, and the desired features are recognized directly from the image with machine vision algorithms, but multi-camera techniques are required for obtaining the depth information. (Pérez et al. 2016, pp. 4–5)

Both active- and passive vision include multiple techniques, and the techniques that are typically applied in robot applications can be seen in table 1. The suitability of different optical sensing techniques for specific robot applications depends on the requirements for sensor accuracy, size, range and processing speed. Also, the disturbances caused by the welding process and environment must be considered, such as external lights, brightness and impurities. Compared to active vision, passive vision techniques have slower processing time due to more complex image processing algorithms, and they are more prone to errors in industrial environment. However, they suit well for applications where the circumstances remain constant, processing delays are acceptable, and the camera can be static during image capture. (Pérez et al. 2016, pp. 11–19)

Different active vision methods have their own advantages in certain applications, but laser triangulation and structured light methods are the most suitable for robot guidance and object recognition applications which demand high accuracy. In structured light method, the object is measured from distance with a static camera and single captures, whereas in laser triangulation the object is measured with continuous scanning motion from closer distance. Light coding and time of flight (ToF) are rather inaccurate methods for robot guidance and path calibration tasks, but they are commonly used in e.g. mobile- and collaborative robot applications to detect objects and people in their working area to avoid collisions. (Pérez et al. 2016, pp. 14–20)

Table 1. Optical sensing methods in robot applications. (Perez et al. 2016, pp. 5–19; Rout et al. 2019, p. 34)

Method	Principle	Advantages	Disadvantages
Active vision			
Time of flight	Light travel time	Compact, not affected by ambient light	Inaccurate
Light coding	Deformation of light pattern	High range, can be in motion during capture	Inaccurate, affected by sun light
Laser triangulation	Trigonometry	Compact, robust, accurate, commonly used, real-time	3D measurement requires scanning motion, short range
Structured light	Trigonometry	Accurate, high range, 3D data with a single capture	Large sensor size, static during capture
Passive vision			
2D vision	Single camera	Compact, cheap, commonly used	Error sensitive, depth data cannot be obtained
Stereo vision & photogrammetry	Multi-camera	Accurate, commonly used, high range and field of view	Static during capture, slow processing time, error sensitive

3.2 Laser triangulation

According to Rout et al. (2019, p. 33–35), laser triangulation is by far the most common optical sensing method utilized in robotic GMAW. Laser triangulation sensors are compact, reliable and accurate, and the technology has proven itself in many industrial applications (Pérez et al. 2016, p. 17). Moreover, the method is versatile for a wide range of tasks and applications in robotic welding, and many different joint types, materials and plate thicknesses can be measured with it (Rout et al. 2019, pp. 34–35).

Laser triangulation sensor consists of a laser diode and a camera based on either CCD (Charge-Coupled Device) or CMOS (Complementary Metal Oxide Semiconductor) sensor. Principle of the method and an example of a typical sensor configuration is presented in figure 7. The laser diode projects laser light to the measured surface, which is captured by the camera from a certain angle. The laser light pattern is typically a single stripe, but also other shapes such as circle, triangle or multiple stripes can be used. The desired feature, for example groove shape, gap size or intersection point of two plates, can be recognized and measured based on the deformed laser line shape. A single measurement provides 2D line geometry data of the width and depth, and as the sensor or object moves, the individual lines form a 3D profile. In addition to the camera and laser diode, laser sensors typically have optical filters and protective glass in front of the optics to reduce the issues caused by external lights, dust and spatters. (Hou et al. 2020, pp. 1758–1759; Lin & Luo 2015, p. 2435)

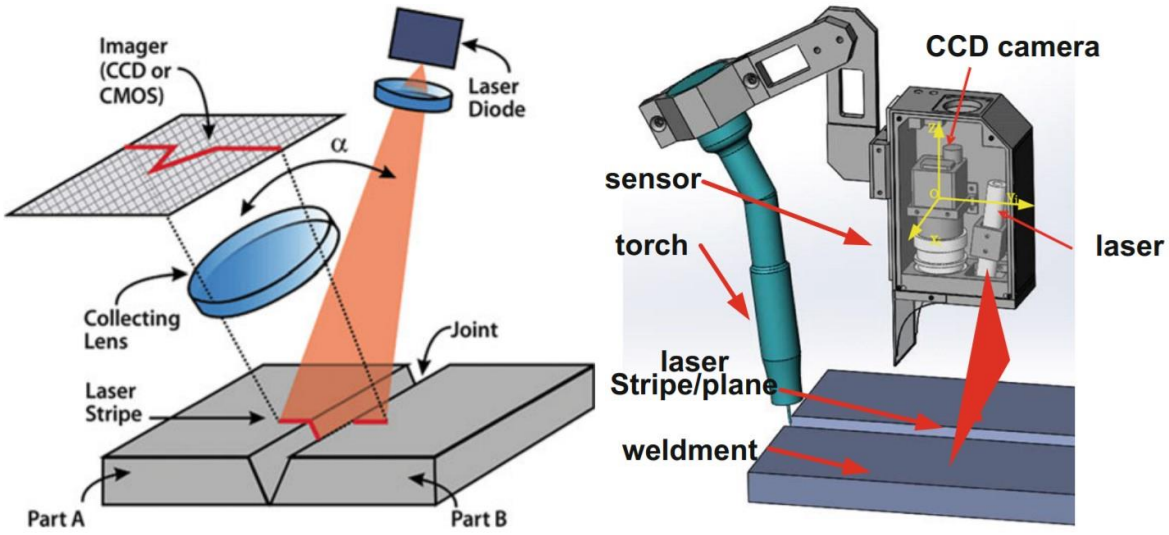

Figure 7. Principle of laser triangulation method (Lin & Luo 2015, p. 2436) and typical sensor structure (Hou et al. 2020, p. 1758).

As only the laser light projection is used for recognizing and measuring the object, it is important to extract the line shape accurately from the image. Disturbances such as arc light, smoke, spatters and reflections cause noise and discontinuities to the image, which can lead to inaccurate and unreliable measurements. This can be tackled by filtering all external lights and redundant noise from the picture with image processing methods. After this, the image can be further processed so that the details are clearly visible, and the laser line can be extracted from the image using different pattern recognition algorithms. One example of this type of image processing procedure for can be seen in figure 8. (Muhammad et al. 2017, pp. 129–136; Gu et al. 2013, pp. 452–454)

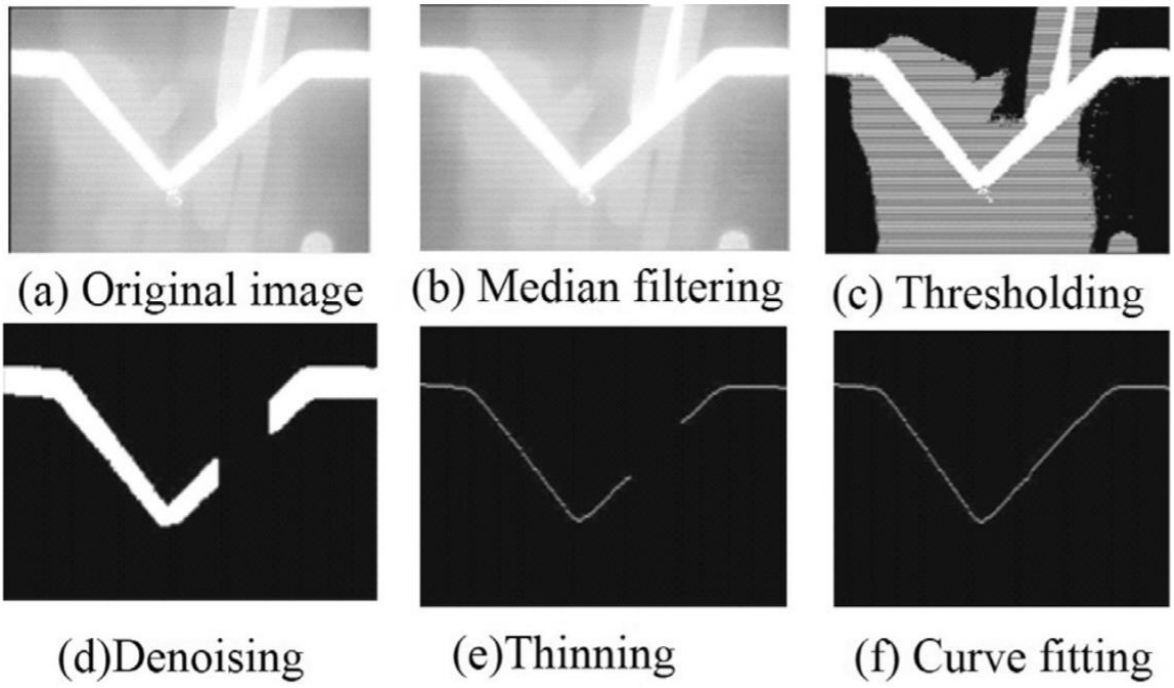

Figure 8. Laser sensor image processing procedure for V-groove. (Gu et al. 2013, p. 453)

After the laser line shape is extracted from the image, the groove shape is identified by extracting the feature points, i.e. the end- and intersection points of the lines. The feature points of some typical joint types are shown in figure 9. As the distance and midpoints between different feature points can be calculated, it is possible to track and measure all the essential dimensions, e.g. groove width, depth, weld bead shape or gap size. (Muhammad et al. 2017, p. 136–142) Commercial laser sensor systems have these image processing- and feature recognition algorithms built into the software, so the end user may just activate the desired features to be measured.

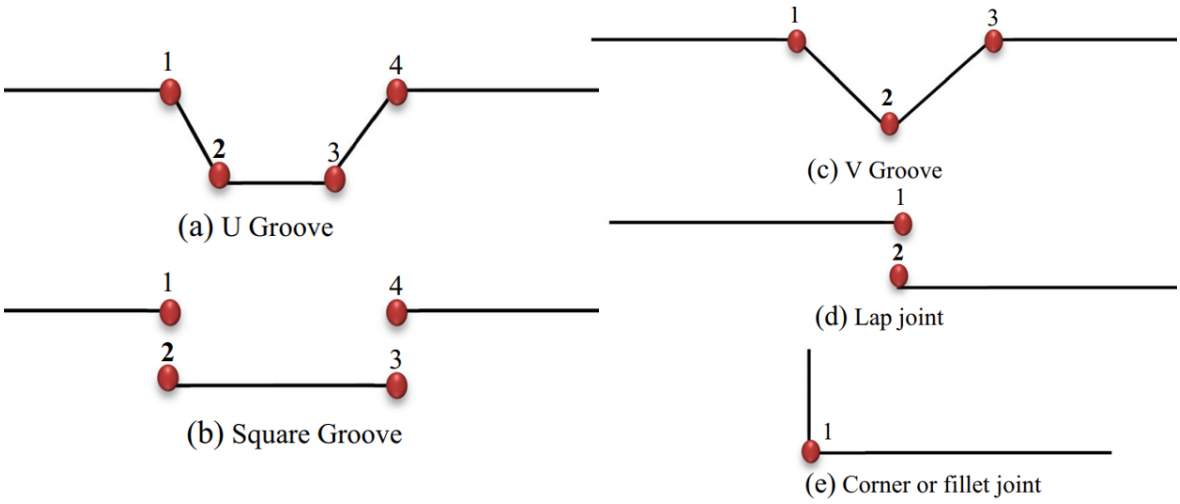

Figure 9. Feature points of typical joint types. (Muhammad et al. 2017, p. 137)

The laser sensor accuracy is dependent on various factors such as camera resolution and quality of the laser beam and optics, and the theoretical accuracy can be as low as few microns. However, typically laser sensors have accuracy in range of 0.01-0.1 mm in practical applications, which is still well sufficient to ensure high weld quality, when the sensor is used for seam tracking and parameter control applications. (Penttilä et al. 2020, pp. 414–415; Rout et al. 2019, pp. 28–34). The measuring range and field of view varies a lot with different laser sensor types, but the maximum measuring distance is typically between 50 and 400 mm, and the maximum scanning width between 20 and 150 mm. (Muhammad et al. 2017, pp. 128–129; Micro-Epsilon 2021, p. 18)

3.3 Optical sensor applications in robotic welding

In the following subchapters, the possibilities and restrictions of optical sensors in seam finding and seam tracking are discussed, and they are compared to the conventional methods used for these purposes. Also, some industrial case examples on how optical sensors are being utilized in flexible robotic welding systems are presented. Other considerable applications for optical sensors in robotic welding are weld pool observation, adaptive process control, quality assurance and visual inspection of welds, but they are not addressed in this review.

3.3.1 Seam finding methods

In robotic welding, the pre-programmed robot path must be adjusted in accordance with the actual seam location due to the cumulative inaccuracies caused by prefabrication, assembly, deformations and workpiece positioning. The seam location and orientation can be detected before welding, which is called seam finding, or during welding, which is called seam tracking. Seam finding technique lacks the real-time control, so heat distortions during welding might still lead to incorrect torch position, but it suits well for short welds. Seam finding can also be combined with seam tracking, in which case only the starting point must be detected before welding. (Zeng et al. 2017, p. 1; Kah et al. 2015, pp. 1-6)

The conventional method for seam finding is touch sensing, either with welding wire tip or gas nozzle. In the method, constant voltage is supplied to the wire or the nozzle, and as it touches the workpiece and the current flows, the robot stops, and the position coordinates are saved. With the touch sensing feature, different types of search functions for detecting edges, planes, points and corners can be created within the robot controller. In a seam finding program, reference points where the surfaces are assumed to be found are given to the search function, and then the searching is done in the required directions. Based on the searches, the shift amount between the pre-programmed path and the actual seam is calculated and the program is corrected. The principle of 2D search function for a lap joint is presented figure 10 as an example. (Gao et al. 2015, pp. 42–46; Yaskawa 2017, pp. 11–14)

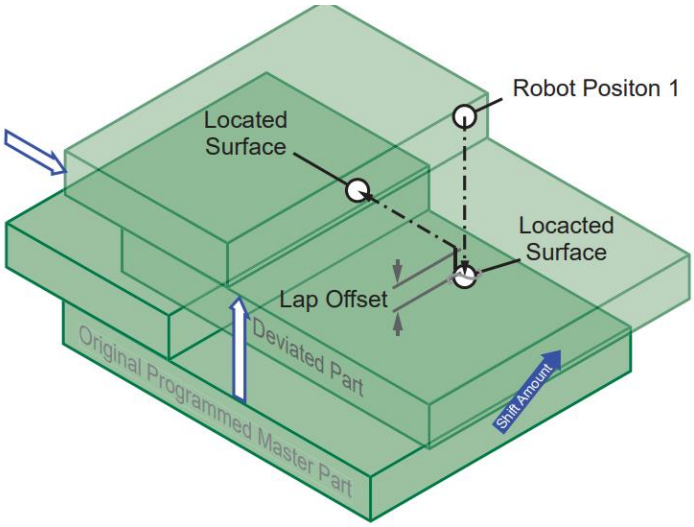

Figure 10. Principle of 2D seam finding of a lap joint. (Yaskawa 2017, p. 12)

Seam finding with touch sensing is sufficient for many robotic welding applications, as it is cheap, simple and does not require bulky sensor near the torch. However, the method is slow, not suitable for all joint types and plate thicknesses, and inconveniences such as bent weld wire and detection delay cause limitations to its accuracy. As can be seen from the figure 11, the same search function principle can be used with 1D laser point sensor, in which case the sensor gives an input signal to the robot controller when it detects the surface at a predetermined distance. Using laser point sensor instead of touch sensing enables faster and more accurate seam finding procedure, as the need to cut the wire after welding is removed, and the search motions can be done with higher speed and from longer distance. On the downside, an external sensor must be attached to the robot, but the accessibility issues can be minimized by using a compact laser point sensor which can be attached to the robot's wrist, as in figure 11. Also, implementation of a laser point sensor in an existing robot system is effortless, since the same control signals and program routines can be used as with touch sensing. (Rout et al. 2021, p. 5; RobotWorx 2018; Yaskawa 2016, pp. 11–16)

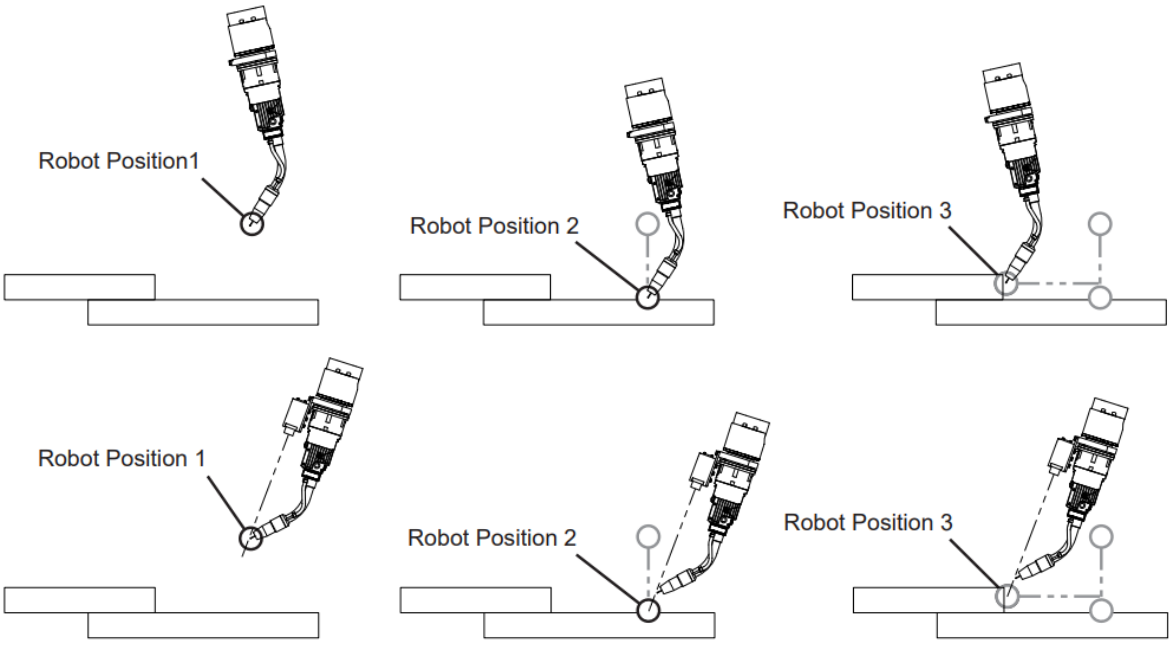

Figure 11. Search motions with touch sensing and with 1D laser point sensor. (Yaskawa 2016, p. 13)

As the regular search functions are not suitable for all joint types and complex weld paths require multiple searches, different vision-based methods for seam finding have been developed. Typical solutions use laser triangulation sensors for detecting and measuring the

seam location, and for calibrating the welding start and end points accordingly. Using a laser sensor enables to locate the seam with a single scan rather than with multiple search motions, and also the groove dimensions can be measured during the seam finding procedure. There are some laser sensor solutions commercially available that are specifically designed for seam finding, and one example is presented in figure 12. Such sensor has a long scanning distance, so it can be attached to the robot's wrist farther from the torch than a seam tracking sensor, so it does not affect the accessibility to the joint as much. (Kah et al. 2015, pp. 5–10; Rout et al. 2021, pp. 1–2)

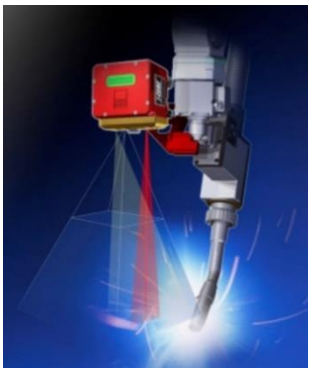

Figure 12. Laser sensor for seam finding. (Servo-Robot 2014)

Seam finding with laser triangulation sensor is suitable for most joint types, but according to Zeng et al. (2017, p. 1), narrow butt joints cannot be detected reliably with the existing solutions. As it is illustrated in figure 13, if the gap is small enough, there is no discontinuity in the captured laser line shape and the joint is not detected.

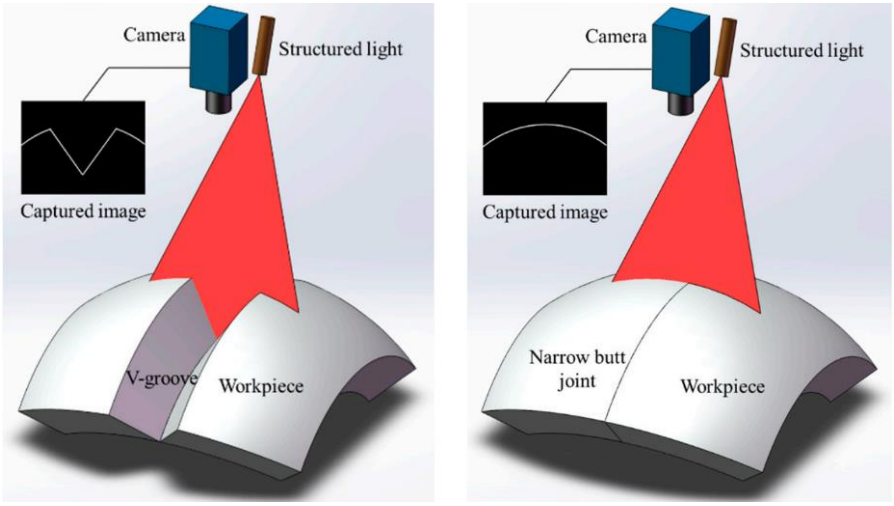

Figure 13. The issue of detecting narrow butt joints. (Zeng et al. 2017, p. 3)

Zeng et al. (2017) solved this problem by combining two different vision techniques in one sensor. The sensor consists of an industrial camera, a led light source and a cross-line laser light source. The different light sources are projected to the surface alternately, and the camera captures images during both periods. The led light source provides uniform lightning to the surface, and as the groove does not reflect the light back, the joint can be detected from the captured 2D image. While the laser light is on, the depth information is obtained with cross-line laser triangulation method. These measurements are then merged, and the 3D geometry data of the seam path is achieved. Reported accuracy of the method is 0.05 mm, and the principle is shown in figure 14 step by step. (Zeng et al. 2017, pp. 3–13)

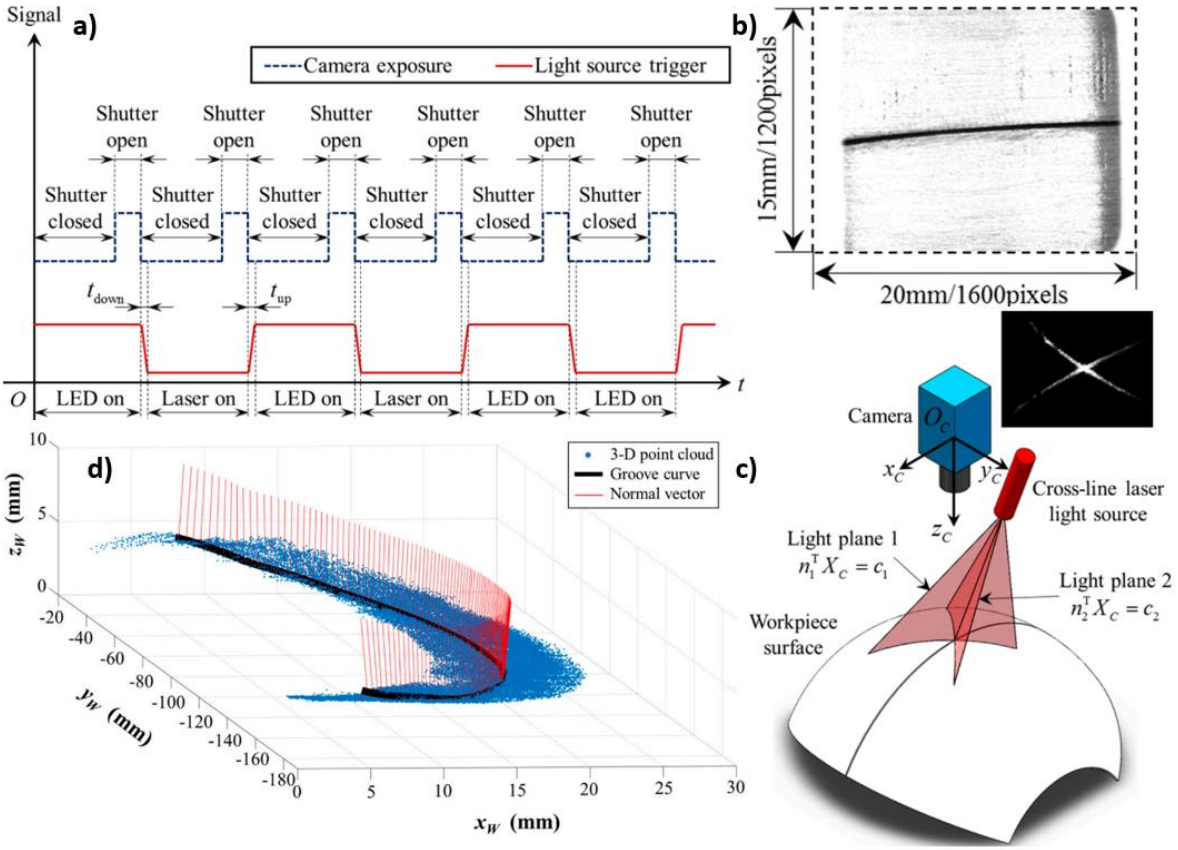

Figure 14. Seam finding of narrow butt joint with dual-action optical sensor. a) Control signal of the sensor light sources b) Received 2D image during uniform lightning c) Cross-line laser measurement to receive the depth information d) Combined 3D position coordinates of the seam. (Zeng et al. 2017, pp. 5–12)

Many studies aim to replace traditional seam finding methods by using different vision techniques to recognize and localise the whole weld seam path before welding. This data can then be utilized for robot program calibration, or even for fully automated program generation. Yang et al. (2020) created a method for automatic seam extraction and robot path planning based on structured light sensor. The sensor consists of a digital light processing (DLP) projector and two CMOS cameras, and its 3D reconstruction principle is shown in figure 15. Scanning of the workpiece results in a 3D point cloud, of which the seam path is recognized, and the robot path planned by using point cloud segmentation and feature extraction algorithms. Finally, the pose of the weld torch is determined by calculating the normal vectors of the weld path. In practical experiments the maximum position error of the torch was 1.9 mm, and the algorithm running time was 4.7 seconds. According to Yang et al. (2020, p. 10), this could be sufficient for industrial applications if seam tracking is used during welding.

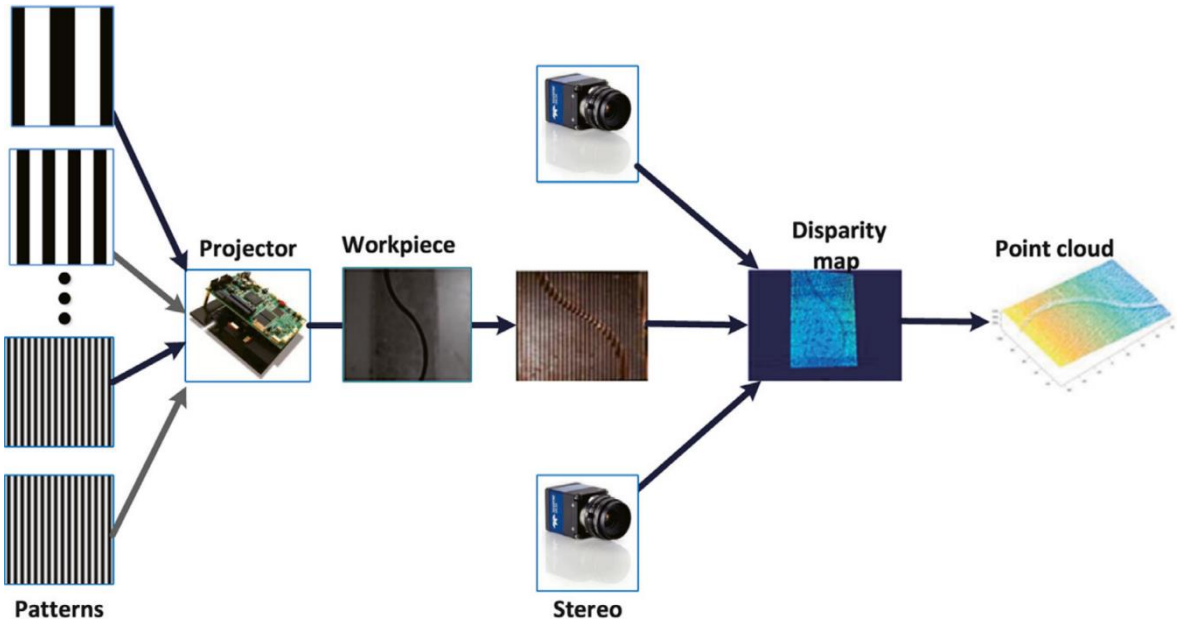

Figure 15. 3D reconstruction of a curved butt joint with structured light sensor. (Yang et al. 2020, p. 4)

Kim et al. (2021, pp. 9703–9705) proposed a novel method for recognizing and measuring the weld path using a 3D vision sensor, which combines 2D colour image and structured light method to obtain the depth information. In the method, the workpiece is measured from different directions and the weld seam is detected from the single 3D images. Then the obtained information is merged with point cloud registration technique to form the complete

weld paths. Although multiple image captures are needed, the view direction can be arbitrary, so the workpiece does not have to be at a specific position or orientation. According to Kim et al. (2021, pp. 9716–9717), the method is suitable for butt-, T-, and lap joints, and multiple seams can be extracted with the same measurements, as shown in figure 16. However, the reported average error in path lengths was 3.4 mm, so seam tracking would be needed to achieve acceptable quality in most applications. (Kim et al. 2021, pp. 9704–9717)

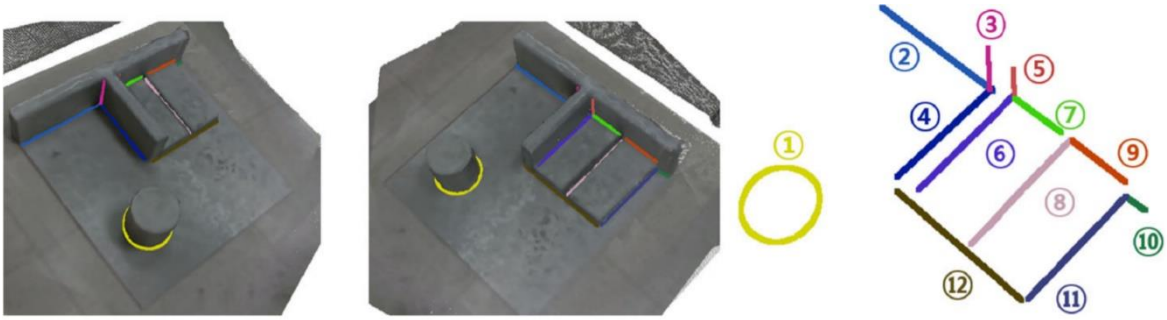

Figure 16. Different types of weld paths extracted using a 3D vision sensor. (Kim et al. 2021, p. 9716)

In the study by Yang et al. (2020), the structured light sensor is operated by the welding robot, and in the study by Kim et al. (2021) it is not stated where the 3D vision sensor is attached to. However, such sensors are often large, and thus cumbersome to use if they are attached to a welding robot, which limits their applicability. Dimensions of the structured light sensor used by Yang et al. (2020) are shown in figure 17 as an example. Therefore, it could be best to mount this type of 3D area sensor to be stationary above the workpiece positioner, or in case of multi-robot welding cell, it could be operated with a separate handling robot.

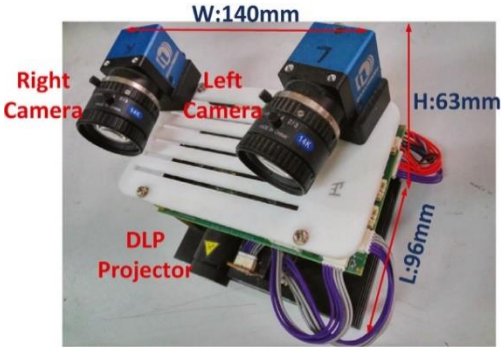

Figure 17. Structured light sensor configuration and dimensions. (Yang et al. 2020, p. 3)

3.3.2 Seam tracking methods

According to Rout et al. (2020, p. 12–13), using sensor technology for seam tracking is often essential for ensuring high weld quality in automated robotic welding. Various types of sensors have been applied for seam tracking purposes, and they can be divided to contact- and non-contact sensors as shown in figure 18. However, other seam tracking methods than arc sensors and vision-based sensors have not been widely adopted in industry. (Rout et al. 2019, pp. 13–14)

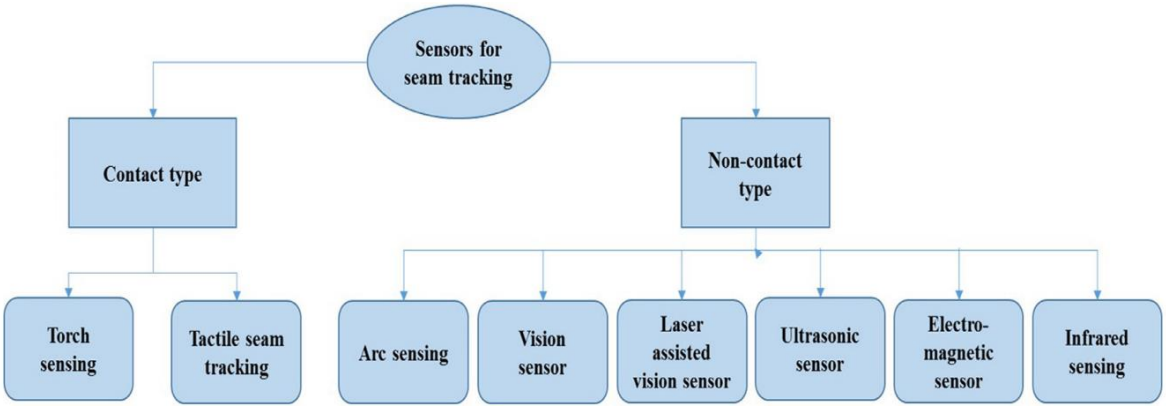

Figure 18. Sensor types that have been utilized in seam tracking. (Rout et al. 2019, p. 14)

The most conventional method for seam tracking is arc sensing, also called through-the-arc sensing. In the method, the robot moves the torch along the seam with a weaving motion, which causes variation to the arc length and thus to the current and voltage. Based on this variation, the tracking algorithm calculates the centerline of the seam and corrects the robot position by giving a voltage signal to the robot controller. This is a simple, cheap and robust method, and there is no need to attach additional equipment to the robot. Although arc sensing is the default solution for seam tracking when it can be used, it has some known drawbacks and restrictions, for example (Kah et al. 2015, pp. 5–6; Rout et al. 2019, p. 34):

- Torch weaving is not suitable for all weld types and processes.
- The method cannot be used reliably for thin sheets (less than 3 mm).
- Tracking can be done only after the arc is ignited, so the starting point cannot be detected.
- Jerking motion and tracking error might occur when there are sudden changes in the weld path.
- Geometric data of the joint cannot be obtained.

Due to the shortcomings in through-the-arc sensing, different optical seam tracking methods have been developed and are commercially available. Majority of the optical seam tracking solutions utilize laser triangulation sensor and feature point recognition method for detecting the seam, which was previously presented in chapter 3.1.1. Many studies that deal with this topic propose different image processing algorithms and feedback control methods, but the general principle of seam tracking with a laser sensor is usually the same, and it is presented in figure 19. The seam tracking algorithm calculates the deviation between the robot position and the detected seam location, and the deviation is converted to a corrective signal which is fed to the robot controller. Since the sensor moves ahead of the welding torch, the corrective motion of the robot can be delayed for the corresponding time. (Rout et al. 2019, pp. 20–29; Lei et al. 2020, pp. 22–25)

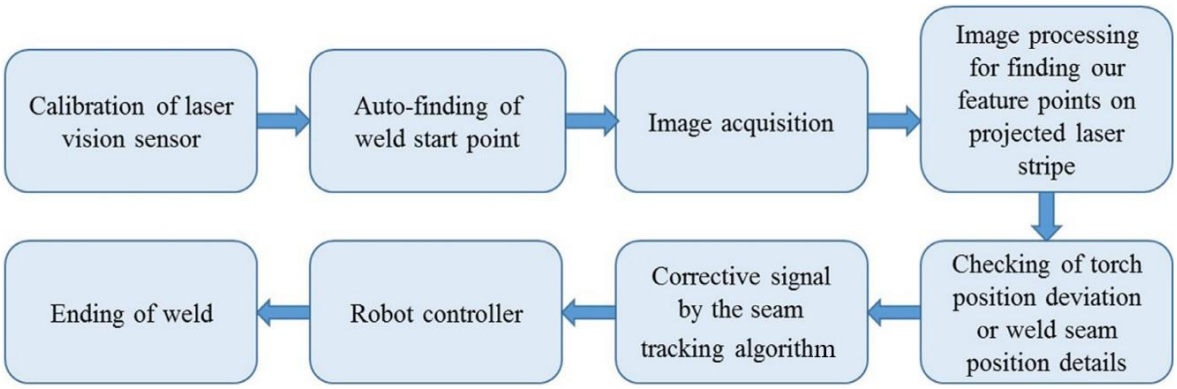

Figure 19. Principle of seam tracking with laser sensor. (Rout et al. 2019, p. 22)

Typical configuration and data flow in robotic welding system with a laser seam tracking sensor is presented in figure 20. The laser sensor sends the raw image data to the computer, which runs the image processing, feature recognition and seam tracking algorithms. Then the digital data is converted to analogue voltage signal which is fed to the robot controller. The voltage signal is always given in certain range, for example ±10 V, and it determines the direction and magnitude of the robot's corrective motion. (Zou et al. 2018, pp. 182–188) In addition, smart sensor solutions with embedded control units are available, in which case an external computer is only needed for running the user interface (Kah et al. 2015, p. 8).

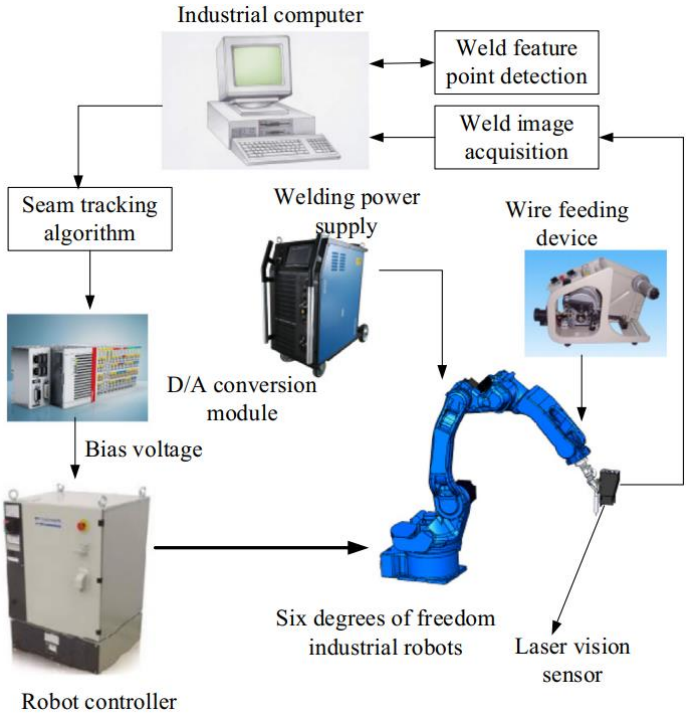

Figure 20. Typical configuration of laser vision sensor based seam tracking system. (Zou et al. 2018, p. 183)

Although seam tracking with a laser sensor is quite widely adopted in the welding industry, a lot of research work is being done to improve the performance and usability of the method. Zou et al. (2018) aimed to make the tracking as real-time as possible by minimizing the distance between the laser stripe and the weld pool. Usually the sensor measures the seam about 50 to 100 mm ahead of the torch, which might lead to tracking errors in some situations, such as on curved weld paths. However, when the distance is smaller, the arc light, smoke and spatters cause more disturbances to the image acquisition, which can lead to tracking failure. The proposed method utilized a laser sensor with three lines instead of one, which increased the reliability of feature point extraction from the noisy image, and the distance between the weld pool and the tracking point could be lowered to 15 mm. The method was verified with welding experiments for curved butt- and lap joints, and the average tracking error was 0.32 mm. The sensor location and the outcome of welding a curved butt joint can be seen in figure 21. (Zou et al. 2018, pp. 182–192)

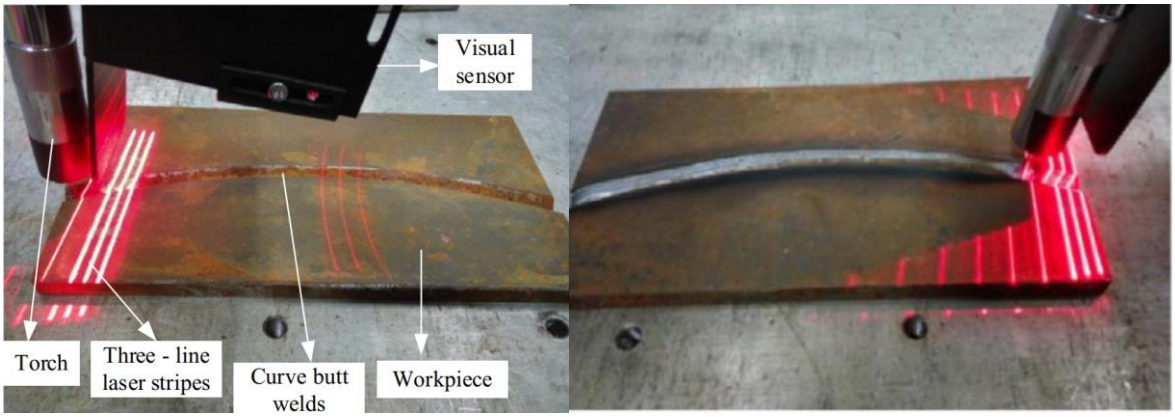

Figure 21. Seam tracking with three-line laser to minimize the distance between the tracking point and torch. (Zou et al. 2018, p. 188–191)

Whereas conventional seam tracking methods are based on correcting the initial weld path that is tought in advance, Hou et al. (2020) proposed a teaching-free method based on real-time path planning and laser sensing. In the method, the robot path must only be programmed so that the laser sensor detects the seam in its field of view. The laser sensor is calibrated in relation to the tool center point (TCP), so as it measures the seam, the correct TCP position for welding can be determined and the robot path can be planned in real-time. The method is enabled with digital control instead of analogue control, and the system schematic is presented in figure 22. (Hou et al. 2020, pp. 1755–1769)

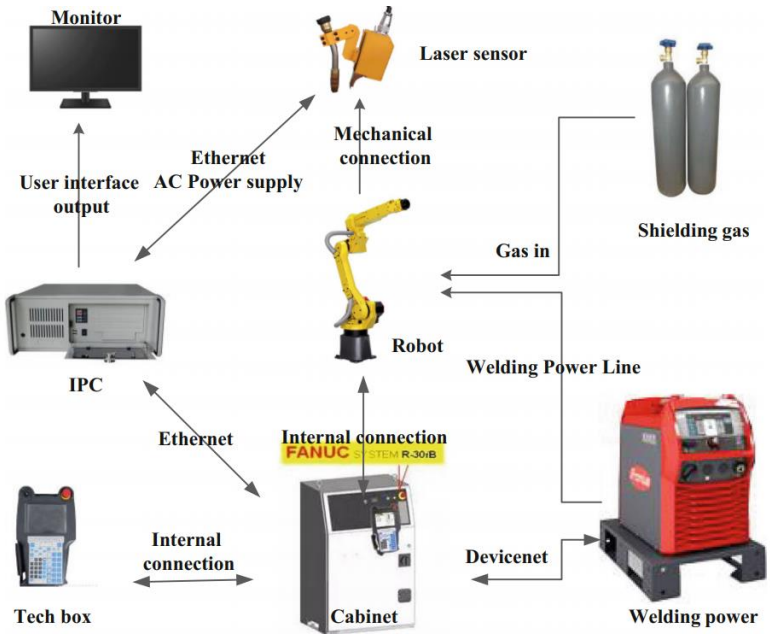

Figure 22. Schematic of digitally controlled welding system for real-time path planning. (Hou et al. 2020, p. 1758)

According to Hou et al. (2020, p. 1757–1758), the information processing center (IPC) communicates with the laser sensor and the robot controller, and it is connected to them via ethernet. The IPC receives the feature point position data from the sensor, converts it to the world coordinate and gives a new target point for the robot. Flow chart of the real-time path planning algorithm is presented in figure 23, where the letter P stands for the detected point and T for the target point. Since the sensor travels in front of the torch, the detected points are saved and given to the robot as target points by following the first-in-first-out principle. Also the identification of the welding start and end points has been taken into account, so that the arc on and arc off commands are executed when the robot stops in the corresponding points. The method was tested by welding straight V-groove and fillet welds and comparing the achieved trajectories to taught weld paths, resulting in maximum tracking error of 0.21 mm. (Hou et al. 2020, pp. 1755–1774)

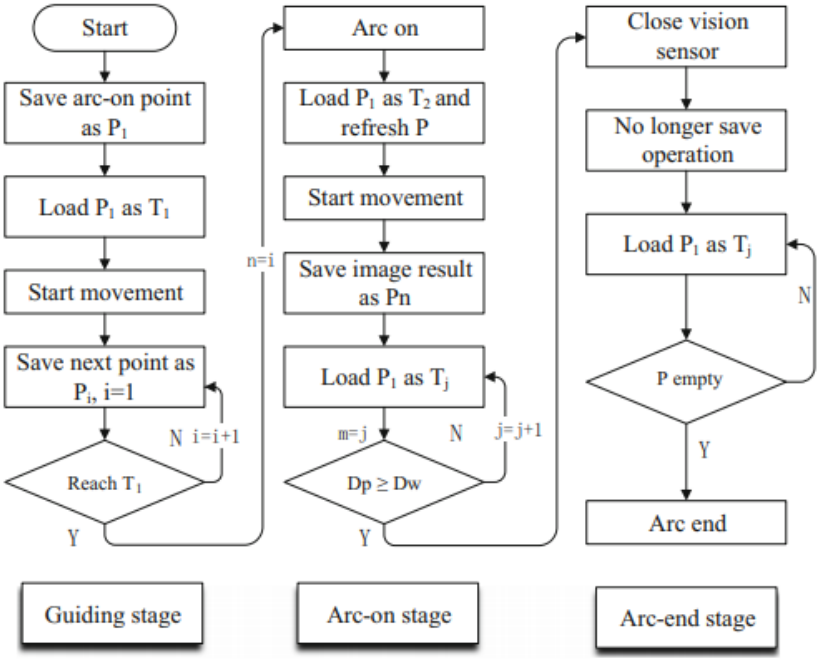

Figure 23. Flow chart of the real-time path planning algorithm. (Hou et al. 2020, p. 1770)

An alternative optical sensing method for seam tracking is based on a passive vision sensor, i.e. a CMOS or CCD camera without a separate light source. In the method, the camera captures the welding process directly, which results in a 2D image such as shown in figure 24, and the tracking is based on the deviation between the weld pool centerpoint and weld seam centerline. Optical filters, which let only light of a certain wavelength through, are used in front of the camera to remove the arc light noise from the image. This enables to

extract the weld pool and weld seam geometries by using different image processing and edge detection techniques. (Xu et al. 2017, pp. 18–22; Lei et al. 2020, pp. 17–27)

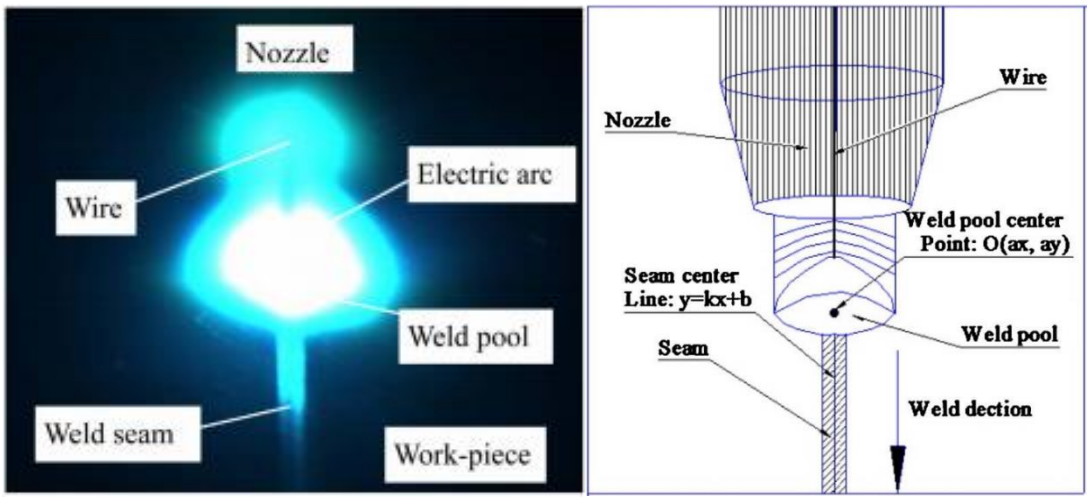

Figure 24. Welding process image of which the weld pool and weld seam features are recognized in passive vision tracking. (Xu et al. 2017, p. 22)

Xu et al. (2017) developed a passive vision sensor unit, software and control algorithm for seam tracking. The sensor unit consisted of two CCD cameras with a dimmer glass, a 660 nm narrow-bandpass filter and a protective glass in front of the optics, and the sensor was attached to the wrist of the robot, as shown in figure 25. The proposed method is suitable for different type of butt joints, but also for fillet welds, which are typically challenging to track with a passive vision sensor. Accuracy of the method was tested with straight joints, and the real-time capability was verified by moving the workpiece randomly during welding. The maximum tracking error was 0.21 mm for static workpiece, and 0.45 mm in case of moving workpiece. (Xu et al. 2017, pp. 19–29)

Figure 25. Seam tracking with a passive vision sensor. (Xu et al. 2017, p. 19)

According to Xu et al. (2017, p. 18), the main benefits of passive vision sensors are that the equipment is cheap, and the tracking is truly real-time since it is based on the weld pool position in relation to the groove. However, the method is more error sensitive and not as versatile when compared to laser sensing. Moreover, using passive vision for controlling the torch height is challenging, because in order to receive the depth information the welding process must be captured with two cameras from different angles. This makes the system more complex and cumbersome as the sensor size increases and the image processing requires more computing power. Therefore, the use of passive vision method is highly situational, and it is not usually proposed as a universal solution for seam tracking. (Rout et al. 2019, pp. 16–20; Lei et al. 2020, pp. 12–19)

Based on the reviewed studies, laser triangulation sensors provide the best features for seam tracking among optical sensing methods, as they are accurate and reliable in production environment. It is also seen as a significant merit that the laser sensor data can be used simultaneously for adaptive process control and seam tracking, and the sensor can be used for a variety of other tasks. On the other hand, passive vision sensors are economical and provide real-time tracking, so they may be more suitable solution in some applications. However, optical sensors in general have some drawbacks that limit their usability in industrial applications, such as (Kah et al., 2015, pp. 5–6; Rout et al., 2019, pp. 20–34):

- Technical integration of the sensor system can be complex.
- The sensor must be attached near the weld torch, which causes restrictions to accessibility.

- One robot axis is locked during seam tracking, as the sensor must travel in front of the torch.
- Disturbances during welding caused by the arc light, spatters, smoke and reflections can lead to tracking errors.

3.3.3 Case examples of optical sensor utilization in industrial applications

This chapters presents some examples on how optical sensors can be used in advanced robotic welding systems. So far, optical sensors have been adopted mostly in high volume production in e.g. seam tracking or parameter control applications to ensure the weld quality in varying circumstances. However, it has become increasingly more popular to use them to increase the flexibility of the robotic system, without sacrificing high level of automation. Characteristic use case has high production volume of similar welded products, where the use of optical sensors enables to do modifications to the product with no need to re-configurate the manufacturing system. This type of optical sensor solutions could be utilized also in development of flexible and jigless multi-robot welding cells for small batch production.

Tavares et al. (2019) utilized optical sensors in development of a semi-automatic robot cell for beam attachment welding, which functions with human-robot collaboration principle. The system configuration and operation steps can be seen in figure 26. Two different vision systems are utilized in the system, SAR (spatial augmented reality) hardware which is located in the gantry, and a laser seam finding sensor which is attached to the robot. The SAR hardware includes an industrial camera and a long-range green laser projector, and it is used for calibrating the beam position in relation to the CAD model. After calibration, an assistive laser light is projected to the beam to visualize the correct position for the attachments, which are then tack welded by manual welder. Finally, the tack welded beam attachments are welded by the robot, which first uses its laser sensor for seam finding and path calibration. (Tavares et al. 2019, pp. 1–11)

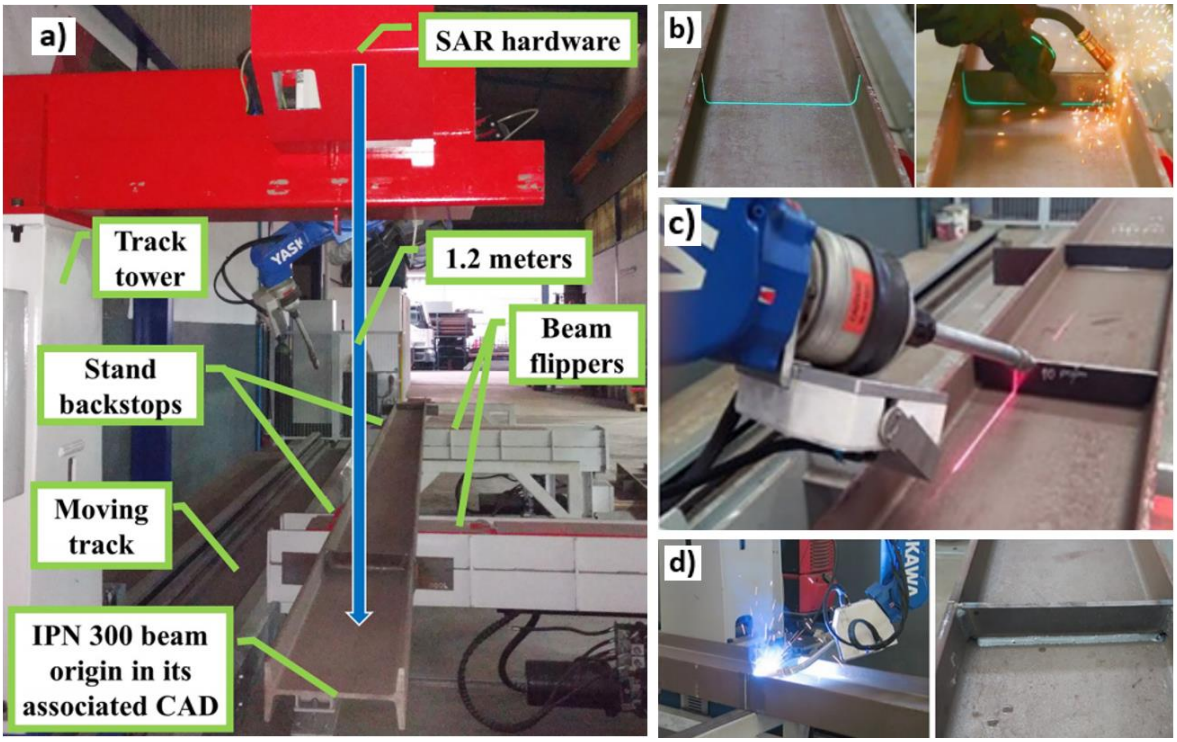

Figure 26. a) Beam welding system configuration b) Assistive laser projection for manual tack welding c) Seam finding with a laser sensor d) Final welding. (Tavares et al. 2019, pp. 4–8)

Robotic systems for beam attachment welding are also commercially available as a turnkey solution. Austrian company Zeman provides fully automatic multi-robot welding cells for beam attachment assembly, which are capable of welding different types of components to the common structural beam profiles. Their welding cell solutions consists of gantry-mounted welding robots equipped with laser sensors, and track-mounted handling robots with magnetic grippers. As can be seen from figure 27, the welding cell functions with the jigless welding principle, and the procedure goes as follows (Zeman 2021):

1. The main beam is clamped by the workpiece positioner.
2. Workpieces to be attached are placed randomly on a conveyor, where they are measured with a static laser scanner mounted above the conveyor.
3. The scanning result is compared to the 3D model, and based on that the handling robot is able to grip the workpieces accurately and in correct orientation.
4. The welding robot measures the location for the attachment with its laser sensor.
5. Based on the measurement, the handling robot positions the workpiece and holds it in place during tack welding.

6. The welding robot finds the seam with its laser sensor and starts tack welding.
7. After all attachments are tacked, the welding robot proceeds to final welding.

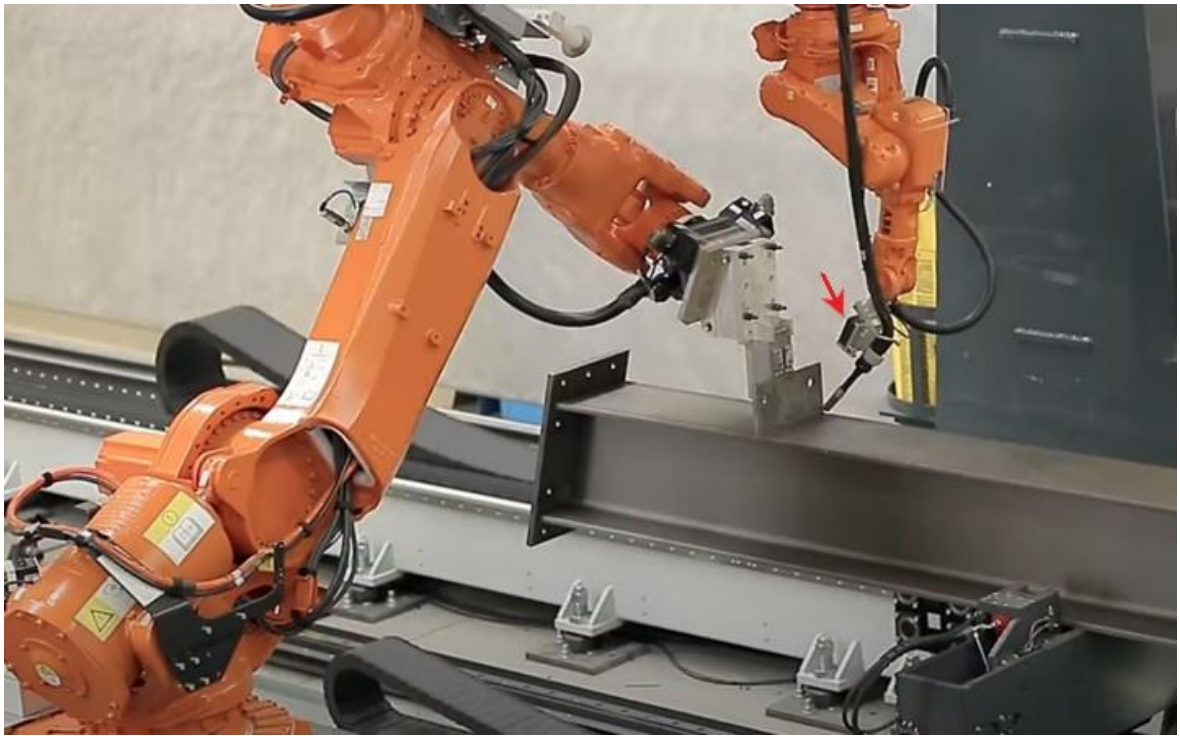

Figure 27. Jigless welding of beam attachments. The red arrow shows the laser sensor location. (Zeman 2021)

Tuominen (2016) presented a novel concept of a measurement-aided welding cell (MAWC) for the automotive industry. The purpose of MAWC is to replace the dedicated welding lines in manufacturing of car body and chassis components with flexible multi-robot welding cells. The MAWC consists of a welding robot and two handling robots with adaptive and interchangeable grippers. The concept uses photogrammetric multi-camera technique for the measurements, and thus the whole welding cell is surrounded with cameras from different directions. The photogrammetric measurements are used to guide the handling robots in workpiece positioning, calibrate the weld path and measure the final product dimensions. The layout design of MAWC is presented in figure 28, and its operation principle for one cycle is the following (Tuominen 2016, p. 371–383):

1. Handling robots grip components from the conveyor and position them in pre-programmed location.
2. Cameras measure the component positions.

3. Handling robots corrects their position based on the measurement.
4. Cameras measure the component positions.
5. Welding robot adjusts its path and performs the welding operation.
6. Cameras measure the final dimensions of the product.

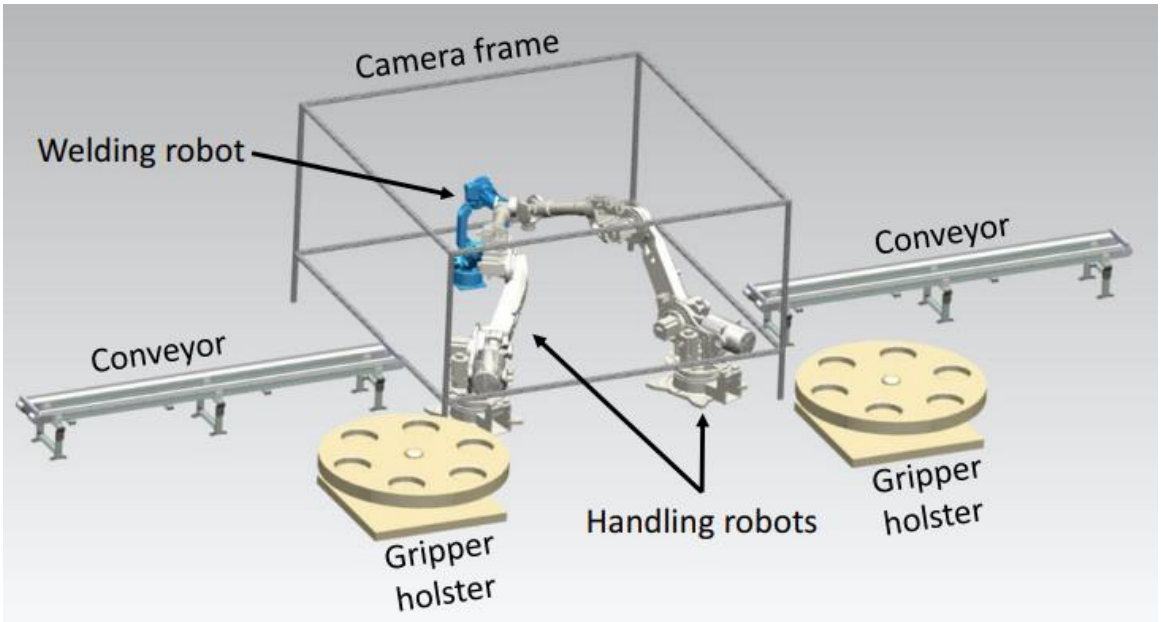

Figure 28. Layout design of MAWC for automotive industry. (Tuominen 2016, p. 374)

A Finland-based welding automation company Pemamek provides vision assisted robot welding portals for welding different type of panels in shipbuilding industry. Their solutions are based on large 3-axis gantries with one or more welding robots, and they utilize vision-based method for robot program generation. Prior to the welding, the panels are scanned with a 3D vision camera which is located in the gantry above the robot, and the scanning result is exported to an offline- programming software. Based on the scanning, the weld paths are determined, and the robot program is created in the software. Thus, the workpieces do not have to be in a predetermined position in the robot's working area. The final path calibration is done by touch sensing and through-the-arc seam tracking by default. This type of a welding portal solution for micro panel welding is shown in figure 29 as an example, where the camera location is marked with the red arrow, and the green area visualizes the field of view of a single scan. (Pemamek 2021)

Figure 29. A vision assisted welding portal for micro panel welding in shipbuilding industry. The camera location is marked with the red arrow, and the green area visualizes its field of view. (Pemamek 2021)

3.4 Summary of the reviewed studies

Based on the review, laser triangulation is the primary vision method utilized in robotic welding applications, and most tasks in multi-robot welding cells can be covered with different variations of laser sensors. 3D camera systems, typically based on structured light method, seems to be an interesting emerging technology for seam recognition, program generation and robot guidance. Passive vision systems can be utilized in certain well-defined tasks, but they do not provide the same flexibility and reliability as active vision methods.

Findings of the reviewed studies and case examples are summarized in table 2. It should be noted that the reported accuracies are not necessarily comparable with each other, due to different testing methods and circumstances. It is also mentioned that where the sensor is mounted to in the system, as it has a critical effect on the usability of the sensor in industrial applications, considering accessibility and reachability limitations.

Table 2. Summarization of the reviewed studies and case examples.

Author	Application	Vision method	Sensor location / Accuracy / Else
Zeng et al. (2017)	Seam finding of narrow butt joints	Combined 2D vision and cross-line laser sensor	Close to torch / 0.05 mm
Yang et al. (2020)	Seam recognition and weld path extraction based on 3D point cloud	Structured light sensor with two cameras	Robot's wrist / 1.9 mm
Kim et al. (2021)	Recognition and path extraction of multiple seams with single image captures	3D vision camera based on 2D color image and structured light method	Not specified / 3.4 mm
Zou et al. (2018)	Seam tracking based on corrective analogue signal	3-stripe laser sensor, measurement point close to the weld pool (15 mm)	Close to torch / 0.32 mm
Hou et al. (2020)	Seam tracking based on real-time path planning	Laser triangulation sensor	Close to torch / 0.21 mm
Xu et al. (2017)	Seam tracking based on weld pool imaging	Passive vision sensor	Robot's wrist / 0.45 mm
Tavares et al. (2019)	Semi-automatic beam attachment welding based on augmented reality and human-robot collaboration	Laser sensor for seam finding, SAR hardware for part calibration and assistive light projection	Robot's wrist / SAR camera apart from the robot
Zeman (2021)	Fully automatic beam attachment welding with jigless welding principle	Laser sensor, used for workpiece positioning and seam finding	Robot's wrist / Part scanning with separate sensor
Tuominen (2016)	Vision- aided welding cell for flexible car body and chassis manufacturing	Multi-camera system based on photogrammetry	Multiple cameras surrounding the welding cell
Pemamek (2021)	Vision- based robot programming for panel welding	3D vision camera	In gantry above the robot

4 LASER SENSOR INTEGRATION TO THE MULTI-ROBOT WELDING CELL

This chapter presents the practical methods for implementing the laser sensor in the LUT welding laboratory's multi-robot welding cell. The central problem is that the laser sensor system that is being integrated does not have built-in features for robotic welding tasks, and the measurement data cannot be transferred digitally to the robot controller. Therefore, all the same functions that laser sensors provide in modern robotic welding systems cannot be realized. The following subchapters presents the system configuration of the multi-robot welding cell, and the operating principle of the developed methods for seam finding, seam tracking and handling robot guidance. Finally, practical tests are conducted to investigate the accuracy and to verify the usability of seam finding and -tracking with the laser sensor.

4.1 System specification of the multi-robot welding cell

The LUT welding laboratory's multi-robot welding cell is shown in figure 30. It is developed to be capable for jigless welding, so that the handling robot brings parts to be tack welded one by one to the workpiece positioner. The cell layout is based on Yaskawa Motoman robots, and the system configuration is the following:

- Welding robot (EA1900N)
    - Mounted on a floor track
    - Laser sensor attached to the weld torch
- Handling robot (ES165N)
    - Mounted on a floor track
    - Custom-made magnetic gripper
- Skyhook- type workpiece positioner (MT1-1000 S2X)
- Two NX100 robot controllers (paired)
- Laser line triangulation sensor (Micro-Epsilon Scancontrol 2960-50)
- GMAW power source (Kemppi A7)
- External computer
    - Laser sensor software (Scancontrol Configuration Tools 6.1)
    - Communication interface for robot controller (MATLAB & MotoNIS)
    - Welding management software (Kemppi Weldeye)

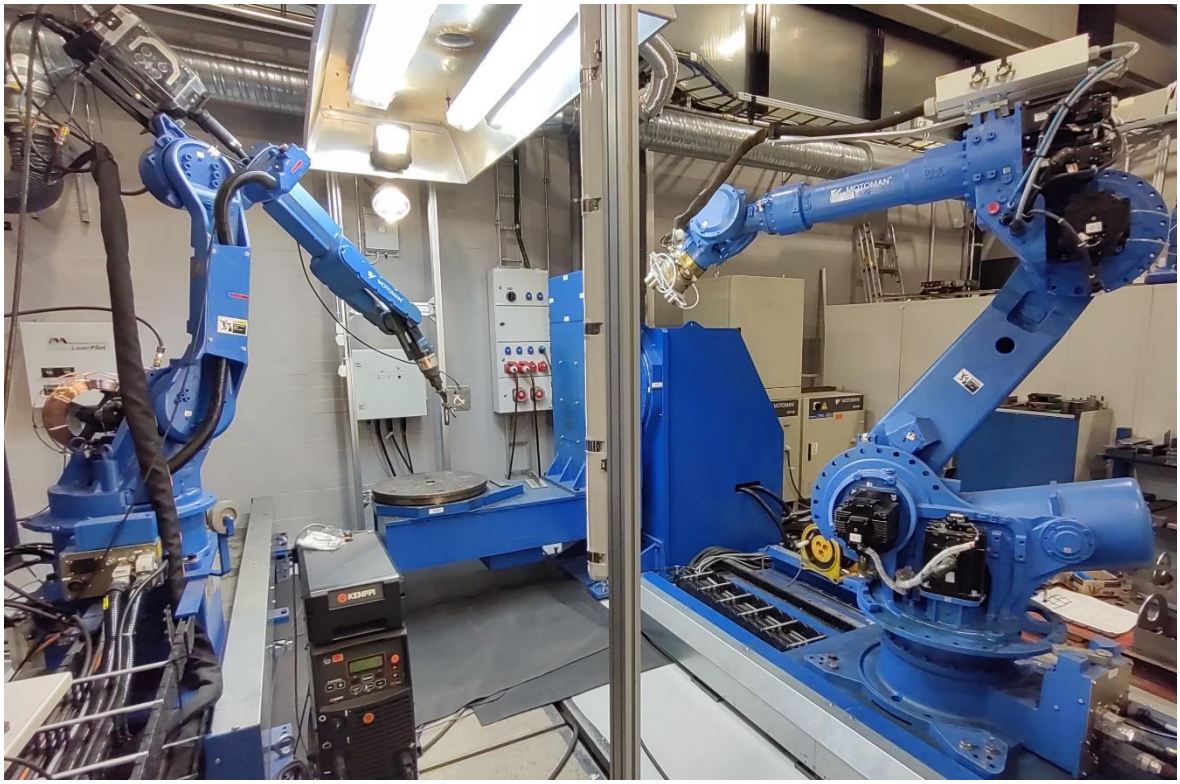

Figure 30. Multi-robot welding cell of the LUT welding laboratory.

Information flow in the welding cell is presented in figure 31. The system is based on two NX100 controllers, but they are paired so that the communication is carried out by only one of them. NX100 is an older generation robot controller, introduced in year 2004. It supports digital I/O (input/output) signals which function with on/off principle, and eight input channels for monitoring analog signals in voltage range of ±10 V. Measurement data of the laser sensor is transferred via ethernet to an external computer with the laser sensor software, where the measured features and output settings are determined. The data is then transferred to the robot controller through a sensor output unit, which has terminals for both digital and analog control signals. The computer is also connected to the welding power source and the robot controller via ethernet. The Kemppi Weldeye welding management software records the welding parameters and enables to fully control the power source with the computer. Communication interface between the computer and robot controller is implemented in MATLAB programming environment by utilizing MotoNIS communication tool, and it was developed in master's thesis by Haapala (2020). It can be used, for example, for giving instructions to the robot station and for reading the robot position and laser sensor data.

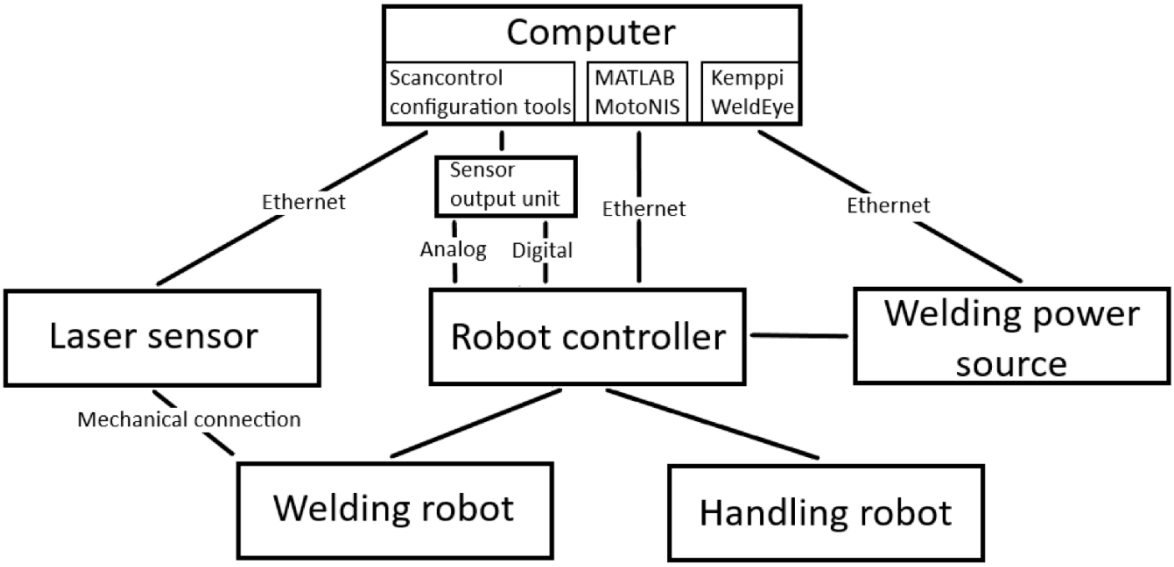

Figure 31. Information flow of the multi-robot welding cell.

The integrated laser sensor is Micro-Epsilon Scancontrol 2960-50, which is based on laser line triangulation method. It is a smart sensor, which means that the profile analyzing is done within the sensor unit. The sensor is suitable for a variety of industrial measurement tasks, e.g. quality control and process parameter optimization. However, it is not specifically designed for robotic welding applications. Table 3 shows the relevant technical data of the sensor. More detailed dimensions of the sensor unit and its measuring range can be seen in appendix I.

Table 3. Technical data of Micro-Epsilon Scancontrol 2960-50. (Micro-Epsilon 2021, p. 18)

Outer dimensions of the sensor	96x85x33 mm
Start of measuring range (minimum distance)	65 mm
Middle of measuring range (nominal distance)	95 mm
End of measuring range (maximum distance)	125 mm
Width of scanning range (depends on the distance)	40–60 mm
Points per profile (resolution of x-axis)	1280
Reference resolution of z-axis (depth)	0.004 mm
Maximum profile frequency	2000 Hz

The sensor is attached to the welding robot with a 3D printed bracket as shown in figure 32. The sensor is located so, that when the welding wire tip (TCP) is at optimal welding position and the torch angle is zero, the sensor measures the seam at a distance of 95 mm, which is in the middle of its measuring range. In welding direction, the measured point is 100 mm ahead of the torch. To reduce disturbances, there is also an additional cover plate under the sensor that prevents direct line of sight to the weld pool and arc.

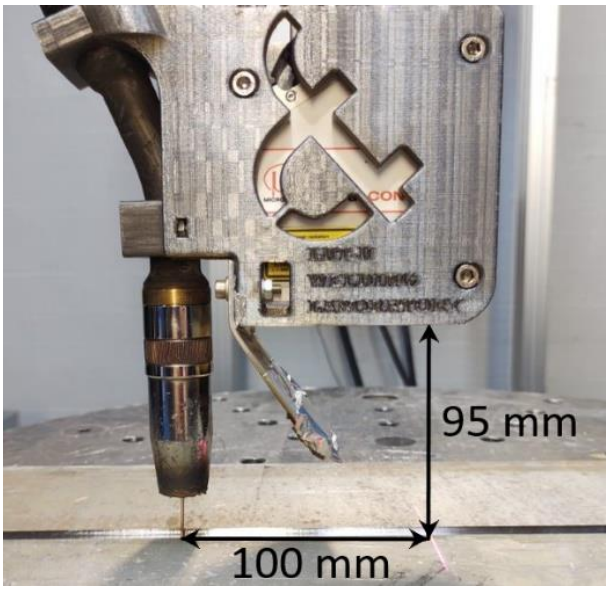

Figure 32. Sensor mounting to the torch and the location of measurement point.

The laser sensor software is Scancontrol configuration tools 6.1 by Micro-Epsilon. The software has built-in programs for measuring different types of features, such as points, gaps, angles and surfaces. The existing programs can be combined to achieve the desired result and output, and the measurement result, i.e. what the sensor sees and what features are detected, is visualized in the software. The sensor system has several digital and analog output ports, and the settings and logic of each port can be modified freely. Also, various sensor settings and parameters can be adjusted, for example camera exposure time, frame rate, region of interest and result filtering. In figure 33 is a screenshot of the main menu, where can be seen the program selector and the different tabs of the software. (Micro-Epsilon 2020, pp. 6–17)

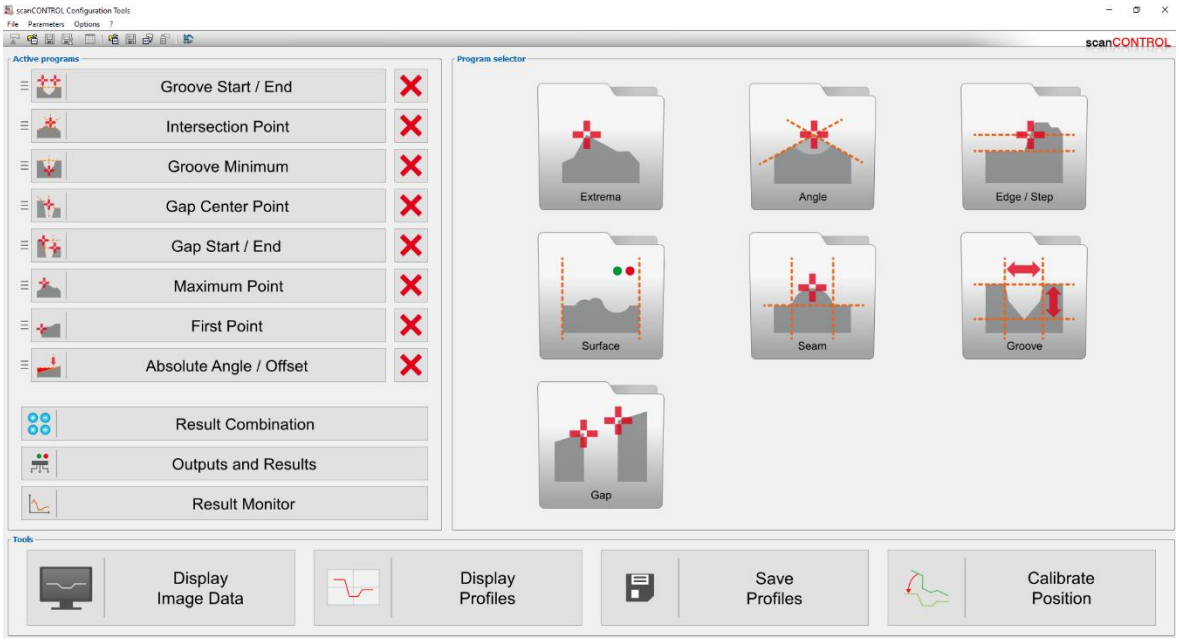

Figure 33. Main menu and program selector of the Scancontrol configuration tools-software.

4.2 Implementation of the laser sensor functions

The NX100 robot controller does not enable to utilize the laser sensor measurement data directly as a correction value for adjusting the robot path. There is also no way to calibrate the relation between the TCP and the features that the laser sensor is measuring. Thus, the communication between the sensor and the robot must be done by using the same control signals and program routines as with touch sensing and through-the-arc seam tracking. Principle of the developed methods for seam finding, seam tracking and handling robot guidance are presented in the following subchapters.

The robot programs are done by online- programming with manual teach pendant. The programming language is called “INFORM”, which is used in most robot controllers by Yaskawa. A single line of the programming language consists of an instruction for the desired operation, and of additional data which specifies e.g. the speed or time of the operation. The INFORM language includes various instructions which are used for creating the robot path, and for controlling the process, I/O and position variables. Also mathematical and logical operations, such as “ADD”, “AND”, “OR” “ELSE” and “IF” can be performed. As an example for the basic instruction, table 4 explains the structure of a simple welding

program, in which seam finding and seam tracking functions are utilized. (Yaskawa 2017, pp. 8–14)

Table 4. The structure of a simple welding program with INFORM programming language.

Row	Instruction	Explanation
0001	MOVJ VJ=100.0	Joint move instruction, 100% joint speed
0002	REFP 3	Sets reference point 3 for search function
0003	REFP 4	Sets reference point 4 for search function
0004	CALL JOB: 1DSRCH	Call for a subprogram to conduct 1D search
0005	MOVL V=50.0	Linear motion towards arc-on point, 50 mm/s speed
0006	TIMER T=2.00	2 second timer before welding starts
0007	ARCON	Arc on
0008	ACORON	Seam tracking on
0009	MOVL V=7.0	Linear motion, 7 mm/s speed during welding
0010	ARCOF	Arc off
0011	ACOROF	Seam tracking off
0012	TIMER T=1.00	1 second timer before departure
0013	MOVL V=100	Departure with linear motion, 100 mm/s speed
0014	END	

4.2.1 Principle of seam finding programs

Due to the limitations set by the controller, seam finding with the laser sensor is performed with the same search function principle that was presented in the literature review in chapter 3.3.1. In the method, searches are performed for each direction in which the correction is to be made, and the search results can be combined to a single correction value. This method is typically used with touch sensing or 1D laser point sensor, but although now it is carried out with the laser line scanner, different surfaces must be measured separately instead of scanning the joint. Thus, the laser sensor is basically used as a one dimensional distance sensor, which triggers an output signal when it detects the surface at a predetermined value.

Principle of the laser sensor for search function and output settings in the sensor software can be seen in figure 34. Digital output port 3 is used for this purpose, which corresponds to direct input port 3 in the robot controller. The selected program measures the maximum value in z- axis, i.e. closest detected distance to the object. Coordinate system of the laser sensor is reversed, so the z-axis value increases as the sensor moves closer to the object. The digital output signal turns on/OK, when the z- axis value exceeds 60 mm, which corresponds to 130 mm distance from the object. The minimum limit value is set at 200 mm, which is outside of the sensor's measuring range, so the output signal remains on as long as the value is over 60 mm. These settings can be modified in different ways, which can be beneficial in some seam finding tasks. For example, the logic for the output signal can be inverted, or the signal can be set to remain on at only certain value range. However, these settings and the same output port were used in all presented search programs.

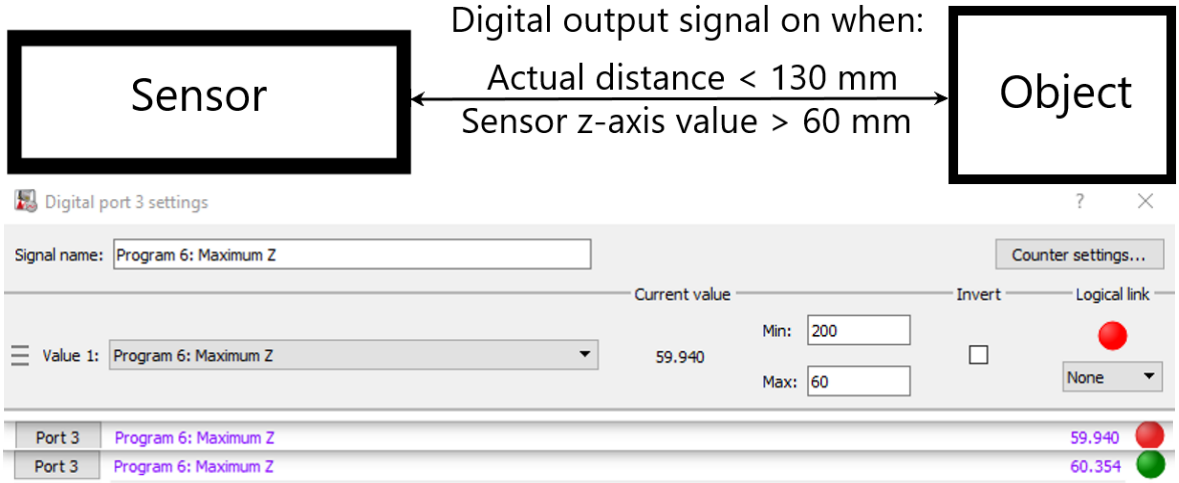

Figure 34. Principle and settings of the digital output port. The output signal turns on as the sensor moves closer to the object, and maximum z- axis value exceeds 60 mm.

Based on the search function principle, seam finding programs for different purposes can be constructed. However, the controller has already existing touch sensing programs provided by Yaskawa. These programs can be utilized also with the laser sensor simply by changing the input port that the search function checks. There are many program variations, mostly for lap- and T-joints, but the programs that are implemented during this work are a 1D search program, and a 3D seam finding program for correcting the corner point of a T-joint.

The structure of the 1D search program can be seen in appendix II, where the function of each instruction is explained. The program calculates the deviation between the detected point and a pre-set reference point, at which the surface is assumed to be detected. The calculation is done by using position variables, that contain the position coordinates and tool angles in the selected coordinate system. All other seam finding programs follow the same principle as the 1D search program, only difference is that more searching motions and position variable calculations are involved. The 3D seam finding program for detecting the starting point from a T-joint can be seen in appendix III. Figure 35 shows an example of position variable data after the 3D seam finding program is executed. The position variable includes the shift value for corrective motion in each direction (X, Y, Z). Tool rotation angles (Rx, Ry, Rz) are set to zero, as only the position of the robot is being corrected.

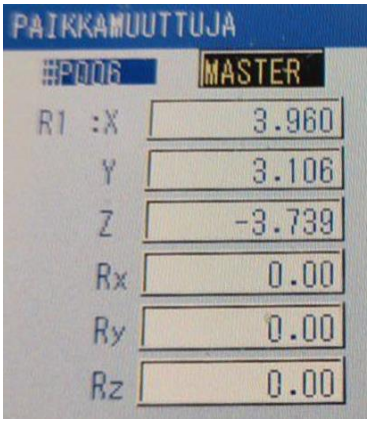

Figure 35. Shift value in position variable P006 after executed 3D seam finding program. Picture taken from the robot teach pendant.

The instructions that are used to construct seam finding programs are presented and explained in table 5. The purpose of most of them is to operate and modify different forms of position variables. The data flows inside a seam finding program as follows. First, the controller saves the reference point as a system variable, which stores the robot position in pulse data form. System variables cannot be utilized directly in robot programs, but they can be saved as a user variable with “GETS” instruction, and then the pulse data can be converted to a desired coordinate system with “CNVRT” instruction. During search function, the robot moves towards the reference point, until the direct input port turns on and the robot stops. At this point, the current position of the robot is saved and converted to a position variable. The desired shift value can be calculated with the different position variables to a single

variable by using “SUB” and “ADD” instructions. Finally, the resulting position variable is run with “SFTON” instruction to make the correction to the robot path. (Yaskawa 2014, pp. 30–42)

Table 5. Instructions used in the search programs. (Yaskawa 2014; Yaskawa 2017)

Instruction and example		**Explanation**
REFP SREFP	REFP 2 SREFP 4	Reference point for search function. REFP pulse is saved as a specific system variable based on the type and number (e.g. REFP 2 -> $PX012, SREFP 4 -> $PX024)
GETS	GETS PX001 $PX024 GETS PX006 $PX000	Saves system variable as a user variable. PX is a position variable group which include position data for all robots in the control group. (e.g. PX001 include P001 and EX001) Used for saving reference points and searching results.
CNVRT	CNVRT PX001 PX001 MTF	Converts position variable group from pulse data to cartesian data in desired coordinate system (MTF=master tool coordinate, BF=base coordinate).
SRCH	SMOVL P001 V=5.0 SRCH RIN#(3)=ON T=0.30 DIS=60	Linear searching motion towards P001 (REFP) until input signal is on, then stops the robot. Format: MOVL<Position variable> V=<speed> SRCH RIN#(Direct IN port number)=<Status ON/OFF> T=<delay time for input check> DIS=<Max. searching distance in mm>
SETE	SETE P003 (4) 0 SETE P003 (5) 0 SETE P003 (6) 0	Sets data to position variable. Used to clear the tool angles. Format: SETE <Position variable> (Axis no.) <Value> 1=X, 2=Y, 3=Z, 4=Rx, 5=Ry, 6=Rz
SUB	SUB P006 P001	Subtracts position variable P001 from P006
ADD	ADD P006 P001	Adds position variable P001 to P006
SFTON	SSFTON P006	Shifts the robot path based on value in P006, starting from the next move instruction.
SFTOF	SFTOF	Ends the active shift operation

The seam finding programs are constructed so, that they do not need to be modified in creation of new welding programs. The suitable seam finding program is called in the main job, and the searching paths are determined with reference points which are set before the call instruction. Setting of the reference points depends on the used program. For example, 1D search program requires only two reference points, whereas 3D outer corner seam finding program requires seven. In addition, the form of reference points differs based on the used control group. The welding programs are typically created as a coordinated program with robot group R1+S1 (welding robot + workpiece positioner), so coordinated seam finding programs are used also in this work. Motion instructions in coordinated programs must be synchronized, so the reference points are set as "SREFP" instead of "REFP".

Principle of setting the reference points of the 3D seam finding program for outer corner of a T-joint is presented in figure 36. There are seven reference points which are used to determine the trajectory for the searching motions for three different surfaces, in this case the web, flange and edge of the web. The searching motions must be done along the axes of the active coordinate system, and preferably perpendicular to the searched surface. The seam finding program is constructed so, that the reference points are executed in order with linear movements, but the robot goes through REFP 1 between each searching motion to avoid collisions.

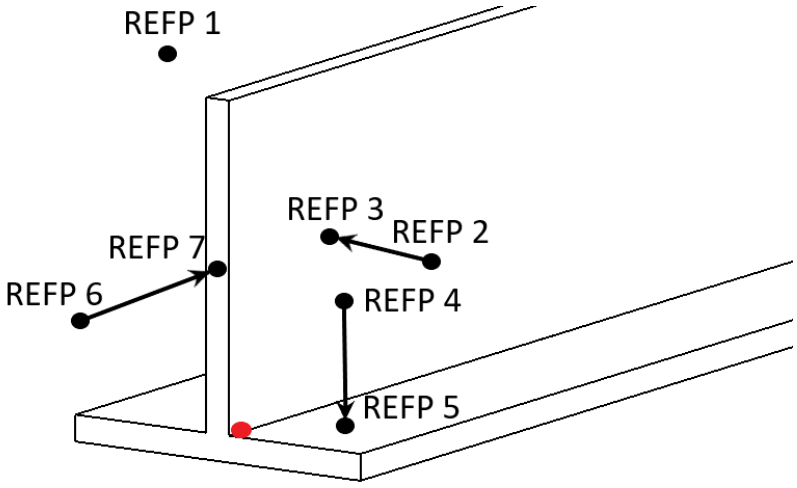

Figure 36. Example of setting reference points of the 3D seam finding program. The red dot is the welding starting point to be corrected.

4.2.2 Principle of seam tracking with the laser sensor

Seam tracking is implemented by the analogue control method, which was introduced in chapter 3.3.2. In the method, the laser sensor measures a specific feature point from the joint that is being tracked. The measurement data is converted to analog signal, which indicates the deviation and its direction from a pre-set target value. The signal is fed to the robot controller as continuous voltage, which is then used by the seam tracking function to correct the initial weld path. Principle of the seam tracking function is, that when there is no deviation from the target value, the output voltage is zero, but when the voltage indicates a deviation, the robot makes a correction to the opposite direction.

The measuring program and output settings for seam tracking must be configurated based on the seam type. In Scancontrol configuration tools- software, a combined signal tool is used for determining the tracked feature from the seam. The point corresponds to values for X- and Z- axes (width and depth), which are used for the analog output. The output coordinate values can be modified separately, for example an offset for the tracking point can be set by adding a constant, and the direction of the corrective signal can be changed by negating the output value. Before converting the measurement data to a voltage signal, it can be filtered for example with median filter to reduce the effect of measurement errors.

Measuring profiles for different joint types and situations can be created and saved in the software. This is recommendable, because for example pulling or pushing torch angle affects to the distance at which the sensor measures the seam, so different tracking parameters must be used. Profiles could be created for example for multi-pass welding, in which case the offset feature can be used to aim the tracking point at the toe of previous weld bead. With the ready-made measurement profiles for different situations, only the active program for the analog output channel must be changed when needed.

Figure 37 shows the sensor software settings that are used for tracking a fillet joint. As can be seen from the result visualisation, the program detects the intersection point between the two plates. In this case, the output values are negated because the sensor travels backwards relative to its own coordinate system. For butt joints, otherwise same settings can be used as with fillet joint, but a measuring program for detecting the midpoint of a gap is selected.

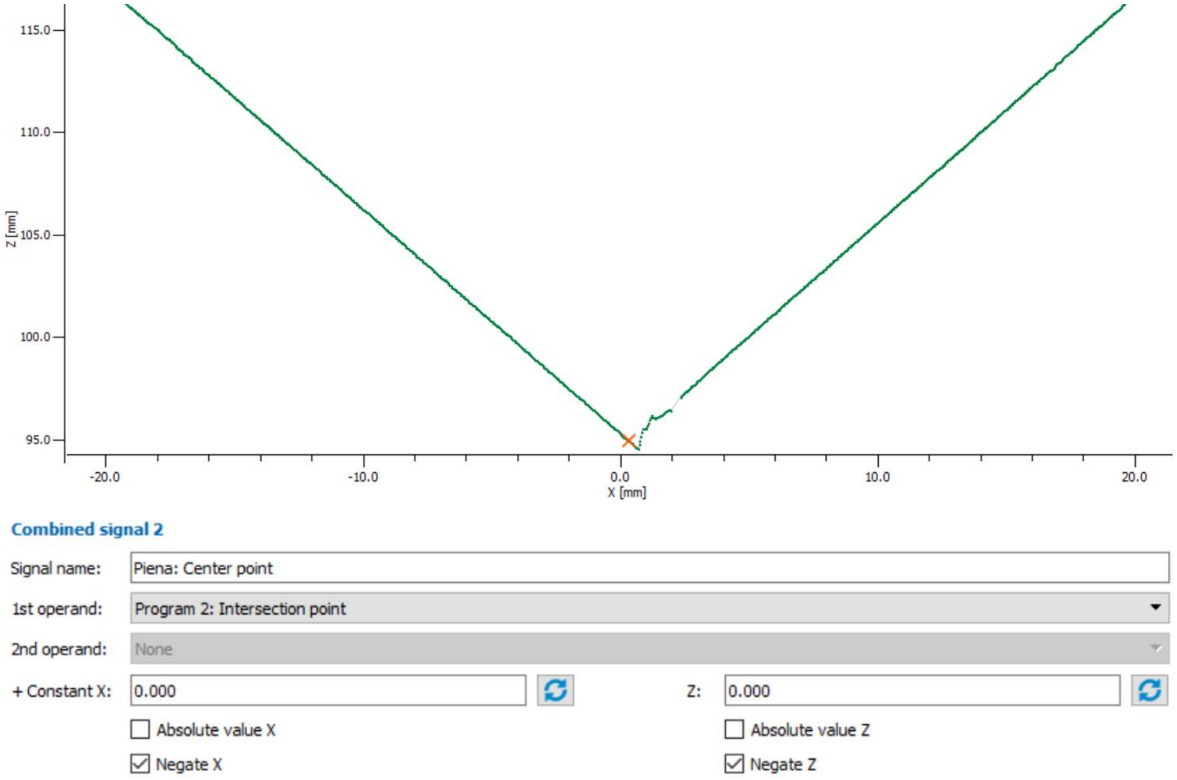

Figure 37. Visualisation and settings of the measurement program for tracking a fillet joint.

The analog output port settings for seam tracking are presented in table 5. Output port 1 is used for X-axis, and output port 2 for Z-axis. The robot controller monitors voltage signals in range of ±10 V, so it is also set as the voltage range for the sensor output ports. The measurement range determines the conversion resolution from millimetres to voltage, as the measurement range values correspond directly to the voltage range values. This resolution does not have a direct effect to the corrective motion of the robot, because a separate mm/V conversion resolution is set in the robot controller. Therefore, limit values of the measurement range are set so, that the analog output signal is active as long as the seam is in the field of view of the sensor. The determinative parameter is the middle point of the measurement range, because it corresponds to 0 V, which is the target voltage during tracking. Hence, the measurement range must be directed based on the measured X- and Z-axis values when the torch is at the optimal welding position. In this case, if pushing or pulling torch angle is not used, the target value for Z-axis is -95 mm, which is also the nominal measuring distance for the sensor. For lateral direction, the target value is X=0, which keeps the torch in the middle of the seam.

Table 5. Analog output port settings in the sensor software for seam tracking.

Analog output port	Voltage range [V]	Measurement range [mm]			Resolution [mm/V]
		Min.	Mid.	Max.	
Port 1 (X- axis, lateral correction)	±10	-65	0	65	6.5
Port 2 (Z- axis, depth correction)	±10	-160	-95	-30	6.5

The analog output port 1 from the sensor leads to input channel 2 of the robot controller, and correspondingly the output port 2 leads to input channel 3. The input channel specifies the direction in which the correction takes place in robot tool frame coordinates. The sensor output status for each channel is displayed in the robot controller as shown in figure 38. As well as from the sensor software, an offset value for each channel can be set here. The dead zone parameter defines the minimum voltage value at which seam tracking function becomes active. (Yaskawa 2005, pp. 17–45)

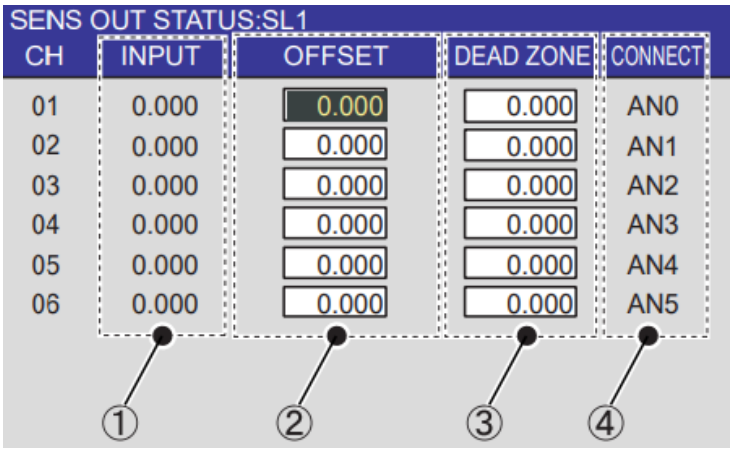

Figure 38. Display of sensor output status for each channel in the robot controller. 1. Input voltage 2. Constant offset value 3. Dead zone 4. Input port. (Yaskawa 2005, p. 45)

Various parameters of the seam tracking function can be changed within the robot controller. The most important parameter is the resolution for the corrective motion, which determines that how much the robot moves in millimetres per voltage unit. It can be set separately for each input channel. Another significant parameter is the maximum correction speed. There are no specific parameter settings that must be used to make the tracking functionable, because the tracking function should always keep the centerline of the path at the correct position. However, the parameters affect to how stable and smooth the robot motions are

during welding, and how the tracking works e.g. when tack welds are crossed, or measurement errors occur. Improper parameters can lead to inaccuracy, jerking motion and even collisions. The parameters that are used in the seam tracking tests can be seen in chapter 4.3.2.

4.2.3 Ensuring the accuracy of workpiece positioning in jigless welding

The concept of jigless welding was introduced in chapter 2.2. The concept has been previously studied and tested in the LUT welding laboratory, but without optical sensor technology. One recognized problem has been to ensure the accuracy and repeatability of workpiece positioning when the handling robot brings new components to the assembly. The variation caused by e.g. inaccurate part manufacturing or incorrect picking position can be so significant, that good weld quality and sufficient dimensional accuracy of the final product cannot be achieved. Also, when offline- programming is used, it is necessary to adapt to the differences between the simulation model and the actual robot station. For these reasons, one of the aims in this study was to investigate how the laser sensor could be used for handling robot guidance in jigless welding.

Workpiece positioning with the laser sensor was not implemented in practice, but the required robot programs were created. A Delfoi Robotics 4.2 simulation software and an existing model of the multi-robot welding cell was utilized in the preliminary planning of the procedure. Figure 39 shows the simulation model during jigless welding of a T-joint, where the base plate is already placed on to magnetic workpiece positioner, and the handling robot holds the vertical plate during tack welding. The simulation was used to visualize how the robot programs should be constructed and how the laser sensor could be operated in this example case.

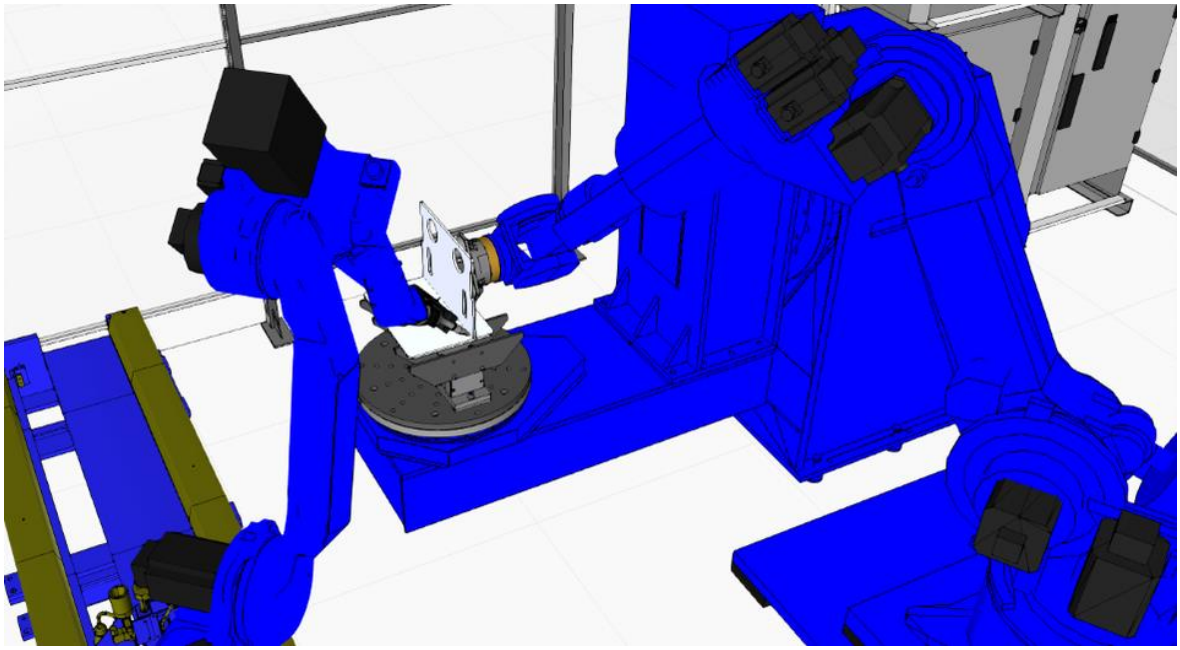

Figure 39. Simulation model of the multi-robot welding cell during jigless welding of a T-joint.

The major restriction to use the sensor in jigless welding is, that the laser sensor output signals cannot be used directly to control the handling robot, for example during movement. This is because the two NX100 robot controllers are paired by master/slave principle, controller of the welding robot being the master, so it conducts the I/O communication. The remaining option is to use the welding robot to perform similar search programs as in seam finding, and to use the resulting position variables to guide the handling robot.

Principle of this method is as follows. The handling robot brings the workpiece to a specific distance from its correct position and holds it in place, while the welding robot performs search functions with its laser sensor in each direction to be corrected. Then, the achieved shift values are used in the handling robot program to correct the final positioning motion, which is originally programmed to place the workpiece to its nominal position. The required searches cannot be done with the existing seam finding programs, so two different modified search programs are created for this purpose. One for correcting the distance between the workpiece to be positioned and the stationary workpiece, and one for correcting the other two directions. They follow the same search function principle and program structure as the seam finding programs presented in chapter 4.2.1, and also the same output settings in the laser senor software can be used.

The positioning programs are created in the base coordinate system, so the position variable data applies to both robots in the same way. The program structure of the 2D position correction program with explanations can be seen in appendix IV. The program saves the shift value in to position variable P008. Unlike in seam finding programs, SFTON instruction for the variable is not ran in the search program since it would apply to the welding robot, but later in the handling robot program. Five reference points must be set in the main job when the 2D correction program is called, and an example of setting them is shown in figure 40. REFP 1 is a standby point at a suitable distance from REFP 2 and 4. The program corrects the workpiece position parallel to the search directions shown in the figure.

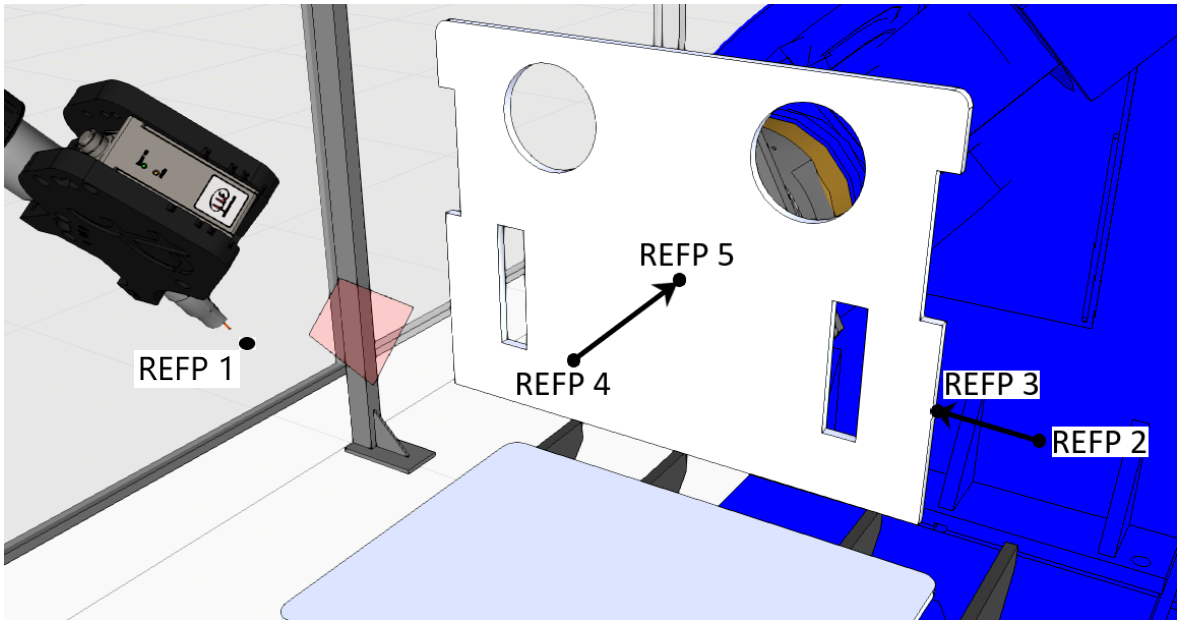

Figure 40. Setting of the reference points for the 2D correction program.

The distance between the stationary workpiece and the workpiece to be positioned is the most crucial to confirm, because positioning errors in depth direction would lead to either collision or too large gap between the parts. As the distance can vary due to incorrect position of either of the workpieces, the location of both of them should be measured. For this purpose, a search program was created which performs two searches in opposite directions along one axis. The program structure with explanations is shown in appendix V. The program mainly follows the same structure as the presented 2D correction program, but it results in 1D correction value. As the search motion for the workpiece to be positioned is done in opposite direction to the final positioning motion, the position variable calculation

is reversed to get the shift value in correct direction. The program saves the distance correction value in position variable P006.

The principle of setting the reference points in main job before calling the distance correction program is presented in figure 41. Distance between the plates in the simulation is 100 mm, but it can be anything as long as there is space to perform the searches. The reference points can be set in different ways and directions depending on the welded product, but the search motions must always be done along one of the base coordinate axes, and REFP 2 and 3 must be used for the plate held by the handling robot. The reference points 2 and 4 could in principle be combined to be the same starting point for both searches. However, this could lead to challenges in performing the search motions with correct tool angles, as it should remain constant during searching, so separate starting points make the program more flexible to use. Moreover, this way the base plate search can take place further away from the vertical plate if needed.

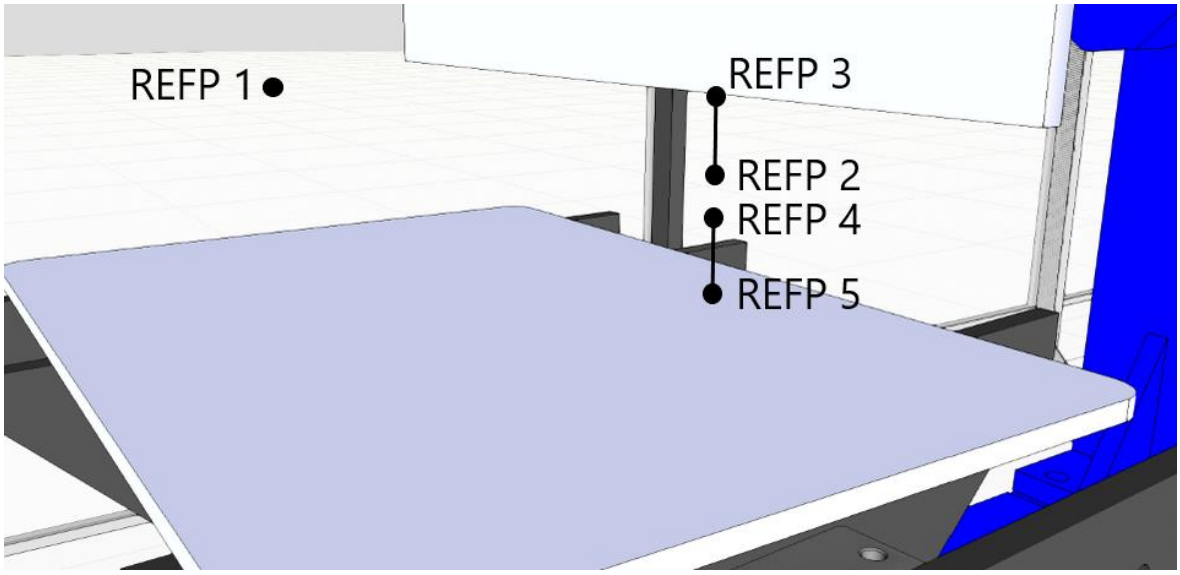

Figure 41. Setting of the reference points for the distance correction program.

Examples of executing the search motions for the presented workpiece positioning methods are presented in figure 42. Measuring range of the laser sensor is visualized in the simulation. The simulation model has a different sensor adapter than the one used in practical tests, but the searching principle remains the same. These tool angles are not the only options to carry out the search motions, but they must always be planned so, that the sensor detects the

surface consistently the same way even if the workpiece position changes. Thus, the sensor orientation and the detected point that activates the digital output signal must be carefully considered.

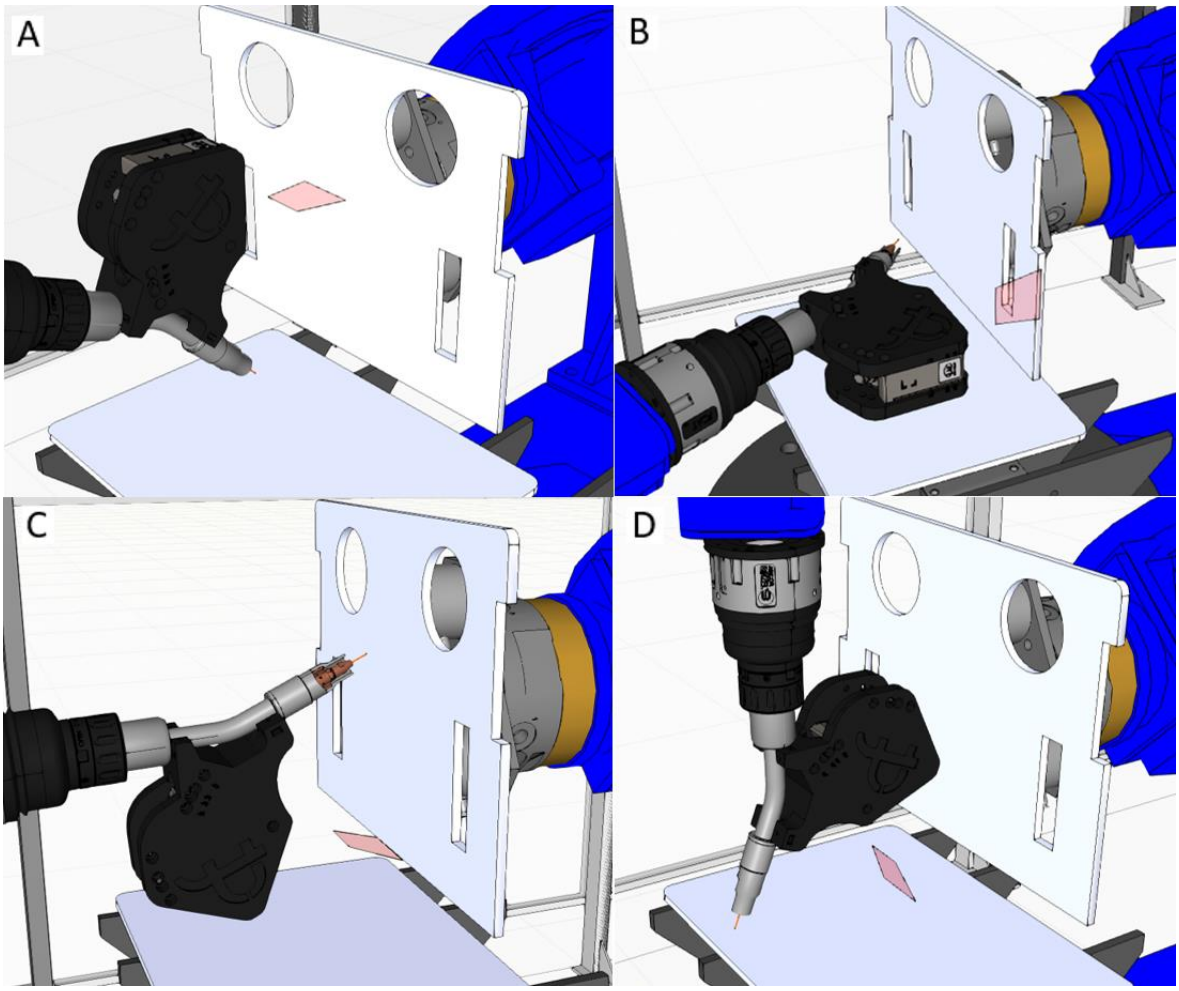

Figure 42. Simulated search motions for workpiece positioning in jigless welding. Pictures A and B are for 2D position correction, and C and D are for distance correction.

These workpiece positioning programs can be used in different situations, as long as the final positioning movement is done parallel to one of the axes of the base coordinate. In terms of programming routines, the workpiece positioning programs can be called in the main job the same way as seam finding programs. After they are executed, the search results are saved in position variables P006 and P008, which can be operated in handling robot programs. For example, they can be merged to a single position variable with “ADD” instruction, which then includes the shift value in along X-, Y- and Z- axes. Finally, the resulting variable can be run with “SFTON” instruction to make the correction to the final positioning motion.

4.3 Testing of the laser sensor functions

Practical experiments were performed to verify the functionality and accuracy of the seam finding and seam tracking methods. The workpiece positioning method was not tested in practice due to scheduling constraints, but a test could be performed based on the presented programs.

4.3.1 Experimental setup for the seam finding test

Testing of the seam finding method is carried out with the 3D seam finding program for detecting the corner point of a T-joint. This program was selected, because it is the most complex to perform among different options, so the achieved accuracy results should apply also for the other seam finding programs. The program structure can be seen in appendix III, and the settings used with the laser sensor in chapter 4.2.1.

Aim of the seam finding test was to investigate the relative and absolute accuracy of the corrective motion. This was done by repeating the same program for a static workpiece to find out the variation of the correction values. The program was repeated for 30 times to ensure the reliability of the results. The correction data was collected from the resulting position variable P006 after every repetition.

The experimental setup and the search motions for each surface can be seen in figure 43. The workpiece is a T-joint which is clamped to the positioner so, that the plates are aligned along the coordinate axes of the robot system. Material of the workpiece is S355 structural steel, with laser cut edges and surface in delivery condition. In the test program, the robot performs the search motions in the order shown in the picture, and the point to be corrected is programmed at the corner of the joint. Speed of the searching motion was 5 mm/s. Because the workpiece is not deviated from its original position in the test, the correction value is expected to be close to zero for each axis.

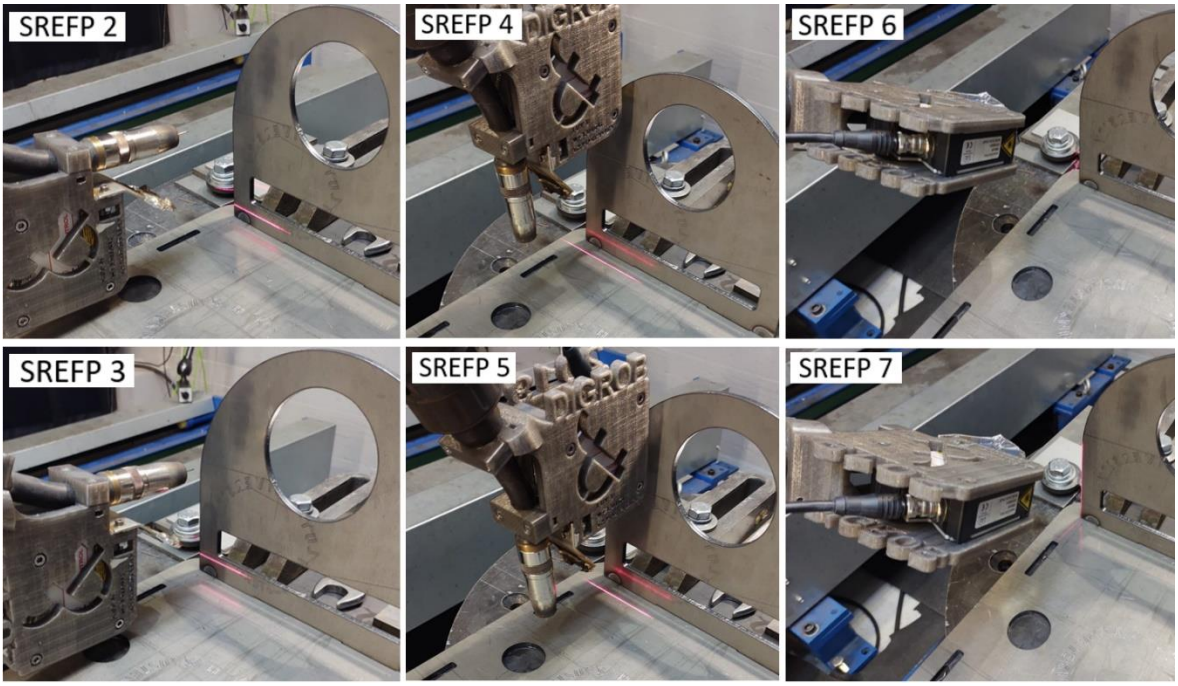

Figure 43. Search motions of the test program.

The reference points 3,5 and 7, which are set in the initial program to define where the surface should be found, must be set as accurately as possible. This is because the correction value is calculated based on the difference between the reference point and the detected point, so also the reference points affect the absolute accuracy of the method. As previously mentioned, the laser sensor activates the digital output signal when the maximum Z-axis value in its coordinate system is 60 mm or more. Thus, reference points 3 and 5 are set so, that the value is as close as possible to 60 mm. This does not apply for the search motion towards reference point 7, because the sensor approaches the surface with different tool angle. The sensor approaches the vertical plate so that it is already close enough in the depth direction, but there is nothing in its field of view until the edge of the plate appears. Therefore, the reference point 7 is set so, that the output signal is just about to activate from the first detected pixels from the plate edge.

The surface detecting principle and the initial sensor values for each search motion can be seen in table 6. Also the direction of each search in the robot coordinate system is mentioned. As can be seen, the difference between the target value (60 mm) and actual reference point value is less than tenth of a millimetre for X and Z axes. Theoretically, this difference is also the expected correction value after the seam finding program is executed.

Table 6. Direction of the search motions in robot coordinate system and the surface detection principle.

Search	Direction	Surface detection principle and initial sensor value
SREFP 2-3	X-axis	Maximum Z value of the sensor 59.94 mm at SREFP 3
SREFP 4-5	Z-axis	Maximum Z value of the sensor 59.97 mm at SREFP 5
SREFP 6-7	Y-axis	First pixels to appear in the sensor's field of view at SREFP 7

After the 30 repetitions for the accuracy test were made, the functionality of the seam finding program was tested visually. The workpiece was deviated from its original position in each direction (x-y-z) by placing 3 mm plates between the workpiece and jig. Then the seam finding program was run once to confirm that it results in the correct welding start point with sufficient accuracy.

4.3.2 Experimental setup for the seam tracking test

The functionality of seam tracking was tested by tracking a T-joint in different situations, and by analyzing the robot position and laser sensor data during the traveled paths. The robot position data during tracking was gathered with the MATLAB program which communicates with the robot controller through MotoNIS. The laser sensor raw data was gathered with the monitoring tool of Scancontrol configuration tools- software. The test was repeated twice for identical workpieces. Same measuring program and analog output settings are used as presented in the chapter 4.2.2.

The test workpieces are symmetrical and straight T-joints made of 500x100x8mm steel plates. They are tack welded from one side with no air gap. The plate material is S355 structural steel with machined edges and surfaces in delivery condition. Figure 44 shows the test setup and the robot position at the start and end of the path. The workpiece is clamped to the positioner along the axes of the base coordinate system of the station. The robot is programmed to move along the joint with constant tool angle and linear motion at a speed of 7 mm/s. At the start point the torch is at the corner of the joint, and at the final point the laser line is at the end of the workpiece, so the path is 400 mm long since the distance between laser line and welding wire tip is 100 mm.

Figure 44. Test setup for the seam tracking tests. Direction of coordinate axes for both the robot and the sensor are marked with the arrows, X = red, Y = green, Z = blue.

The initial path was programmed so, that the welding wire tip was optimally at the center of the joint, and the sensor detected the intersection point at coordinates X=0, Z=95, at both the start and end points. Thus, the robot position coordinates of the initial path also corresponds to the position of the fillet joint. The initial path was calibrated for both workpieces separately, but it was not modified between the different test runs. The program was run, and the robot position data was plotted in four different occasions:

1. Initial path without tracking.
2. Initial workpiece position with tracking.
3. Deviated workpiece position with tracking.
4. Deviated workpiece position with tracking and welding.

In the tests, the seam was first tracked in the original workpiece position to see, if the tracked path follows the initial linear path. Then, the workpiece was deviated along the X-axis of the robot coordinate system by placing a 3 mm thick steel plate between the workpiece and jig, and the tracking was repeated to verify that the robot adjusts its path accordingly. It must be noted that the actual deviation was not exactly 3 mm, but this has no effect on the results. Finally, the deviated workpiece was welded to investigate how the arc light and other disturbances affect the tracking, and if the tracking is accurate enough to achieve high weld quality. Direction of the deviation, and the relation of the torch in the starting position to the different workpiece positions is presented in figure 45.

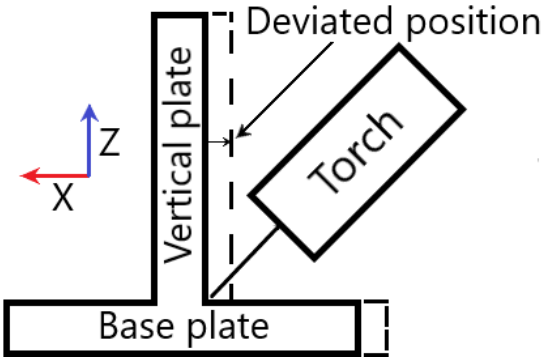

Figure 45. Initial and deviated workpiece positions and torch in the starting position.

The same procedure was performed, and the same parameters were used for both test workpieces, only exception being that for the second workpiece the number of sequential measurements for median filtering was increased from 3 to 15. The significant parameters for the laser sensor, seam tracking function and welding are compiled in table 7.

Table 7. Parameters used in the seam tracking tests.

Parameter	Value
Sensor parameters	
Profile frequency	100 Hz
Exposure time	0.50 ms
Median filter size	3 for first, 15 for second workpiece
Analog output resolution	6.5 mm/V
Tracking function parameters	
Voltage – correction resolution	2 mm/V
Dead zone	0.01 V
Maximum correction speed	3 mm/s
Welding parameters	
Wire feed rate	11 m/min
Travel speed	7 mm/s
Torch angle	45° / perpendicular
Wire stickout length	18 mm

5 RESULTS AND ANALYSIS

Results of the tests are presented and analysed in this chapter. The seam finding test data was fed to an Excel spreadsheet, where the key statistics for accuracy were calculated. The robot position and laser sensor data were processed and plotted with MATLAB.

5.1 Results of the seam finding tests

Figure 46 shows the correction values for each axis in the seam finding test set. The test program was constructed so, that the target correction value for each axis was zero, and the accuracy of the pre-set reference points was ±0.06 mm. With this accuracy of the test arrangements, the resulting absolute accuracy of the method is ±0.3 mm. However, relative accuracy of the method is higher, as the correction values for each axis separately are roughly in range of 0.1 mm. As can be seen, the X-axis values are close to zero on average, whereas Y- and Z-axis values are at over 0.2 mm distance from the target. In principle, the Y and Z axes could be calibrated based on this result, by setting the reference points of the seam finding program to an equivalent distance from the nominal value which triggers the output signal. However, more testing in different circumstances would be needed to ensure that the magnitude and direction of the error are always the same.

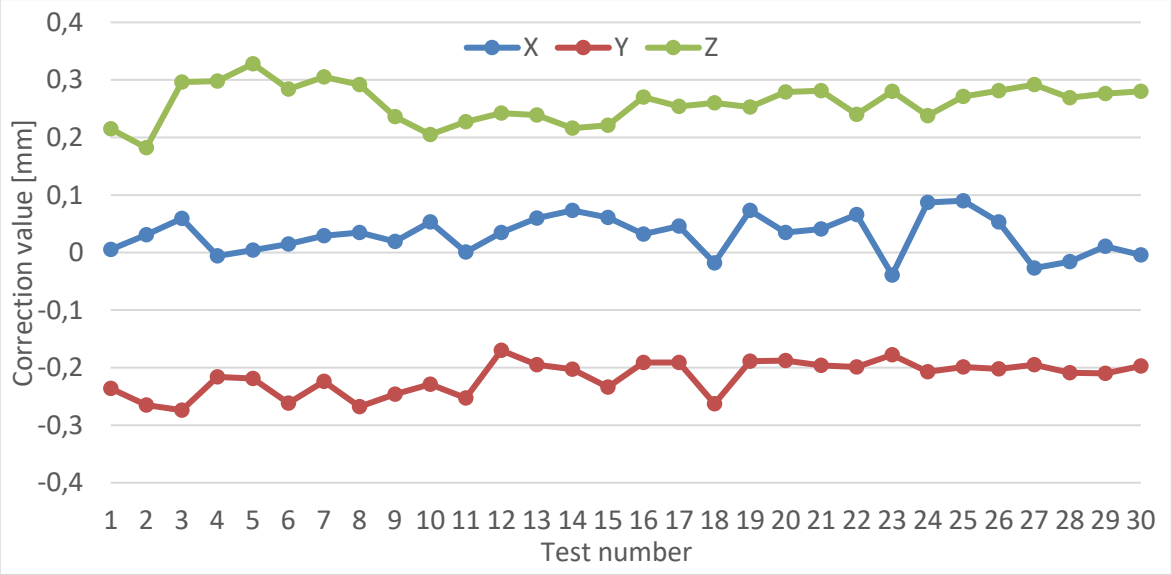

Figure 46. Correction value for each axis in the seam finding test set of 30 repetitions.

Statistics on the correction value variation for each axis are shown in the table 8. Theoretical accuracy of the laser sensor is 4 µm, so the results are rounded to hundredth of a millimetre. The maximum error from mean, range and standard deviation indicates high repeatability and precision. Based on this result, an absolute accuracy of ±0.1 mm would be realistic to achieve, if the Y and Z axes can be calibrated as accurately as X-axis.

Table 8. Variation of the correction values for each axis based on test set of 30 repetitions.

Axis	Minimum value [mm]	Maximum value [mm]	Mean [mm]	Maximum error from mean [mm]	Range [mm]	Standard deviation [mm]
X	–0.04	0.09	0.03	0.07	0.13	0.03
Y	–0.27	–0.17	–0.22	0.06	0.10	0.03
Z	0.18	0.33	0.26	0.09	0.15	0.03

After the repeatability test, the workpiece was deviated from its original position in three directions to confirm that the seam finding program works as it should. The result is shown in figure 47. As a reference for the dimensions, the welding wire is 1 mm thick. As it can be seen, the correction was successful, and the welding wire is at the welding start point with sufficient accuracy. It can be stated that this seam finding method could be used in practical applications even if the shift values for Y and Z axes are not calibrated more precisely.

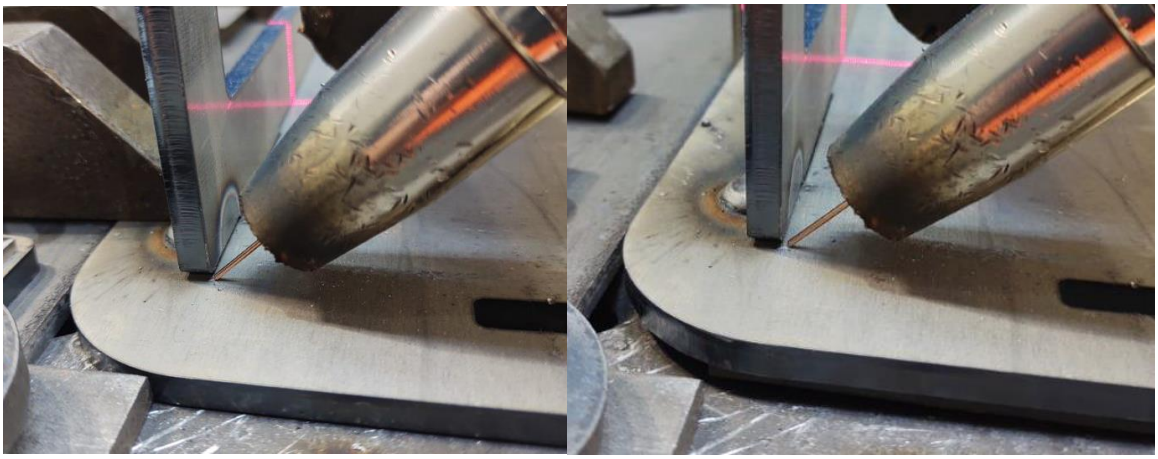

Figure 47. Welding wire position after the seam finding program. On the left, the workpiece is in its original position, and on the right, the workpiece is deviated in three directions.

5.2 Results of the seam tracking tests

The seam tracking test results are presented for both workpieces separately. The results include graphs of the robot tool path (TCP coordinates) and the laser sensor data during different test runs. When reading the graphs, it should be noted that the coordinate systems of the sensor and robot are not parallel, as was illustrated in figure 44. The X-axis of the laser sensor corresponds to width and Z-axis to depth, whereas X-axis of the robot coordinate system is parallel to the bottom plate, and Z-axis is parallel to the vertical plate. Therefore, a deviation measured by the sensor in either X- or Z- axis direction causes a corrective motion which reflects to both X- and Z- coordinates of the robot. Moreover, position of the TCP (welding wire tip) in relation to the joint is determined by these two coordinates.

The robot position graphs include the coordinate data of the four different test runs. First, the initial path without tracking, then the initial workpiece position with tracking, then the deviated workpiece position with tracking, and finally the deviated workpiece position with tracking and welding. Each test run has the same starting point since the robot program was not modified between the runs, and it is scaled to zero in the graphs. The graphs show that the position coordinates of the initial paths do not remain at zero throughout the paths. In addition, for either of the test workpiece the actual deviation is not 3 mm, and the deviated position is not exactly parallel to the initial position, i.e. the deviation is not constant. These factors are caused by inaccuracy of the test setup, and they are insignificant to the reliability of the results, because the functionality of seam tracking can be determined by comparing the different test run paths to each other.

5.2.1 Test workpiece 1

The robot X-axis coordinate during the tracking test for workpiece 1 is presented in figure 48, where the test runs are indicated with different line colours. The green and violet line show that tracking in the initial workpiece position follows the initial robot path as expected, and variation in the robot position was only some tenths of a millimetre. The red line shows that when the workpiece was deviated along X-axis, the tracking function started immediately to correct the torch position farther from the joint, and it was fully corrected after the robot had advanced 10 mm from the starting point. After the correction, tracking of the straight joint was as accurate as in the initial workpiece position for the rest of the path. However, the blue line shows that during welding the tracking becomes remarkably

inaccurate, as it should follow the red line that indicates the optimal welding path. For the first 10 mm, the position is being corrected to the right direction, but then the tracking error occurs, which takes the torch too close to the workpiece and causes a continuous weaving motion in range of 1 mm. At worst, the tracking error is 4.5 mm, and the torch is mostly closer to the workpiece than it would have been with the initial path, despite the deviation.

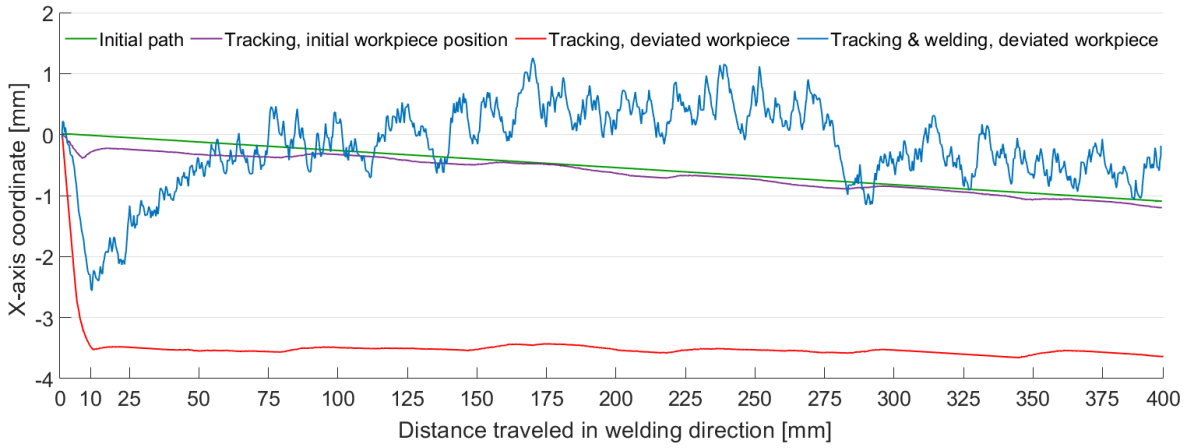

Figure 48. Robot X-axis position coordinate, test workpiece 1.

Figure 49 shows the Z-axis position coordinate for workpiece 1, where the same tracking error during welding can be seen. The workpiece was deviated only in X-axis direction, so the Z-axis coordinates of the optimal path are the same for the initial and deviated workpiece positions. The maximum error in this direction is 4 mm, and the torch is on average 3 mm too close to the base plate along the whole path. As the torch is too close to the vertical plate due to the X-axis error, and too close to the base plate due to the Z-axis error roughly for the same amount, it can be concluded that the welding wire stays moderately at the center of the fillet joint, but the wire stickout length is decreased drastically. Decrease of the stickout length is equivalent to the hypotenuse of the errors these two directions, so the wire stickout during welding has been about 5 mm shorter than the 18 mm nominal stickout length. This has an effect to the welding parameters and weld quality, and moreover the gas nozzle has been traveling quite close to the workpiece, causing a risk of collision.

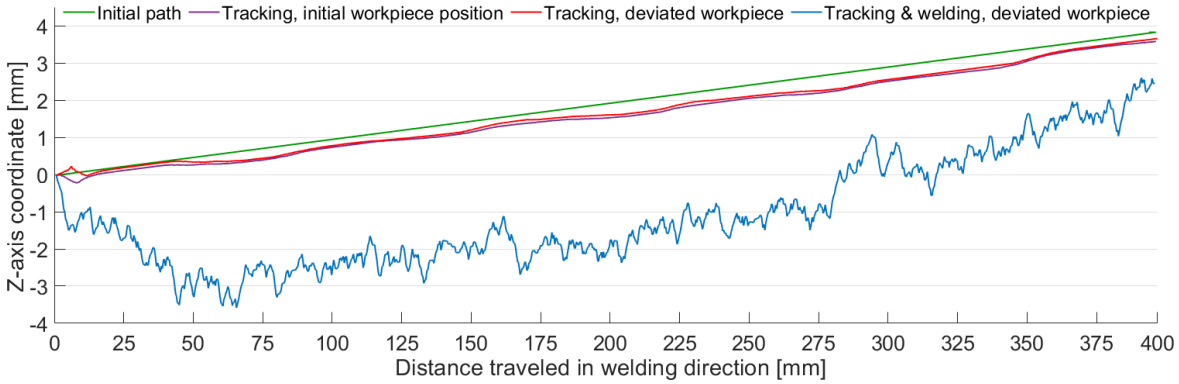

Figure 49. Robot Z-axis position coordinate, test workpiece 1.

Reason for the tracking error can be found from the laser sensor data. The two test runs with the deviated workpiece position are investigated to see the effect of welding to the sensor measurements. The robot position data indicated that the tracking works moderately in lateral direction (sensor X-axis), but not in depth direction (sensor Z-axis).

The laser sensor X-axis data for workpiece 1 is shown in figure 50. The red line shows the tracking data without welding, in which case the tracking functioned accurately and flawlessly. At the start, the sensor measures a deviation from the target value (zero), based on which the robot corrects its path. After the correction, the sensor measurements stay close to the target value, as every non-zero value leads to a correction that keeps the robot in the optimal path, of course considering the dead zone set in the seam tracking function. On this scale, any measurement errors during tracking only cannot be detected. However as the blue line shows, during welding there are continuous measurement errors in range of ±10 mm. The mean is nevertheless close to zero as it should be, and the errors are evenly distributed to both directions. This means that the robot is fed with too high correction values alternately in opposite directions, causing the robot to move along the correct path on average, but with a constant weaving motion. As can be seen, some measurement errors are up to -65 mm, which is the pre-set limit value of the analog output port. They occur, because the sensor gives the limit value of the measurement range as an output, when it does not detect the intersection point of the T-joint at all. This is an unexpected feature, probably caused by an incorrect setting in the laser sensor software, and it should be changed in further use. In addition, note that this data has been filtered with a median filter of three sequential measurements, so the amount of measurement errors in the raw data is much higher.

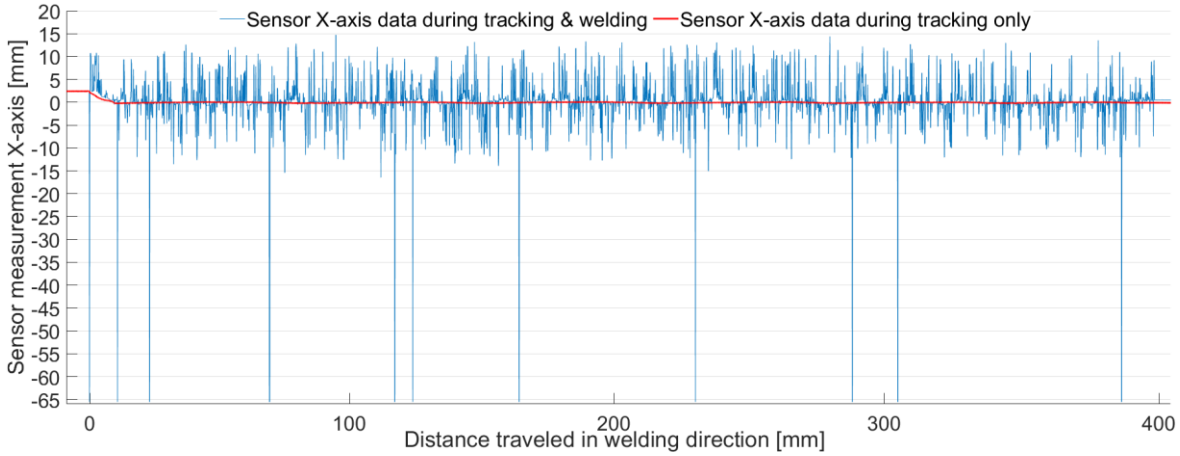

Figure 50. Laser sensor X-axis data during tracking, test workpiece 1, median filter 3.

The laser sensor Z-axis data for workpiece 1 can be seen in figure 51. The red line shows that the tracking without welding functioned optimally also in depth direction. On the contrary, the data during welding shows the reason to the major tracking error. The large measurement errors up to the limit of the measurement range occur for the same reason as for X-axis. However, for Z-axis there are more significant errors, and measurements are not evenly distributed around the target value (-95 mm / red line). The large measurement errors are weighted so, that the sensor detects the joint further away than it actually is. Therefore, the magnitude of voltage signals which corrects the path closer the joint is higher than to the opposite direction, causing the robot to travel constantly too close.

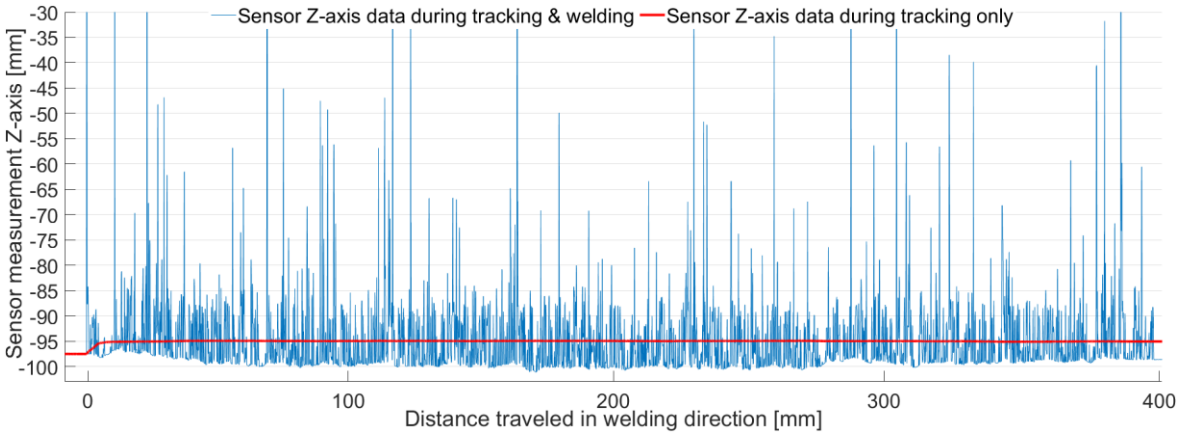

Figure 51. Laser sensor Z-axis data during tracking, test workpiece 1, median filter 3.

5.2.2 Test workpiece 2

Since the results for test workpiece 1 showed that median of three sequential measurements was not enough to filter out the obvious measurement errors, median filter of 15 was used for the second test workpiece. Due to increased filtering, the rate at which voltage signals are fed to the seam tracking function decreases from 5/mm to 1/mm, based on the travel speed and sensor's measuring frequency.

Figure 52 shows the robot X-axis coordinate for the test workpiece 2. First, it should be noted that the actual deviation for this workpiece was five to six millimetres instead of three, so the scale of the graph is larger. Again, without welding the tracking worked optimally, but the tracking error during welding did not disappear. On average, the error between the weld path and the optimal path (red line) is 3 mm. However, the maximum error is over 5 mm, because the amplitude of the weaving motion is higher than for workpiece 1. This is likely caused by the increased filtering, as the measurement values are more stable, and the individual correction signal affect the robot position for a longer period of time.

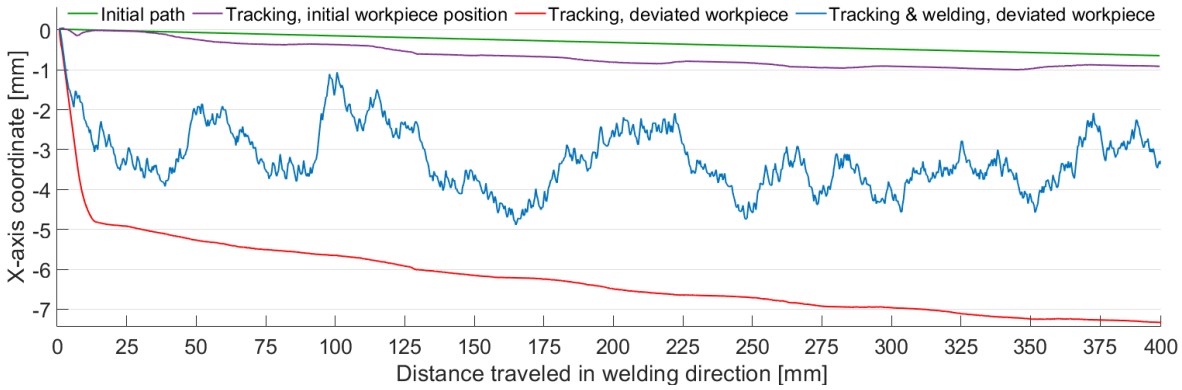

Figure 52. Robot X-axis position coordinate, test workpiece 2.

The robot Z-axis position coordinate for workpiece 2 can be seen in figure 53. It shows that the tracking error during welding is on average 2 mm, and thus not equal to the error in X-axis. This means, that the centerline of tracking in lateral direction is not exactly in the middle of the joint, and the wire is directed slightly more towards the vertical plate. However, the central problem is still the same as for workpiece 1, that is the tracking in depth direction takes the torch too close to the joint. For workpiece 2, the wire stickout length was on average 4 mm shorter than it should (18 mm), which is slightly better than with workpiece 1, but the position variation throughout the welding path was higher.

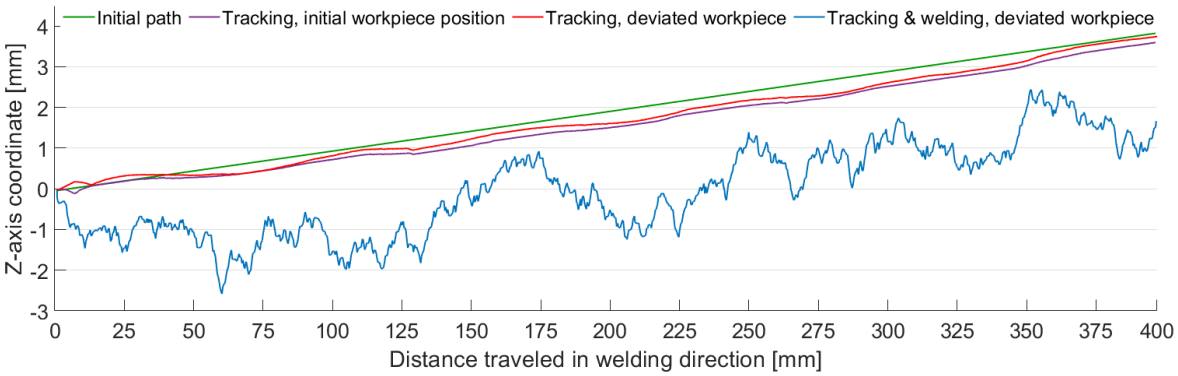

Figure 53. Robot Z-axis position coordinate, test workpiece 2.

The sensor data is again shown for the two test runs with the deviated workpiece position. The effect of increased filtering to the laser sensor X-axis data can be seen in figure 54. With this scale it can be well seen, how the sensor values during tracking only remain accurately near zero with a stable wave motion. For the data during welding, the large measurement errors are filtered off, and the values stay in range of ±8 mm. However, still obvious measurement errors get through the filtering, as the robot position did not vary enough to explain the spikes of several millimetres. The measurement errors, together with the less frequent correction signals, lead to the high variation in the robot position throughout the path. When compared to the optimal tracking data, it can be seen that the mean is slightly over the target value during welding. This explains the finding from the position data, that the lateral tracking did not direct the wire at the center of the joint on average.

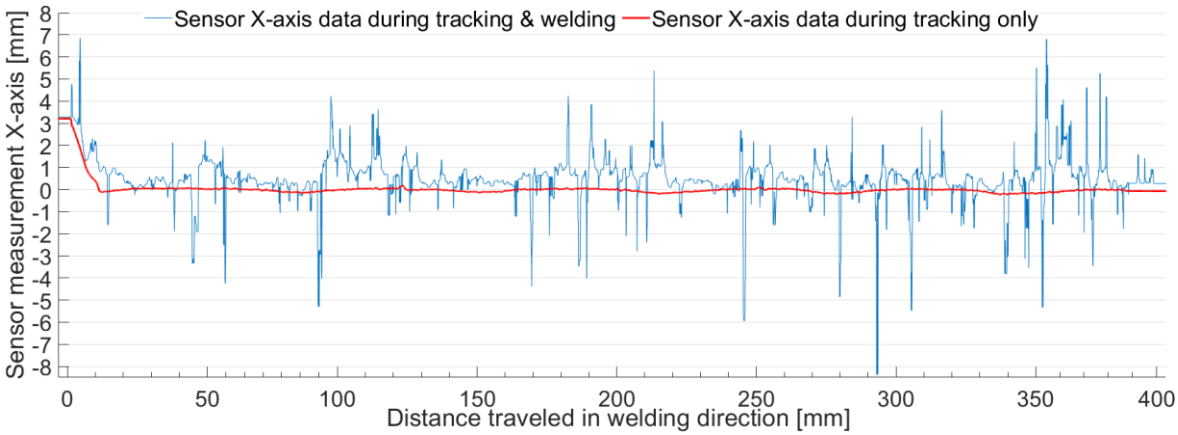

Figure 54. Laser sensor X-axis data during tracking, test workpiece 2, median filter 15.

Figure 55 shows the sensor Z-axis data for workpiece 2. The largest errors are now filtered off, and the measurement values stay in range of 20 mm. However, the same phenomenon that causes the depth tracking error can be seen as with test workpiece 1, just on a smaller scale. The sensor alternately detects the joint being too close (values under the red line), which is correct, but then the measurements errors occur to the opposite direction (values over the red line). As the errors have a bigger deviation to the target value than the correct measurements, they result in higher correction signal voltage, and the robot position is constantly incorrect.

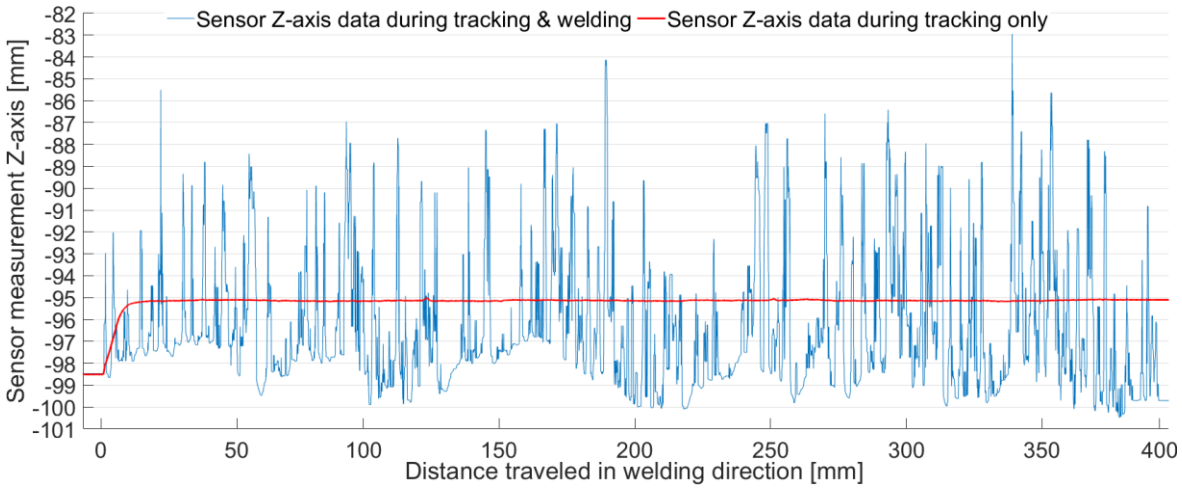

Figure 55. Laser sensor Z-axis data during tracking, test workpiece 2, median filter 15.

Based on the results with increased median filtering, it is clear that any additional filtering in the sensor software does not solve the tracking error, because the measurement errors cover so significant percentage of the raw data. The tests proved that the seam tracking method itself works correctly and with high accuracy. The tracking function corrected the robot tool path according to the deviated workpiece position, and the variation in the robot tool position was very low. By investigating the laser sensor- and robot position data on a smaller scale, it was observed that the robot position stayed in range of 0.2 mm during tracking a straight joint. However, the disturbances caused by welding led to significant measurement errors, which made the tracking unreliable and inaccurate. The laser sensor X-axis measurement errors caused uncontrolled weaving/jerking motion in lateral direction, but the traveled path was close to optimal on average. For Z-axis, the welding caused more significant measurement errors, and they occurred mainly in one direction, which caused the

torch to travel too close to the joint. The root causes of the measurement errors are discussed, and development proposals are given in chapter 6.2.2.

5.2.3 Visual quality of the welds

Resulting weld quality of the seam tracking tests was inspected visually, and figure 56 shows a close up of both test workpieces. No significant difference could be observed between the two test runs. The tracking error in depth direction reflected to the welding parameters, as the current increased and voltage decreased to due to the shorter wire stickout length. The average current and voltage were 353 A and 27.5 V for workpiece 1, and 340 A and 27.6 V for workpiece 2, which is not a normal ratio, considering that the wire feed rate was 11 m/min. This had an effect to the weld shape, as can be seen from the figure, both welds are quite convex and the transition is not smooth. The non-linearity of the fusion line is likely caused by the uncontrolled weaving/jerking motion during welding. However, otherwise the welds are quite symmetrical and uniform, which indicates that the welding wire was directed to the joint moderately in lateral direction.

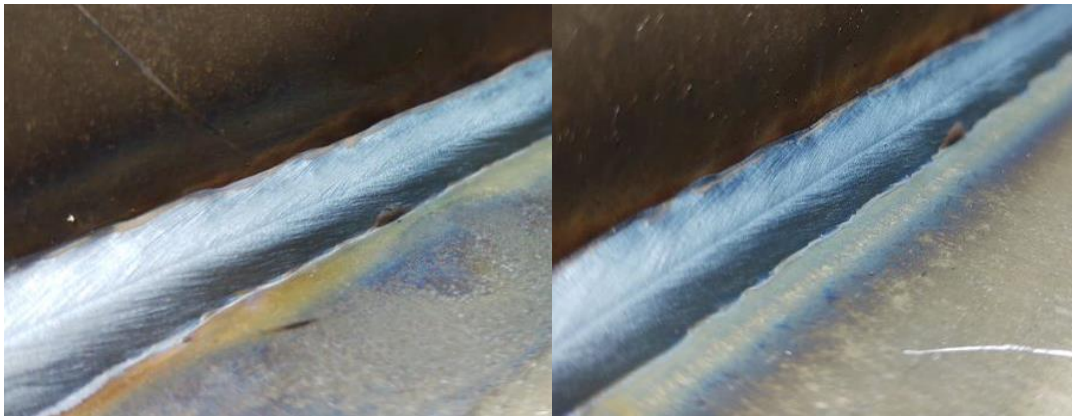

Figure 56. Visual quality of the welds of test workpieces 1 and 2.

The welds were also scanned with the laser sensor, and the visual quality was assessed with a Winteria- weld quality assurance software. The software analyses the weld quality based on the laser scanning, and estimates the quality level in accordance with a desired standard. Based on the Winteria inspection, both welds were level C in accordance with standard ISO 5817. The welds are not accepted to quality level B due to excessive convexity and too small weld toe angle, but e.g. excessive unequal leg length or undercuts were not detected. The excessive convexity of the welds is well seen in figure 57, which shows the weld profile of

test workpiece 1 at a certain point. The figure also shows how the software visualizes the results of the quality inspection. The desired weld quality feature can be selected for detailed view, which shows the dimensions and exact locations of the defects. In the figure, the selected imperfection for detailed view is weld toe radius, which was in range of 0.2-0.8 mm for both workpieces. (Winteria 2021)

Figure 57. Visualization of the inspection results in Winteria- weld quality assurance software.

6 DISCUSSION

This chapter discusses the findings of this thesis. First, the main observations of the literature review are summarized. Then the success of the laser sensor implementation is critically evaluated from the aspect of usability and applicability. Furthermore, the results of the practical tests are compared to other studies and development proposals are given.

6.1 Literature findings

Literature review in this thesis was rather general and it covered a lot of different topics. In chapter two, which discussed the future outlook of robotic welding, was found that different types of optical sensors are involved in various advanced robotic welding applications. Besides of the conventional use cases related to robot guidance, they can be used for collecting measurement data from e.g. groove geometry, weld shape, weld pool, distortions, defects and workpiece dimensions. This measurement data can be utilized in applications such as adaptive welding, robot programming and weld quality assurance. Moreover, all this data could be managed in a digitized welding production environment, where the design information, manufacturing parameters and quality data could be linked and traced throughout the production chain, and then again utilized in the design of new products and manufacturing procedures. All in all, it is apparent that optical sensing is one of the key technologies in enabling of the intelligent and flexible welding systems of the future.

Based on the closer view on optical sensing methods in chapter 3, laser triangulation sensors are the most suitable for robotic welding tasks due to their reliability, accuracy and versatility for a wide range of tasks. Laser sensors have been proven to be beneficial in various industrial applications, and it is the default option when utilization of optical sensors is considered. Another promising technology for robot guidance is 3D camera systems, based on either structured light or passive multi-camera methods. Their advantage is that the camera system can be attached apart from the robot, and the field of view covers a large area when compared to laser line scanners. Many reviewed studies addressed this topic, but any studies on practical integration of a 3D camera system to a robotic welding station were not found. However, the presented case examples showed how they can be utilized in industrial applications already with the existing technology. The 3D camera systems also enable

interesting new applications, such as automated weld path recognition and robot program generation, which will certainly evolve in years to come.

6.2 Applicability of the laser sensor methods and discussion of the test results

During practical implementation of the laser sensor functions, it first became clear that full potential of the laser sensor cannot be realized in the multi-robot welding cell, because the robot controller does not support fully digital sensor integration. This set some major restrictions, as the sensor measurement data cannot be directly utilized in guidance of the robot, and the relation between the sensor data and robot tool cannot be calibrated. Nevertheless, methods for utilizing the laser sensor in seam finding, seam tracking and workpiece positioning were proposed, of which seam finding and seam tracking were implemented and tested in practice. The next subchapters discuss the restriction and possible improvements of each method in more detail.

Utilization of this type of laser sensor functions in industrial applications is often challenging due to practical constraints. Even if the method itself works flawlessly, factors such as sensor size, mounting, maintenance, achieved benefits and complexity of operating the system must be considered. A simple example is the sensor location, as it is obvious that seam tracking sensors near the torch cannot be used when high level of flexibility is required, because accessibility to the joint suffers drastically. In this thesis, the sensor was mounted to the robot with a bracket designed for seam tracking, which restricts the freedom of movement, and e.g. welding of inner corners becomes basically impossible. However, usability of the proposed seam finding and workpiece positioning methods could be improved by mounting the sensor higher to the robot’s wrist. Also one solution could be developing an interchangeable sensor mounting system, so that the robot can pick up the sensor and use it only when needed.

6.2.1 Seam finding

Seam finding was implemented by utilizing the conventional search function principle, but instead of touch sensing, the laser sensor gives the direct input signal for the function. This is a simple and reliable method, and it is widely used in industry to adapt to the variation in workpiece position. Using the laser sensor over touch sensing provides better usability, as the searches can be done with higher speed and from longer distance. However the usability

is not optimal as a separate search motion is required in each direction to be corrected. Programming of the search motions is time consuming, and there is not always enough space to perform them. For comparison, with modern robot controllers that enable fully digital sensor integration, the seam finding can be done simply by scanning the joint at the required points, which is obviously much faster and more flexible method.

Since in search function method the sensor is used only to signal when the surface is at a specific distance, using this type of a laser line scanner does not add any value when compared to a 1D laser point sensor, which would be a more compact option for this purpose. In fact, the usability of the seam finding method could be improved by changing the field of view in the laser sensor software so, that it would be practically a laser point sensor. This would give more freedom to perform the search motions with different tool angles. In the seam finding tests, the search motions were performed with perpendicular tool angle in relation to the searched surface, but this is not mandatory as long as the sensor detects consistently the same point from the workpiece, even if its orientation varies.

Practical implementation of seam finding with the laser sensor succeeded well. Absolute accuracy of the method was ±0.3 mm, which is already sufficient for ensuring high weld quality, and it can be calibrated to be even more precise since the repeatability is so high. The accuracy is also in the same range as the accuracies of the laser sensor methods in the reviewed studies, which were summarized in table 4. Based on previous seam finding tests conducted in the LUT welding laboratory, the laser sensor provides superior accuracy when compared to touch sensing with the welding wire. The test of this thesis showed that standard deviation of seam finding with the laser sensor is 0.03 mm, whereas in bachelor's thesis by Paananen (2020, p. 31), the reported standard deviation with touch sensing is 0.16 mm. The results are comparable, because both experiments were carried out with the same robot and with similar testing procedures.

6.2.2 Seam tracking

Seam tracking with the laser sensor was implemented with analog control method, which sets limitations to its usability in some situations. The method is best suitable for straight welds, and it can be used for all different joint types. Also different torch angles can be used, but for this purpose new measurement profiles and analog port settings should be created in

the sensor software. However, problems occur if the weld path is curvature. This is because the tracking is real-time and it is solely based on the sensor data instead of the torch position, and the sensor measures the seam 100 mm ahead of the torch. Thus, if the weld path changes significantly during the 100 mm distance, it leads to a corresponding positional error of the torch. For the same reason, endings of weld paths are an issue, as the torch should still move towards the end point, while the sensor no longer detects the joint. It might be possible to set a delay for the tracking function to take account this difference, but then in turn the sensor would measure the seam constantly from an incorrect position, which would lead to unnecessary corrections. A more viable option would be to reverse the sensor mounting so that the sensor measures the seam closer to the torch.

The practical tests verified that the proposed seam tracking method can be utilized in the multi-robot welding cell. Tracking without welding was highly accurate, and it worked flawlessly also when the workpiece was deviated from its original position for several millimeters. During tracking of a straight joint, variation in the robot position was only a few tenths of a millimeter. According to Penttilä et al. (2020, p. 414–415), in order to produce a fillet weld that meets the requirements for level B in standard ISO 5817, positional error of the torch should be less than 1 mm. Therefore, if the same level of accuracy can be realized during welding, the presented seam tracking method can ensure high weld quality even if there is significant variation in the workpiece position.

However, due to the disturbance caused by welding, reliable tracking could not be achieved, as the sensor raw data consisted mostly of measurement errors. Root cause for the measurement errors is the bright light from the arc, which prevents the sensor from detecting the laser line shape and the feature points of the joint with sufficient accuracy, or even completely. According to Rout et al. (2019, p. 20), the arc light disturbance can be reduced by using optical filtering, and many studies propose bandpass filters for this purpose. This solution was also used in the study by Zou et al. (2018, p. 184) with good results. A bandpass filter transmits light only in a certain wavelength range, so it must be selected based on the laser light wavelength. For the Scancontrol 2960-60 sensor, wavelength of the laser is 658 nm, so a bandpass filter with equivalent central wavelength should remove majority of the measurement errors and solve the tracking error during welding.

Optical filters are commonly used in seam tracking sensors, but as the implemented laser sensor is not specifically designed for welding applications, it does not have such filters by default. Severity of the tracking error was not noticed in preliminary testing, because the robot path and laser sensor data was not recorded until the final tests. Measurement errors during welding were expected due to the lack of optical filtering, but only to an extent that the errors would not pass the median filtering, and thus they would not affect the tracking accuracy. Also, a cover plate was used to block the direct line of sight between the sensor and the weld pool, which was expected to be a sufficient precaution to reduce the disturbance. However, the use of optical filtering seems essential in order to realize reliable tracking. Practical integration of optical filtering could be done by designing a new sensor bracket, that has a slot for the bandpass filter between the protective glass and the sensor.

Besides arc light, also other factors can cause measurement errors for the sensor, such as spatters and reflections, but the median filtering removes this type of occasional errors as long as majority of the raw data is correct. Also, the tests showed that when the sensor did not detect the joint at all, it gave the limit value of the measurement range as an output, which led to large measurement errors. Thus, the sensor settings should be changed so, that if the feature point is not detected, the output is the target value of tracking. In this way, erroneous measurements do not convert to a correction signal even if they pass through filtering.

Effect of the tracking error to the weld quality was rather small, as the welds were symmetrical and uniform. This is because the lateral tracking error appeared only as a weaving motion of the torch, which in itself do not necessarily cause imperfections, contrarily it may be beneficial. The major problem was the torch travelling constantly too close to the joint due to the tracking error in depth direction, which led to excessive convexity of the welds. However, also other factors contribute to the weld shape, such as torch angle, e.g. a pushing torch angle would have been resulted in less convex welds. Despite the errors, weld quality level C was achieved in accordance with standard ISO 5817, based on the visual inspection with Winteria quality assurance software.

6.2.3 Workpiece positioning in jigless welding

A method for ensuring the accuracy of workpiece positioning in jigless welding was developed by utilizing the same search function principle as with seam finding. Therefore, the same practical restrictions apply to it, and correspondingly the same level of accuracy can be expected. The method was not tested in practice, but the required programs were created.

Correction of the workpiece position is carried out with two different search programs, one for correcting the distance of the final positioning motion, and one for correcting the other two directions. These programs could in principle be merged into a single search program, but it would be more cumbersome to use. The method is suitable for correcting the handling robot position prior to the final positioning motion, but the tool angles cannot be adjusted. Therefore, collisions may occur if the handling robot picks the workpiece at a wrong angle, because distance between the stationary plate and the plate to be positioned can be measured at one point only. In addition, the search motions must be performed along the main axes of the robot coordinate system, so the workpiece orientation must be considered in programming.

Due to the mentioned shortcomings, usability of the search function principle for workpiece positioning is not optimal, so further research is needed. Any relevant studies regarding specifically this topic were not found. However, a lot of studies have been made on utilizing optical sensors for handling robot guidance in pick-and-place tasks, which could potentially be applied for the multi-robot welding cell as well. For example, if the handling robot position is already adjusted in the workpiece picking phase, it could be enough for ensuring sufficient accuracy of positioning, and thus the dimensions of the welding assembly. However, the integration of new sensor technology for this purpose might turn out to be impossible due to the limitations set by the robot controller, considering that direct guidance of the handling robot could not be realized with the laser sensor either.

7 CONCLUSIONS

The purpose of this study was to implement a laser sensor system in the multi-robot welding cell of LUT University's welding laboratory, and to gather information about modern optical sensor solutions in robotic welding. Three research questions were set to direct the focus of the study, which are answered below.

To answer the first research question "What are the possibilities and restrictions of using optical sensors in robotic welding?", an extensive literature review was conducted on the topic. Based on the review, optical sensors are mainly used to adjust the robot position and process parameters to the inevitable variation in the position, orientation and geometry of the joint. Therefore, the use of optical sensors can ensure better weld quality and improve flexibility of the robot system, and correspondingly it enables to set less strict requirements for the precision of prefabrication and weld preparations. Optical sensors can also be used to gather process-level data, which can be utilized not only in process optimization, but also throughout the whole production chain of welded structures. As for restrictions, practical challenges such as accessibility issues due to sensor location, as well as error sensibility during welding limits the usability of optical sensors. In addition, implementation of an optical sensor increases complexity of the system and adds another source of error to the process, so it is not always sensible in relation to the achieved benefits.

The second research question was "For what tasks and how the laser sensor can be utilized in the multi-robot welding cell?", which refers to the practical implementation of laser sensor functions. Three main tasks were defined: seam finding, seam tracking and workpiece positioning in jigless welding. Different options for utilizing the sensor in these tasks were investigated based on literature, user manuals and consultation of the robot manufacturer's technical support. It was found out that compatibility issues between the robot controller and the sensor system limits the possibilities of the sensor integration significantly. Despite the restrictions, methods for using the laser sensor in seam finding, seam tracking and workpiece positioning was proposed.

The third research question “Is the accuracy of the laser sensor methods sufficient to ensure high weld quality?” was answered by carrying out practical tests. The test results were compared to findings of similar studies, and the visual quality of the welds was inspected in accordance with standard ISO 5817. Based on the tests, the seam finding method is reliable and the accuracy is sufficient for ensuring high weld quality, but further development is needed in order to make the seam tracking method functionable also during welding.

As a conclusion, the laser sensor system can be utilized for the desired tasks in the multi-robot welding cell, but not in an optimal manner due to the limitations set by the old generation robot controller.

7.1 Key results

The results of this thesis are both qualitative and quantitative, as new information was compiled, practical methods were proposed, and accuracy and functionality of the developed methods were determined by experiments. The key results are as follows:

- Summarization of the literature findings in table 4, which includes the different optical sensing methods and their accuracies in various robotic welding applications.
- Developed methods for using a laser sensor system for seam finding, seam tracking and workpiece positioning in jigless welding.
- For seam finding with the laser sensor, an absolute accuracy of ±0.3 mm and standard deviation of 0.03 mm could be determined.
- Theoretical accuracy of the seam tracking method was proven to be sufficient for ensuring high weld quality, but an optical filter should be integrated to the sensor in order to realize reliable seam tracking during welding.

The thesis sets a basis for further development of the optical sensor methods in the LUT-university’s multi-robot welding cell. The developed methods can also be applied directly in welding robot systems by Yaskawa. Generally, the results can be utilized in designing of robotic welding cells, in evaluation of pros and cons of optical sensor methods in different applications, and in integration of an optical sensor system into an older generation robot system. The reported accuracies of the laser sensor methods can be used as a reference for similar studies, but it should be noted that they are truly valid only for the system under investigation in the described conditions, and for non-reflective materials.

7.2 Reliability of the study

Objectivity of the literature review was ensured by selecting several and different type of references on the same topics. In total, the references of this work consisted of 22 peer reviewed articles, 3 books, 14 technical or commercial documentations, and 3 theses. The collected information is up to date, since majority of the cited articles are published after year 2015, and many of them during past two years.

Validity of the developed methods was confirmed with practical experiments. However, the workpiece positioning method was not tested, so the created search programs involve a risk of principle error, and they should be carefully reviewed before testing.

The seam finding test was repeated for 30 times to ensure the statistical reliability of the results. Reliability of the seam tracking test consist of various factors. The testing procedure included four test runs in different occasions, and the same procedure was repeated twice. Functionality and accuracy of the method was evaluated based on robot position coordinates and laser sensor data during tracking. A single test run was 400 mm long, and consisted of approximately 1600 data points of the robot position data, and 6000 data points of the sensor measurement data, so the sample size was large. The results of the tests were consistent, and the detected errors and other phenomena could be explained by both the robot position and the sensor data. Furthermore, the reason and solution to the tracking error was identified by comparing the test results to the findings of other studies on the same topic.

7.3 Key development proposals and topics for further research

Although the robot controller sets some insurmountable restrictions in unlocking the full potential of the laser sensor system, more development could be made to better utilize the sensor in the multi-robot welding cell. The key development proposals are as follows:

- Making the seam tracking method functionable during welding by integrating an optical filter in front of the sensor, and by optimizing the sensor settings in case of measurement errors.
- Designing of new sensor bracket that takes the optical filter integration into account. It could also reverse the sensor to reduce the distance between the torch and the measuring point, so the significance of the tracking delay issue decreases.

- Creation of measurement profiles and output settings to the sensor software for tracking different types of joints with different torch angles. These profiles could be saved systematically to a library to increase the usability of the seam tracking.
- Testing the effect of different parameters to the accuracy of seam finding and seam tracking, e.g. the searching speed in seam finding could be significantly increased, as it has a direct effect to productivity.
- Testing the usability of all the proposed laser sensor methods in jigless welding.
- Investigating the possibilities of other NX100 sensor functions. For example, a search function based on analog control method might be a possible option for the presented seam finding and handling robot guidance methods.

Topics for further research that emerged from the literature review are listed below:

- The possibilities and restrictions of utilizing 3D camera technology based on structured light method in a multi-robot welding cell.
- A study of the features and differences of modern, commercially available laser sensor systems for robotic welding, also considering their compatibility with different robot manufacturers in terms of sensor integration.
- A research of optical sensor utilization for handling robot guidance in pick-and-place tasks, and the applicability of similar solutions for the jigless welding concept.

8 SUMMARY

This thesis was done for the welding laboratory of LUT University as a part of ENI CBC project EFREA (Energy-efficient systems based on renewable energy for Arctic conditions). One of the goals of the project is to develop solutions that ensure the quality and productivity in welding manufacturing of lightweight structures, and this thesis aimed to contribute to this goal by investigating the possibilities of optical sensing in robotic welding.

The thesis gave an overview on the possibilities and restrictions of optical sensor utilization in different robotic welding applications, which were studied on the basis of literature and industrial case examples. Based on the review, optical sensors have a key role in the development of increasingly more flexible and adaptable robotic welding systems, which are capable of ensuring the weld quality in varying circumstances. Laser triangulation was found out to be the typical and most suitable optical sensing method for robotic welding, but also other methods based on e.g. 3D camera technology are being developed. The restrictions are mainly related to various practical issues encountered when an optical sensor is integrated to a welding robot, such as restricted accessibility due to sensor location.

The main purpose of the thesis was to implement a laser sensor system in the multi-robot welding cell of LUT University's welding laboratory. Practical methods for utilizing the laser sensor for seam finding, seam tracking and workpiece positioning in jigless welding were presented in chapter 4. However, compatibility issues between the sensor system and the robot controller limited the possibilities of the integration, so the developed methods have some drawbacks in terms of usability, which were discussed in chapter 6.

Practical experiments were carried out to investigate the accuracy and functionality of the seam finding and seam tracking methods. Seam finding with the laser sensor functioned optimally, and it showed superior accuracy when compared to conventional touch sensing method. Theoretical accuracy of the seam tracking method was proven to be sufficient for ensuring high weld quality. However, arc light disturbance during welding caused measurement errors which led to a significant tracking error. As a key development proposal, an optical filter should be integrated to the sensor to solve the tracking error during welding.

LIST OF REFERENCES

Bejlegaard, M., Brunoe, T.D. & Nielsen, K. 2018. A Changeable Jig-Less Welding Cell for Subassembly of Construction Machinery. In: Advances in Production Management Systems. Production Management for Data-Driven, Intelligent, Collaborative, and Sustainable Manufacturing. Cham: Springer International Publishing. pp. 305–311.

Bell, M. 2020. Robotic welding station increases strength by ensuring consistency. [web article]. In: Fabricating and Metalworking. [Referred 19.2.2021]. Available: https://www.fabricatingandmetalworking.com/2020/03/robotic-welding-station-increases-strength-by-ensuring-consistency/

Gao, F., Qinlan, C. & Lanzhong, G. 2015. Study on arc welding robot weld seam touch sensing location method for structural parts of hull. Proceedings of the International Conference on Control, Automation and Information Sciences (ICCAIS 2015). IEEE. pp. 42–46.

Gu, W.P., Xiong, Z.Y. & Wan, W. 2013. Autonomous seam acquisition and tracking system for multi-pass welding based on vision sensor. International Journal of Advanced Manufacturing Technology, vol. 69. pp. 451–460.

Haapala, J-P. 2020. Design and implementation of a welding robot control system based on laser measurements. Master's thesis. LUT University. 67 p.

Hou, Z., Xu, Y., Xiao, R. & Chen, S. 2020. A teaching-free welding method based on laser visual sensing system in robotic GMAW. International Journal of Advanced Manufacturing Technology, vol. 109. pp. 1755–1774.

Kah, P., Shrestha, M., Hiltunen, E. & Martikainen, J. 2015. Robotic arc welding sensors and programming in industrial applications. International journal of mechanical and materials engineering, vol. 10. pp. 1–16.

Kim, J., Lee, J., Chung, M. & Shin, Y.-G. 2021. Multiple weld seam extraction from RGB-depth images for automatic robotic welding via point cloud registration. Multimedia Tools and Applications, vol. 80. pp. 9703–9719.

Larkin, N., Short, A., Pan, Z. & van Duin, S. 2017. Automated Programming for Robotic Welding. In: Transactions on Intelligent Welding Manufacturing. Springer, Singapore. pp. 48–59.

Lei, T., Rong, Y., Wang, H., Huang, Y. & Li, M. 2020. A review of vision-aided robotic welding. Computers in Industry, vol. 123. pp. 1–30.

Lin, W. & Luo, H. 2015. Robotic Welding. In: Handbook of Manufacturing Engineering and Technology. Springer, London. pp. 2403–2444.

Lund, H., Penttilä, S. & Skriko, T. 2020. A knowledge-based multipass welding distortion estimation method for a multi-robot welding off-line programming and simulation software. Procedia manufacturing, vol. 51. pp. 302–308.

Lund, H. 2019. Development of a multi-robot welding cell for jigless welding. Master's thesis. LUT University. 90 p.

Micro-Epsilon. 2021. Operating instructions: Scancontrol 29xx laser scanners. User manual. [web document]. Micro-Epsilon Messtechnik. 64 p. [Referred 5.4.2021]. Available: https://www.micro-epsilon.com/download/manuals/man--scanCONTROL-29xx--en.pdf

Micro-Epsilon. 2020. Operating instructions: Scancontrol Configuration Tools 6.5. User manual. [web document]. Micro-Epsilon Messtechnik. 202 p. [Referred 8.4.2021]. Available: https://www.micro-epsilon.fr/download/manuals/man--scanCONTROL-Configuration-Tools--en.pdf

Muhammad, J., Altun, H. & Abo-Serie, E. 2017. Welding seam profiling techniques based on active vision sensing for intelligent robotic welding. International Journal of Advanced Manufacturing Technology, vol. 88. pp. 127–145.

Paananen, N. 2020. Usage of industrial robots for measuring welding assemblies. Bachelor's thesis. LUT University. 38 p.

Pemamek. 2021. PEMA welding and production automation for shipbuilding. Product information. [Pemamek webpage]. [Referred 29.3.2021]. Available: https://pemamek.com/welding-solutions/shipbuilding/

Penttilä, S., Kah, P., Ratava, J. & Eskelinen, H. 2019. Artificial Neural Network Controlled GMAW System: Penetration and Quality Assurance in a Multi-Pass Butt Weld Application. International Journal of Advanced Manufacturing Technology, vol. 105. pp. 3369–3385.

Penttilä, S., Lund, H., Martikainen, A., Gyasi, E. & Skriko, T. 2020. Weld Quality Verification by Using Laser Triangulation Measurement. Procedia manufacturing, vol. 51. pp. 408–415.

Pérez, L., Rodríguez, Í., Rodríguez, N., Usamentiaga, R. & Daniel, F.G. 2016. Robot Guidance Using Machine Vision Techniques in Industrial Environments: A Comparative Review. Sensors, vol. 16. pp. 335–361.

Pires, J.N., Loureiro, A. & Bölmsjo, G. 2005. Welding Robots: Technology, System Issues and Applications. Springer London. 180 p.

Ratava, J., Penttilä, S., Lund, H., Lohtander, M., Kah, P., Ollikainen, M. & Varis, J. 2019. Quality assurance and process control in virtual reality. Procedia manufacturing, vol. 38. pp. 497–504.

Reisgen, U., Mann, S., Middeldorf, K., Sharma, R., Buchholz, G. & Willms, K. 2019. Connected, digitalized welding production—Industrie 4.0 in gas metal arc welding. Welding in the world, vol. 63. pp. 1121–1131.

RobotWorx. 2018. Accufast II Tackles Seams Quickly and with Quality. [web article]. [Referred 10.3.2021]. Available: https://www.robots.com/articles/accufast-ii-offers-reduced-cycle-times-and-improved-quality

Rout, A., Deepak, B.B.V.L. & Biswal, B.B. 2019. Advances in weld seam tracking techniques for robotic welding: A review. Robotics and Computer-Integrated Manufacturing, vol. 56. pp. 12–37.

Rout, A., Deepak, B.B.V.L., Biswal, B.B. & Mahanta, G. 2021. Weld seam detection, finding and setting of process parameters for varying weld gap by the utilization of laser and vision sensor in robotic arc welding. Transactions on industrial electronics. IEEE. pp. 1–10.

Servo-Robot. 2014. Universal robot sensor system provides 3-D part measurements. [web article]. In: The Fabricator. [Referred 12.3.2021]. Available: https://www.thefabricator.com/thefabricator/product/testingmeasuring/universal-robot-sensor-system-provides-3-d-part-measurements

SFS-EN ISO 5817. 2014. Welding. Fusion-welded joints in steel, nickel, titanium and their alloys (Beam welding excluded). Quality levels for imperfections. Finnish standard association. Helsinki. 28 p.

Tavares, P., Costa, C.M., Rocha, L., Malaca, P., Costa, P., Moreira, A.P., Sousa, A. & Veiga, G. 2019. Collaborative Welding System using BIM for Robotic Reprogramming and Spatial Augmented Reality. Automation in Construction, vol. 106. pp. 1–12.

Tuominen, V. 2016. The measurement-aided welding cell—giving sight to the blind. International journal of advanced manufacturing technology, vol. 86. pp. 371–386.

Wang, B., Hu, S.J., Sun, L. & Freiheit, T. 2020. Intelligent welding system technologies: State-of-the-art review and perspectives. Journal of Manufacturing Systems, vol. 56. pp. 373–391.

Winteria. 2021. Weld quality assurance software based on laser scanning. Product information. [Winteria webpage]. [Referred 11.6.2021]. Available: https://winteria.se/products/

Yang, L., Liu, Y., Peng, J. & Liang, Z. 2020. A novel system for off-line 3D seam extraction and path planning based on point cloud segmentation for arc welding robot. Robotics and Computer-Integrated Manufacturing, vol. 64. pp. 1–14.

Yaskawa. 2005. Operators manual: NX100 options, Instructions for sensor function. Motoman instructions. Manual No. HW0483000. 51 p.

Yaskawa. 2014. Operator's manual: DX200/DX100/NX100 Options, Instructions for basic operation of starting point detecting function. Motoman instructions. Manual No. 157327-1CD. 44 p.

Yaskawa. 2016. Operator's manual: Touchsense and Accufast with macro jobs. Motoman Instructions. Manual No. 166153-1CD. 105 p.

Yaskawa. 2017. Operator's manual: YRC1000 Options, Instructions for inform language. Motoman instructions. Manual No. 178649-1CD. 398 p.

Yaskawa. 2020. Robotic Welding, solutions for all industries. Product information. [web document]. [Referred 15.2.2021]. Available: https://www.motoman.com/getmedia/22a7db10-4c85-4c67-a352-372f9089e9e7/ds_RoboticWeldingBrochure.pdf.aspx

Zeman. 2021. Steel beam assembler, fully automated tacking and welding of steel beams. SBA Compact. Product information. [Zeman webpage]. [Referred 10.4.2021]. Available: https://www.zebau.com/machines/sba/

Zeng, J., Chang, B., Du, D., Peng, G., Chang, S., Hong, Y., Wang, L. & Shan, J. 2017. A Vision-Aided 3D Path Teaching Method before Narrow Butt Joint Welding. Sensors, vol. 17. pp. 1099–1114.

Zou, Y., Wang, Y., Zhou, W. & Chen, X. 2018. Real-time seam tracking control system based on line laser visions. Optics and Laser Technology, vol. 103. pp. 182–192.

Appendix I

Dimensions and technical data of the Scancontrol 2960-50 sensor (Micro-epsilon 2021)

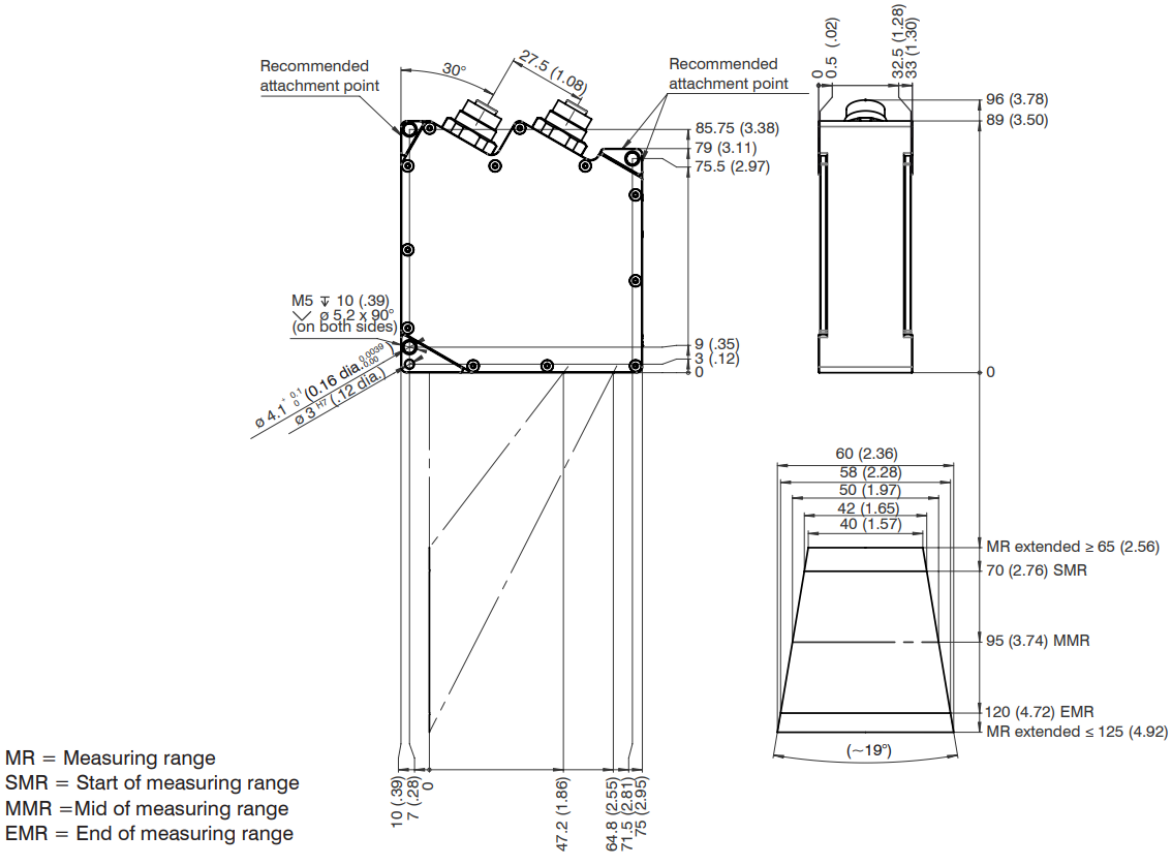

MR = Measuring range
SMR = Start of measuring range
MMR =Mid of measuring range
EMR = End of measuring range

	Model	scanCONTROL	29xx-10/BL	29xx-25	29xx-50	29xx-100
Z-axis (height)	Measuring range	Start of measuring range	52.5 mm	53.5 mm	70 mm	190 mm
		Mid of measuring range	56.5 mm	66 mm	95 mm	240 mm
		End of measuring range	60.5 mm	78.5 mm	120 mm	290 mm
		Height of measuring range	8 mm	25 mm	50 mm	100 mm
		Extended start of measuring range	-	53 mm	65 mm	125 mm
		Extended end of measuring range	-	79 mm	125 mm	390 mm
	Linearity [1]	2 sigma	±0.17 % FSO	±0.10 % FSO		
	Reference resolution [2 3]		1 µm	2 µm	4 µm	12 µm
X-axis (width)	Measuring range	Start of measuring range	9.4 mm	23.4 mm	42 mm	83.1 mm
		Mid of measuring range	10 mm	25 mm	50 mm	100 mm
		End of measuring range	10.7 mm	29.1 mm	58 mm	120.8 mm
		Extended start of measuring range	-	23.2 mm	40 mm	58.5 mm
		Extended end of measuring range	-	29.3 mm	60 mm	143.5 mm
	Resolution X-axis		1280 points/profile			
	Profile frequency	Standard	Up to 300 Hz			
		Highspeed	Up to 2000 HZ			

Appendix II

Program structure and functioning principle of 1D search program with laser sensor

"1DLSRCH" program structure:

ROW	Instruction	Explanation
0000	NOP	
0001	SSFTOF	Turns off any previous shift instructions
0002	GETS PX000 $PX023	Saves SREFP 3 from system variable $PX023 in to position variable group PX000
0003	GETS PX001 $PX024	Saves SREFP 4 from system variable $PX024 in to position variable group PX001
0004	CNVRT PX000 PX000 MTF	Converts position variable group (PX000 & PX001) into specific coordinate system
0005	CNVRT PX001 PX001 MTF	MTF=master tool frame in case of synchronized motion seam finding programs
0006	SUB P006 P006	Subtracts position variable P006 from itself to clear the data
0007	SMOVL P000 V=60.0 PL=0 +MOVJ EX000	Instruction to move to the reference point SREFP 3 (P000) with linear motion and 60 mm/s speed. (MOVJ EX000 for the workpiece positioner)
0008	SMOVL P001 V=5.0 SRCH RIN#(3)=ON T=0.30 DIS=60	Search instruction towards the SREFP 4, sets searching speed (V), input port no. (RIN 3 for laser), input status (on/off), delay time (T) and searching distance (DIS)
0009	GETS B000 $B002	Saves $B002 as B000. $B002 specifies if the searching was succesful or not
0010	JUMP *HUTI IF B000=0	If B000=0, nothing was detected. JUMP to row 0020 to cancel the program
0011	GETS PX006 $PX000	Saves the searching result ($PX00=current pulse) into position variable group PX006
0012	CNVRT PX006 PX006 MTF	Converts PX006 (which includes P006) to MTF coordinate system
0013	SUB P006 P001	Subtracts P001 (SREFP 4) from position variable P006 (detected point)
0014	SETE P006 (4) 0	Sets the tool rotation angles of the position variable to zero along all three axes
0015	SETE P006 (5) 0	4=x, 5= x, 6=x. P006 now includes the deviation between reference point and
0016	SETE P006 (6) 0	detected point along the search motion axis. (e.g. x=0, y= 0, z=3,5mm)
0017	SMOVL P000 V=60.0 PL=0 +MOVJ EX000	Instruction to move back to the reference point SREFP 3 (P000) with linear motion and 60 mm/s speed.
0018	SSFTON P006	Instruction to shift the robot's path according to the calculated deviation in P006
0019	RET	Return to the main program
0020	*HUTI	JUMP instruction from row 0010 leads here if nothing was detected
0021	SUB P006 P006	Clears the position variable P006
0022	PAUSE	Pauses the seam finding program
0023	SMOVL P000 V=60.0 PL=0 +MOVJ EX000	Move instruction back to SREFP 3
0024	RET	Return to the main program
0025	END	

A simple example of calling the search function in a main job:

NOP	
SREFP 3	Reference point for starting the searching motion
SREFP 4	Reference point at which the surface is assumed to be detected
CALL JOB: 1DLSRCH	Call for the search function sub-program
MOVL V=20.0	Point that is being corrected by the search program
END	

Appendix III

3D Seam finding program for T-joint which was used in the seam finding test.

(Job name S1H4LASR)

```
0000        NOP
0001        '--------
0002        'KOORDINOIDUN LIIKKEN HAKU
0003        'HAKUPISTEET SREFP- MUODOSSA
0004        'ULKONURKAN 3D HAKU
0005        'KAYTA HAKUUN ROBOTIN
0006        'OMIA AKSELEITA
0007        '---------
0008        SSFTOF
0009        GETS PX000 $PX021
0010        GETS PX001 $PX022
0011        GETS PX002 $PX023
0012        GETS PX003 $PX024
0013        GETS PX004 $PX025
0014        GETS PX005 $PX026
0015        GETS PX007 $PX027
0016        CNVRT PX000 PX000 MTF
0017        CNVRT PX001 PX001 MTF
0018        CNVRT PX002 PX002 MTF
0019        CNVRT PX003 PX003 MTF
0020        CNVRT PX004 PX004 MTF
0021        CNVRT PX005 PX005 MTF
0022        CNVRT PX007 PX007 MTF
0023        SUB P006 P006
0024        SUB P008 P008
0025        SUB P009 P009
0026        SUB P010 P010
0027  001   SMOVL P000 V=30.0
            +MOVJ EX00
0028  002   SMOVL P001 V=30.0 PL=0
            +MOVJ EX001
0029  003   SMOVL P002 V=10.0 SRCH RIN#(3)=ON T=0.30 DIS=40
            +MOVJ EX002
0030        GETS B000 $B002
0031        JUMP *HUTI IF B000=0
0032        GETS PX008 $PX00
0033        CNVRT PX008 PX008 MTF
0034        SUB P008 P002
0035        ADD P001 P008
0036        ADD P000 P008
0037        ADD P003 P008
0038        ADD P004 P008
0039  004   SMOVL P001 V=30.0
            +MOVJ EX001
0040  005   SMOVL P000 V=30.0
            +MOVJ EX000
0041  006   SMOVL P003 V=30.0 PL=0
            +MOVJ EX003
0042  007   SMOVL P004 V=10.0 SRCH RIN#(3)=ON T=0.30 DIS=40
            +MOVJ EX004
0043        GETS B000 $B002
0044        JUMP *HUTI2 IF B000=0
0045        GETS PX009 $PX000
0046        CNVRT PX009 PX009 MTF
0047        SUB P009 P004
0048        ADD P003 P009
0049        ADD P003 P009
0050        ADD P000 P009
0051        ADD P005 P009
0052        ADD P007 P009
0053  008   SMOVL P003 V=30.0
            +MOVJ EX003
0054  009   SMOVL P000 V=30.0
            +MOVJ EX000
0055  010   SMOVL P005 V=30.0 PL=0
            +MOVJ EX005
0056  011   SMOVL P007 V=10.0 SRH RIN#(3)=ON T=0.30 DIS=40
            +MOVJ EX007
0057        GETS B000 $B002
0058        JUMP *HUTI3 IF B000=0
0059        GETS PX010 $PX000
0060        CNVRT PX010 PX010 MTF
0061        SUB P010 P007
0062        SET P006 P008
0063        SUB P009 P008
0064        ADD P006 P009
0065        ADD P006 P010
0066        SETE P006 (4) 0
0067        SETE P006 (5) 0
0068        SETE P006 (6) 0
0069  012   SMOVL P005 V=30.0
            +MOVJ EX005
0070  013   SMOVL P000 V=30.0
            +MOVJ EX00
0071        SSFTON P006
0072        RET
0073        *HUTI1
0074        'No contact
0075        SUB P006 P006
0076        PAUSE
0077  014   SMOVL P001 V=30.0
            +MOVJ EX001
0078  015   SMOVL P000 V=30.0
0079        RET
0080        *HUTI2
0081        'No contact
0082        SUB P006 P006
0083        PAUSE
0084  016   SMOVL P003 V=30.0
            +MOVJ EX003
0092  017   SMOVL P000 V=30.0
            +MOVJ EX00
0086        RET
0087        *HUTI3
0088        'No contact
0089        SUB P006 P006
0090        PAUSE
0091  018   SMOVL P003 V=30.0
            +MOVJ EX003
0092  019   SMOVL P000 V=30.0
            +MOVJ EX00
0093        RET
0094        END
```

Appendix IV

2D correction program for workpiece positioning

Operating principle explained above figure 40

ROW	Instruction	Explanation
0000	NOP	
0001	SSFTOF	Turns of previous shift operations
0002	GETS PX001 $PX011	Reference points 1-5 are saved as position variable (REFP1 -> P001 etc.)
0003	GETS PX002 $PX012	Data transfer steps: $PX01x stores the pulse data of REFP x
0004	GETS PX003 $PX013	GETS saves the system variable in to position variable group PX00x
0005	GETS PX004 $PX014	PX00x includes P00x
0006	GETS PX005 $PX015	
0007	CNVRT PX001 PX001 BF	The position variable is converted from pulse data to the desired
0008	CNVRT PX002 PX002 BF	coordinate system
0009	CNVRT PX003 PX003 BF	BF=Base coordinate, applies the same way for both robots
0010	CNVRT PX004 PX004 BF	
0011	CNVRT PX005 PX005 BF	
0012	SUB P008 P008	Clears the position variables used for saving the search results
0013	SUB P009 P009	
0014	MOVL P001 V=60.0	Move to REFP 1 (standby point)
0015	MOVL P002 V=60.0	Move to REFP 2 (starting point of first search)
0016	MOVL P003 V=5.0 SRCH RIN#(3)=ON T=0.30 DIS=60	Search motion towards REFP 3 until RIN#(3)=ON (laser sensor digital output)
0017	GETS B000 $B002	Checks if the search was succesful
0018	JUMP *MISS IF B000=0	If not, jumps to row 38 to cancel the program
0019	GETS PX008 $PX000	Saves the search result (robot's current position) to position variable P008
0020	CNVRT PX008 PX008 BF	Converts P008 to base coordinate system (BF)
0021	SUB P008 P003	Subtracts REFP 3 from the search result to obtain the first shift value in P008
0022	MOVL P002 V=60.0	Move back to REFP 2
0023	MOVL P001 V=60.0	Move back to REFP 1
0024	MOVL P004 V=60.0	Move to REFP 4 (starting point of second search)
0025	MOVL P005 V=5.0 SRCH RIN#(3)=ON T=0.30 DIS=60	Search motion towards REFP 5 until RIN#(3)=ON (laser sensor digital output)
0026	GETS B000 $B002	Checks if the search was succesful
0027	JUMP *MISS IF B000=0	If not, jumps to row 38 to cancel the program
0028	GETS PX009 $PX000	Saves the search result (robot's current position) to position variable P009
0029	CNVRT PX009 PX009 BF	Converts P009 to base coordinate system (BF)
0030	SUB P009 P005	Subtracts REFP 5 from the search result to obtain the second shift value in P009
0031	ADD P008 P009	Adds the shift value from P009 to P008
0032	SETE P008 (4) 0	Sets the tool rotation angles of P008 to zero (4=Rx, 5= Ry, 6= Rz)
0033	SETE P008 (5) 0	P008 is now ready to be used as a shift value in the handling robot program
0034	SETE P008 (6) 0	to correct two directions in positioning (P008 values e.g. x=2, y=4, z=0)
0035	MOVL P004 V=60.0	Move back to REFP 4
0036	MOVL P001 V=60.0	Move back to REFP 1 (standby)
0037	RET	Return to main job
0038	*MISS	If either of the searches was unsuccesful, JUMP instruction leads here
0039	'No contact!	to run the rest of the instructions to pause the program
0040	SUB P008 P008	
0041	SUB P009 P009	
0042	PAUSE	
0043	MOVL P001 V=60.0	
0044	RET	
0045	END	

Appendix V

Distance correction program for workpiece positioning

Operating principle explained above figure 41

ROW	Instruction	Explanation
0000	NOP	
0001	SSFTOF	Turns of previous shift operations
0002	GETS PX001 $PX011	Reference points 1-5 are saved as position variable (REFP1 -> P001 etc.)
0003	GETS PX002 $PX012	Data transfer steps: $PX01x stores the pulse data of REFP x
0004	GETS PX003 $PX013	GETS saves the system variable in to position variable group PX00x
0005	GETS PX004 $PX014	PX00x includes P00x
0006	GETS PX005 $PX015	
0007	CNVRT PX001 PX001 BF	The position variable is converted from pulse data to the desired
0008	CNVRT PX002 PX002 BF	coordinate system
0009	CNVRT PX003 PX003 BF	BF=Base coordinate, applies the same way for both robots
0010	CNVRT PX004 PX004 BF	
0011	CNVRT PX005 PX005 BF	
0012	SUB P006 P006	Clears the position variables used for saving the search results
0013	SUB P007 P007	
0014	MOVL P001 V=60.0	Move to REFP 1 (standby point)
0015	MOVL P002 V=60.0	Move to REFP 2 (starting point of search for the plate to be positioned)
0016	MOVL P003 V=5.0 SRCH RIN#(3)=ON T=0.30 DIS=60	Search motion towards REFP 3 until RIN#(3)=ON (laser sensor digital output)
0017	GETS B000 $B002	Checks if the search was succesful
0018	JUMP *MISS IF B000=0	If not, jumps to row 38 to cancel the program
0019	GETS PX007 $PX000	Saves the search result (robot's current position) to position variable P007
0020	CNVRT PX007 PX007 BF	Converts P007 to base coordinate system (BF)
0021	SUB P003 P007	Subtracts the searching result (P007) from the REFP 3 to get the shift value in correct direction (reversed when compared to seam finding programs)
0022	MOVL P002 V=60.0	Move back to REFP 2
0023	MOVL P001 V=60.0	Move back to REFP 1 (standby)
0024	MOVL P004 V=60.0	Move to REFP 4 (starting point of stationary plate search)
0025	MOVL P005 V=5.0 SRCH RIN#(3)=ON T=0.30 DIS=60	Search motion towards REFP 5 until RIN#(3)=ON (laser sensor digital output)
0026	GETS B000 $B002	Checks if the search was succesful
0027	JUMP *MISS IF B000=0	If not, jumps to row 38 to cancel the program
0028	GETS PX006 $PX000	Saves the search result (robot's current position) to position variable P006
0029	CNVRT PX006 PX006 BF	Converts P006 to base coordinate system (BF)
0030	SUB P006 P005	Subtracts REFP 5 from the search result to obtain the second shift value
0031	ADD P006 P003	Adds the shift value from P003 to P006
0032	SETE P006 (4) 0	Sets the tool rotation angles of P006 to zero (4=Rx, 5= Ry, 6= Rz)
0033	SETE P006 (5) 0	P006 is now ready to be used as a shift value in the handling robot program
0034	SETE P006 (6) 0	to correct the positioning distance (P006 values e.g. x=0, y=0 z= 3,5mm)
0035	MOVL P004 V=60.0	Move back to REFP 4
0036	MOVL P001 V=60.0	Move back to REFP 1 (standby)
0037	RET	Return to main job
0038	*MISS	If either of the searches was unsuccesful, JUMP instruction leads here
0039	'No contact!	to run the rest of the instructions to pause the program
0040	SUB P006 P006	
0041	SUB P007 P007	
0042	PAUSE	
0043	MOVL P001 V=60.0	
0044	RET	
0045	END	